Neural Coding of Real and Implied Motion in the Human Brain

Dissertation

zur Erlangung des Grades eines
Doktors der Naturwissenschaften

der Mathematisch-Naturwissenschaftlichen Fakultät
und
der Medizinischen Fakultät
der Eberhard-Karls-Universität Tübingen

vorgelegt
von

Gizem Altan

aus Adana, Türkei

November – 2019

Tag der mündlichen Prüfung:	20.12.2019
Dekan der Math.-Nat. Fakultät:	Prof. Dr. W. Rosenstiel
Dekan der Medizinischen Fakultät:	Prof. Dr. I. B. Autenrieth
1. Berichterstatter:	Prof. Dr. Andreas Bartels
2. Berichterstatter:	Prof. Dr. Birgit Derntl
Prüfungskommission:	Prof. Dr. Andreas Bartels
	Prof. Dr. Birgit Derntl
	Prof. Dr. Uwe Ilg
	Prof. Dr. Ziad M. Hafed

Erklärung / Declaration:

Ich erkläre, dass ich die zur Promotion eingereichte Arbeit mit dem Titel:

„Neural coding of real and implied motion in the human brain"

selbständig verfasst, nur die angegebenen Quellen und Hilfsmittel benutzt und wörtlich oder inhaltlich übernommene Stellen als solche gekennzeichnet habe. Ich versichere an Eides statt, dass diese Angaben wahr sind und dass ich nichts verschwiegen habe. Mir ist bekannt, dass die falsche Abgabe einer Versicherung an Eides statt mit Freiheitsstrafe bis zu drei Jahren oder mit Geldstrafe bestraft wird.

I hereby declare that I have produced the work entitled

*"*Neural coding of real and implied motion in the human brain*", submitted for the award of a doctorate, on my own (without external help), have used only the sources and aids indicated and have marked passages included from other works, whether verbatim or in content, as such. I swear upon oath that these statements are true and that I have not concealed anything. I am aware that making a false declaration under oath is punishable by a term of imprisonment of up to three years or by a fine.*

Tübingen, den 19.11.2019 .....

Datum / Date Unterschrift /Signature

This thesis is dedicated to Koffee,

the best dog ever.

ACKNOWLEDGEMENTS

I am extremely grateful to my supervisor Professor Dr. Andreas Bartels for his patience, guidance, time and knowledge. He has been very supportive with his positive comments, encouragements, critical questions and suggestions. I feel privileged to have had the chance to work with him and learn about functional magnetic resonance imaging, neural processes in the human brain, and visual neuroscience from him.

I am very thankful to the other members of my thesis committee, Professor Dr. Birgit Derntl and Professor Dr. Uwe Ilg, for their availability, support, feedback and insightful comments. It was a great pleasure to have had the chance to collaborate with Professor Dr. Birgit Derntl in addition to my thesis project, and to be included in her group.

Many thanks to the Graduate Training Centre of Neuroscience staff for their educational and financial support that allowed me to acquire new skills and improve my existing skills. Especially without their support the Neuromag could not exist, as well as the NeNa.

Thanks to all the members of the Vision and Cognition lab for their help, and to all the participants who participated in my experiments. Thanks to my friends for their encouragement and emotional support.

Last but not least, thanks to Koffee, for being the best dog ever.

CONTENTS

LIST OF ABBREVIATIONS

BOLD – Blood oxygen level-dependent

CSv – Cingulate sulcus visual area

EVC – Early visual cortex

fMRI – Functional magnetic resonance imaging

IPS – Intraparietal sulcus

LGN – Lateral geniculate nucleus

LH – Left hemisphere

LO – Lateral occipital area

LOC – Lateral occipital complex

MST – Middle superior temporal visual area

MT – Middle temporal visual area (V5)

MT+ – Middle temporal visual complex (V5+)

MVPA – Multivariate (multivoxel) pattern analysis

Pc - Precuneus

PHC – Parahippocampal cortex

PPC – Posterior parietal cortex

RH – Right hemisphere

ROI – Region of interest

SEM – Standard error of the mean

SPL – Superior parietal lobule

TE – Echo time

TMS – Transcranial magnetic stimulation

TR – Repetition time

V1 – Primary visual cortex

V2 – Secondary visual area

V3 – Third visual area

VIP – Ventral intraparietal area

VO – Ventral occipital area

SUMMARY

Perceiving and processing visual motion is crucial for all animals, including humans. Brain regions in the human brain that are responsive to real motion have been extensively studied with different neuroimaging methods. However, the neural codes that are related to real motion have been primarily addressed using highly reductionist and mostly artificial motion stimuli, mostly using so-called random dot kinematograms. Studies using more natural forms of motion that the brain evolved and developed to deal with are comparably rare. Moreover, real, physical motion is not the only type of stimulus that induces motion perception in humans. Implied motion stimuli also induce motion perception although the stimuli do not carry physical motion information. Implied motion stimuli are for example still images containing a snap-shot of an object in motion. Various contextual cues mediate the percept of motion, including the context of the object in its background, and in particular the object composition and its axial position in the image that mediate both, the impression of implied motion as well as its direction. This means that at the neural level, object processing must be used to generate the implied motion percept. The work described in this thesis investigated the neural coding of real and implied motion in the human brain. The investigation was done using functional brain imaging of human adults and data were collected with a 3-Tesla MRI scanner while the participants viewed a variety of distinct visual stimuli. The visual stimuli contained directional real and implied motion and were created specifically for this study. For real motion stimuli, the aim of was to engage a maximal number of directionally selective units, in order to maximize the overlap to the subset of units potentially involved in coding implied motion. Hence, real motion stimuli were created such that the static component frames had natural image statistics (known to activate neurons more effectively) by using Fourier-scrambled natural images, and motion was presented at a wide range of motion velocities. Similarly, implied motion stimuli were derived from photographs of natural scenes. They were created by placing objects such as airplanes, birds, cars, or snapshots of walking humans on a set of contextual background images such as skylines or streets. For both, real motion and implied motion, stimuli for four directions were created: forwards and backwards, and left- and rightwards.

Given that the key interest in this study concerned coding of directional motion information, multivariate decoding methods were used for the analysis and modelling of the response activity patterns. However, we also examined univariate effects, as to our knowledge no prior study systematically examined neural response preferences for forward versus backward motion across brain regions, even though there are numerous behavioural studies

reporting differences of their saliency. Also, for stimuli containing natural image statistics, no prior study examined preferences for distinct motion-axes (right-left versus forward-backward) across motion regions.

Finally, it is noteworthy that the sheer number of cortical regions examined in this study far exceeded that of prior research on implied motion, in particular because we explicitly added ventral stream and object processing regions to our analysis, as, according to our hypothesis, implied motion processing must also rely on object-based processing. Regions of the ventral pathway have been overlooked in the past for such involvement and this is one of the questions I aimed to answer in this thesis. In the end, including the parietal cortex areas, high visual areas and early visual areas, I had the most extensive direction information search within 27 regions of interest for real and implied motion, to my knowledge.

The main findings of this thesis are presented in four separate results chapters.

Chapter I examines multivariate encoding of direction information evoked by our real motion stimuli that were generated with natural image statistics and variable velocities (i.e. right, left, forward, backward). The results show that directional information is encoded within numerous visual areas, from early visual to higher parietal and ventral areas, and that directions can be predicted with linear machine learning classifiers from BOLD activity responses. The areas that encode motion direction information are not limited to motion responsive areas, and include even some of the object responsive areas as well as anterior ventral regions. I found that the primary visual area (V1) and the peripheral early visual cortex (Peripherasl EVC) have a preference for encoding right and left motion directions, whereas motion area MST has a preference for encoding forward and backward motion directions.

Chapter II examines multivariate encoding of implied motion evoked by viewing static images containing objects in context. The results show that directional information in implied motion stimuli can be decoded from all early visual areas and some higher visual areas. Visual area V4 encodes patterns that allow correct prediction of right and left implied motion directions, while the motion areas V5/MT and MST only allows decoding of forward and backward implied motion directions. A key finding is that the peripheral part of the early visual cortex encoded all implied motion directions. Importantly, this part of cortex was not stimulated by the foreground object and hence did not receive bottom-up information about directionality. This result can only be accounted for by considering that feedback information from higher-level regions informs the peripheral early visual cortex (EVC) representations about foveally presented implied motion information.

Chapter III examines whether directional motion information is encoded by similar patterns for both, real and implied motion. Classifiers were hence trained on real motion patterns and tested on implied motion patters. I found that in select cortical regions, the neural codes for motion directions are shared between real and implied motion. For right and left directions the shared information is encoded in the lateral occipital area LO2, for forward and backward directions it is encoded in the ventral occipital area VO1. These findings highlight the importance of ventral and object responsive areas in human brain for motion processing.

Chapter IV examines net-BOLD signal amplitudes across distinct motion direction and motion axes. I found that motion regions and some regions in the posterior parietal cortex show a bias for processing backward real motion in contrast to forward real motion, which is surprising given that forward real motion simulates “looming” that has been shown as salient stimulus for humans.

Overall, the research in my thesis advances the field of motion processing in the human brain on several levels, by examining multi- and univariate encoding of directional information as perceived in physically moving and static stimuli, all of which were optimized to be both controlled yet also as close as possible to real-live naturalistic vision.

1 INTRODUCTION

In this thesis I aim to answer some of the unanswered questions about the neural mechanisms of real and implied motion processing in the human brain. In the following I will introduce the fundamental concepts and review the previous relevant research that was done on the topic.

1.1 Implied motion

Beyond recognizing physical motion, humans can infer visual motion even when none is present in the physical stimulus. Such as, human brain perceives motion when viewing static images in which some action or movement is performed. This perceptual phenomenon is known as implied motion. Implied motion is a type of perceptual extrapolation of the brain when viewing static images with motion content when actually no real-time change occurs. This perceptual processing relies on the knowledge of statistics of the world (e.g. gravity, acceleration) and the anticipation (expectancy) of action continuation. That means, when looking at a static image, a photograph or an art-piece, in which there is some movement going on, the brain processes this visual input not only in a feed-forward way. For instance, in cartoons the use of simple lines behind moving objects indicates presence of motion. The extraction of dynamic information, or the inference of motion, from static images requires brain to use prior knowledge about the movements of objects and involves top-down processing of the visual information (Schlack and Albright, 2007). To the date, implied motion perception is the strongest evidence of the importance of motion and that perceiving motion is a fundamental organizing principle of human perception and cognition (Gibson, 1966; Freyd, 1983).

Implied motion is different than apparent motion that is the illusion of motion when sequential presentation of images that captures a displacement of an object. The first description of implied motion goes back to experiments of Freyd on the mental representation of motion. She tested her idea that representation of movement occurs under static conditions while using frozen-action photographs. These photographs included both humans and other animals. For example, image of a person jumping off a wall. She reasoned that when a photograph that contains an object undergoing a unidirectional movement is presented to the human subjects, they would represent continuation of the movement that is presented, and therefore perceive motion when there is actually no change. The results of her experiments showed that humans represent motion when viewing static stimuli and there is a systematic tendency for humans to remember a captured event as extending beyond its actual ending point (Freyd, 1983, 1987).

Furthermore, in later experiments Freyd and Finke coined the term “representational momentum” to describe the forward extrapolation of mental representation of an object in the direction of that objects implied motion direction (Freyd and Finke, 1984).

Since humans do not attribute motion to every static images, the characteristics of the image content are relevant to induce implied motion perception in experimental settings. For example, a clear picture of cars aligned by the side of a road does not imply motion but stillness (i.e. the cars are parked). In contrast, an image of a blurred car in the middle of a road implies motion, not stillness. In both examples the images contain car(s) and road, however there is a difference in context and also in the second example the characteristics of the image is different since it includes blur. Blurring is one type of image cue to imply motion while conveying information about direction and speed. The most used and noted other static cues are dynamic balance, stroboscopic effects, affine shear and action lines (Cutting, 2002).

1.2 Implied motion processing in the human brain

One of the most studied set of brain regions involved in visual motion processing is the middle temporal visual complex (V5/MT+) that contains several distinct regions (such as V5/MT, MSTd, MSTl, and potentially additional regions) (Greenlee, 2000; Orban et al., 2004; Ilg, 2008; Zeki, 2015). Neurons in V5/MT+ are selective for the direction of motion of the stimulus (Dubner and Zeki, 1971; Albright, 1984; Albright et al., 1984; Tootell et al., 1995). Previous human (Zeki, 1991; Tootell et al., 1995; Goebel et al., 1998; Moutoussis et al., 2005; McKeefry et al., 2008; Vetter et al., 2015) and monkey (Newsome and Pare, 1988; Logothetis and Schall, 1989; Salzman et al., 1990) studies suggest a direct involvement of V5/MT+ in the perception of motion. Moreover, as previous imaging studies have shown V5/MT+ is not only involved in processing of physical motion, but also in the processing of apparent motion (Goebel et al., 1998; Muckli et al., 2002), illusory motion (Zeki et al., 1993), motion imagery (Goebel et al., 1998) and implied motion (Kourtzi and Kanwisher, 2000; Senior et al., 2000; Senior et al., 2002; Krekelberg et al., 2003).

In the following I provide brief reviews of the most relevant studies providing insights into neural substrates linking real motion processing to that of implied motion processing.

1.2.1 Enhanced fMRI responses in V5/MT+ to static images of implied motion

One of the first studies investigating neural responses of implied motion is that of Kourtzi and Kanwisher (2000). Given all that has been known about the involvement of V5/MT+ in processing of different types of motion, Kourtzi and Kanwisher designed fMRI experiments to test whether this area is also involved in processing implied motion (Kourtzi and Kanwisher, 2000). In the first experiment they showed human participants sets of images of athletes in action, athletes at rest, people at rest and houses while measuring their cortical activation. For the analysis they contrasted V5/MT+ activation to the images of athletes in action with athletes at rest, people at rest and houses. In the second experiment they contrasted activation to variety of animal and nature scenes that either implied motion or not. For instance, cortical activation to animals in action was contrasted with animals at rest, dynamic nature scenes were contrasted with static nature scenes. For both experiments they looked at the percent BOLD signal change in functionally localized V5/MT+. The percent signal change in V5/MT+ was greater for conditions with implied motion in comparison to conditions without implied motion in both of the experiments. Their interpretation of the results was that the activity in V5/MT+ most likely was modulated in a top-down fashion by high-level perceptual inferences occur elsewhere in the brain.

1.2.2 V5/MT+ is causally involved in implied motion processing

Another neurobiological research on the topic was done by Senior and colleagues (2000) who conducted an fMRI experiment with the hypothesis of experience of implied motion and perception of real motion should be sharing a common neural substrate (Senior et al., 2000). As real motion stimuli they used video samples of dynamic scenes such as a man jumping from a ledge, a kettle pouring water into a cup and for contrast still conditions of the same objects, such as kettle standing without movement, man standing without jumping. As implied motion stimuli they used the frames of the dynamic content containing videos, for contrast they used the frames of the video of the still condition. They looked at the whole brain activity of subjects and found that the overlapping area was V5 and its satellites (which I assume they both correspond to V5/MT+). With this finding, they arrived to the conclusion that V5 system is capable of perception of implied motion besides actual motion. Moreover, similar to Kourtzi and Kanwisher (2000), they mentioned about higher-order information to be acting on this motion-specific region. Later, Senior and colleagues (2002) wanted to test for functional necessity of V5/MT+ for implied motion perception and experience of representational momentum. For this they disrupted coherent firing in V5/MT+ with transcranial magnetic stimulation (TMS) 100 ms after the onset of implied motion stimulus. They observed that application of TMS on V5/MT+ resulted in

disappearance of the representational momentum effect compared to when it was applied on vertex. They concluded that there is a functional necessity for V5/MT+ for processing of implied motion (Senior et al., 2002).

1.2.3 Prior knowledge is crucial for neural responses to implied motion

Kim and Blake (2007) investigated the activation of V5/MT+ and primary visual cortex V1 in response to paintings that portray motion versus paintings that motion was not intended (Kim and Blake, 2007). At first they conducted an experiment in which participants rated the chosen paintings with and without implied motion according to which extend those paintings portray motion. They tested two groups of observers, one with experience viewing abstract paintings using multiple stroboscopic images and one without any experience. For both groups they got average rating higher for paintings with implied motion than for paintings without implied motion. Afterwards, they conducted an fMRI experiment with two groups of participants, one group (n = 5) that had prior experience observing kinetic art paintings and the other group (n = 5) had no prior experience of such. As stimuli they selected the two of the highest rated paintings with implied motion (for 'motion' condition) and two of the lowest rated painting without implied motion (for 'static' condition, as control), plus two chronophotographs. Their rapid event-related fMRI results showed that for both groups the chronophotographs produced larger BOLD response in V5/MT+ compare to the paintings, but in V1 this effect was not present. For the experienced group they found significant difference in BOLD activation in response in V5/MT+ to paintings with implied motion than paintings without implied motion, in V1 the difference was not significant. Interestingly, for the inexperienced group there was no difference in BOLD activation response neither in V5/MT+ nor in V1. Overall, they reproduced higher BOLD response in V5/MT+ with photographs with implied motion in both group of participants. Moreover, they showed that prior experience and knowledge modulates BOLD response in V5/MT+ but not V1 when viewing kinetic art stimuli. Therefore, their results are consisted with the previous research (Schlack and Albright, 2007) on the topic and highlights the importance of prior knowledge in perceiving implied motion.

1.2.4 Feedback is involved in implied motion processing in V5/MT+

Lorteije and colleagues (2007) conducted an EEG experiment in which recorded visually evoked potentials (VEP) to real and implied motion (Lorteije et al., 2007). Their aim was to test if motion-sensitive neurons are also responsive to implied motion. In an adaptation paradigm they used three types of adaptation stimuli. The first one was a static random dot pattern, second was a random dot pattern moving in the same direction as the implied motion stimuli and the

third was a random dot pattern moving in the opposite direction of the implied motion stimuli. The implied motion stimuli that they used to test the adaptation included pictures of humans either running toward left or right or standing still while facing left or right. Importantly, these pictures were cut-off images meaning that as stimuli these human pictures were surrounded with random dot patterns instead of having a coherent background image. They looked at positive (P100 and P280) and negative (N150) peek responses after implied motion stimuli onset from where they identified as visual motion areas. What they found out was that only the amplitude of the P280 was significantly different after adaptation to the random dots moving in the same direction as the test stimuli, in comparison to other adapted stimuli. Adaptation to a moving random dot pattern resulted in reduction in the amplitude of the P100 peak regardless of the direction of motion. Finally, N150 response was not modulated by adaptation to any of the stimuli. They concluded that real motion can adapt visually evoked responses to implied motion and the positive peak after around 280 ms stimulus onset is modulated by implied motion. This late positive response finding is in line with their previous research on the topic in which they reported that implied motion response is delayed compared to the real motion responses (Lorteije et al., 2006). Altogether these findings suggest that implied motion responses from V5/MT+ is related to feedback from higher areas.

1.2.5 Adaptation to implied motion stimuli recruits direction selective neurons

In order to infer whether direction-selective neural circuits are employed for implied motion processing as it is the case for real motion processing, Winawer and colleagues (2008) conducted three experiments with the motion aftereffect (MAE) paradigm (Winawer et al., 2008). The motion aftereffect is a well-studied psychophysical phenomenon that can be used as a psychophysical test for the involvement of direction selective neural mechanisms. The task during all three experiments was to make two-alternative forced-choice judgements about the motion direction while attending to the pictures for a memory test afterwards. In the first experiment participants (n = 26) were adapted to directional implied motion stimuli (either to the left or to the right) and tested with dot displays containing real leftward or rightward motion. In the second experiment (n = 19) everything was same as in the first experiment except that after half of the implied motion stimuli presentation they introduced a delay of 3 s between the offset of the pictures and the onset of the test trials with moving dots. In the third experiment (n = 32) participants were adapted to mirror-reversed pairs of implied motion stimuli and tested with inward or outward moving dots. The results of each experiments revealed that viewing implied motion stimuli systematically shifts participants' responses to real motion stimuli in a way that test stimuli were judged as moving in the opposite direction of the adapted implied motion

images. This means there was a transfer of adaptation from implied motion to real motion and suggests that implied motion processing recruits direction selective neurons.

1.2.6 Neural responses to implied and real motion involve overlapping neural populations: evidence from fMRI adaptation experiments

Krekelberg and colleagues (2005) conducted an fMRI experiment with adaptation paradigm to determine to what extent the subpopulations of neurons that are selective for implied motion overlap with those selective for real motion in V5/MT+ (Krekelberg et al., 2005). They used radial and concentric static Glass patterns as implied motion stimuli and presented in a sequence (for 300 ms, change of pattern in every 83 ms). For real motion they used random dot patterns that were arranged in the same way in the static Glass patterns and had either concentric or radial motion. They presented each class of Glass patterns in pairs of matching (e.g. concentric – concentric) and non-matching type (e.g. concentric – radial) sequentially. In their event-related adaptation design their interpretation of pattern-selective adaptation was dependent on the lower average peak BOLD response of V5/MT+ in the conditions where the same pattern was shown twice than in the conditions where two different sequences were shown. For both implied and real motion, they found adaptation to the same pattern to cause reduced BOLD response in V5/MT+. Within different experiments they expanded the adaptation paradigm to test whether adaptation to implied motion would transfer to real motion. They found evidence for a transfer of the adaptation to the same pattern from implied motion to real motion (i.e. concentric to concentric, radial to radial). Their results led them to estimate that about 45% of the neurons in V5/MT+ that are selective for real motion were also selective for implied motion. They concluded that in V5/MT+ the cells extract motion signals independent of the real or implied motion cue that delivers the signal. Moreover, they also investigated some of the early visual (V1, V2), ventral (V4, LOC) and other dorsal areas (V3, V3a and V3b) for their selectivity to real and implied motion. Their findings show that there is overlap between neural populations responding to implied and real motion stimuli, and that the overlap is twice as large in dorsal areas compared to early visual or ventral areas.

1.2.7 Conclusion

The fore mentioned experiments focused primarily on the V5/MT+ complex, and show that it has a higher mean response to images with implied motion stimuli compared to images without implied motion, and that, most interestingly, neural substrates (i.e. most likely direction selective neurons) responding to visual motion overlap with those responding to implied motion.

A key question that arises from this prior research, and that has to our knowledge not been addressed, is whether the actual information content about motion direction is encoded the same way when humans view physical motion compared to when implied motion is perceived. Only modern multivariate pattern analysis (MVPA) techniques allow to answer this question that concerns the actual neural information encoding. This is the core the question I aimed to answer in this thesis. As it is a complex question, it led to the collection of a multitude of fMRI datasets that allowed to ask several additional questions related to neural encoding of real and implied motion in the human brain.

Furthermore, since we used human fMRI, we focused our questions not only on the V5/MT+ complex, but included various additional motion responsive brain regions, early visual cortex, higher visual areas, posterior parietal cortex areas and, inspired by the study from Krekelberg and colleagues, also ventral areas for processing implied motion as well. After all, as outlined in the introduction, implied motion processing relies on object recognition and context, hence by definition requiring some input from brain regions capable to process information beyond motion.

1.3 Motion processing in the human brain

Humans, as well as most of the known species of the animal kingdom, rely on their visual system to detect changes in their own movements and their environment both when being stationary and while navigating. Since perceiving and recognizing visual motion and visual motion direction is crucially important for animals to survive in dynamic world, these are fundamental tasks of the visual systems.

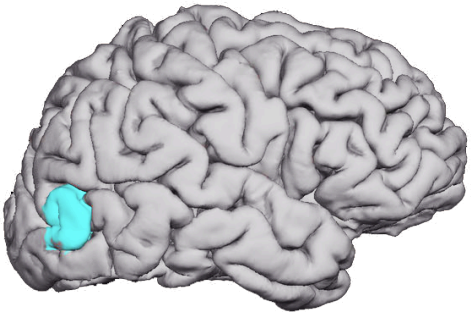

Figure 1: Cortical location of the middle temporal visual complex (V5/MT+) of a single subject.

Visual motion processing is a well-examined function of the visual cortex in primates. The direction selective cells in primary visual cortex (V1) of primates are considered to be the basic motion processing units (Livingstone and Hubel, 1988). In V1, where the first stage of processing visual information occurs, up to 20% of the neurons respond direction selectively to visual motion and project to the middle temporal area (V5/MT) (Mikami et al., 1986; Movshon and Newsome, 1996). As previously mentioned in the implied motion processing chapter, middle temporal visual complex (V5/MT+) has been extensively studied in both human and monkey studies and the activation of this area is tightly linked to perception of visual motion (see Figure 1 for its location). Being in the dorsal stream (or dorsal pathway) and having high amounts of direction selective neurons are the two most known characteristics of V5/MT+. However, it was also shown that the activity of V5/MT+ does not always correlate with awareness of the motion, suggesting that motion perception relies on activity of and interactions between multiple brain regions (Moutoussis and Zeki, 2006, 2008; Hedges et al., 2011). Indeed, there is mounting evidence that feedback from specialized motion regions to early visual cortex facilitates motion processing (Muckli et al., 2005; Wibral et al., 2009). Interestingly V5/MT+ activation was observed when motion is perceived tactilely in the absence of visual stimuli (Hagen et al., 2002) or when motion is held in working memory (Bisley et al., 2004). These findings suggest that V5/MT+ is not only an area that processes visual information but it has complex reciprocal connections with higher visual areas.

1.3.1 Decoding motion and motion direction from fMRI activity patterns

It has been shown that with MVPA on fMRI BOLD data it is possible to decode seen and attended direction of motion in early visual areas (V1-V4) and motion responsive complex V5/MT+ (Kamitani and Tong, 2006). In their first experiment, Kamitani and Tong (2006) wanted to test whether motion direction of observed stimuli can be decoded from BOLD activity patterns. For this they presented random dots moving to eight possible motion directions (four cardinal and four inter-cardinal directions) as visual stimuli to the participants (n = 4) while recorded their fMRI BOLD responses. They found that the linear classifier (SVM) was able to decode the correct directions from the activity patterns in early visual areas (V1-V4) and V5/MT+ significantly above chance. In the second experiment, they wanted to test whether it would be possible to decode the attended motion direction from the BOLD activity patterns. This time the random-dots were presented in rotational motion (clockwise and counter-clockwise). To train the classifier they used response patterns to stimuli that either rotated clockwise or counter clockwise. The test data were collected when both directions were simultaneously presented (i.e. half of the dots moving clockwise, the other half counter-clockwise). They found that after training the classifier on the data that was collected when participants were viewing clockwise or counter-clockwise stimuli, the classier was able to correctly identify the rotation direction that participants attended when both rotation directions were presented simultaneously. Similar results were obtained by Seymour and colleagues (2009) who investigated whether linear support vector machines (SVM) could discriminate between voxel-activity patterns by colourful dot stimuli containing clockwise or counter-clockwise motion direction (Seymour et al., 2009). They performed group analysis (n = 5) for decoding motion directions in V1, V2, V3, V3A/B and V5/MT+ and found that all of the areas performed better than chance.

1.3.2 Direction selective response patterns do not directly relate to the conscious perception of motion

Do the direction-selective response patterns directly relate to the conscious perception of motion? Serences and Boynton (2007) conducted an fMRI study to investigate exactly this question. They also used random-dot motion patterns as visual stimuli and asked their participants (n = 10) to report perceived direction of motion either of an ambiguous or an unambiguous dot patterns (Serences and Boynton, 2007). They looked at the response patterns in V1-V4v, V3A and V5/MT+ within a multivariate pattern analysis. For the unambiguous motion condition, they replicated that all these areas encoded directional information. For the ambiguous motion condition, they expected over chance level decoding only in cortical regions is perceptual state of the observer. Indeed, after training the classifier on with ambiguous motion

stimuli, they were able to classify motion directions of unambiguous stimuli only in V5/MT+ and V3A. Thus, they concluded that decoding response patterns in these motion areas relate to their cortical specialization for motion processing.

1.3.3 Decoding some motion types can be explained by aperture-inward bias

What allows motion decoding in early visual areas? The assumption behind the decoding motion direction is that the response patterns of the direction selective columnar organization in cortex. However, the study done by Wang and colleagues (2014) found evidence for decoding accuracy of motion to be result of what is called “the aperture-inward bias” in early visual cortex (Wang et al., 2014). In an fMRI experiment they showed subjects (n = 5) moving random dot patterns at different eccentricities (between 2 to 11 degrees radius from fixation) moving at differing direction coherence. Motion directions of the coherent dot groups varied in eight possible directions. They mapped the motion direction preferences in visual cortex in a similar way to neuronal population receptive field mapping. They reported that in V1-V3 voxels encoding visual field locations at the edges of the annular stimulus aperture showed a systematic preference for motion directions orthogonal to the aperture edge and pointing into the aperture. When they performed a multivariate classification analysis of the eight motion directions in V1-V3 and V5/MT+ they were able to decode the corresponding directions from these areas. However, when they binned the voxels in these areas according to their motion direction preferences they found that aperture-inward prediction was sufficient for motion decoding in early visual areas but not in V5/MT+. Therefore, they concluded that motion decoding was not the result of the direction-selective columnar organization but rather reflected the motion direction preferences in the early visual areas. However, their results only apply to decoding of motion types that lead to aperture-inward biases, such as planar, expansion, or contraction motion. Several other MVPA studies have successfully decoded motion direction for motion types where this does not apply, such as circular motion (Seymour et al., 2009). This decoding also worked across visual cortex (V1-V3, V3A, hV4, V5/MT+).

1.3.4 Motion processing beyond V5/MT+

Besides V5/MT+ there are other areas in the human brain that were identified as motion responsive. For instance, V3A has been shown to be involved in motion processing (Tootell et al., 1997). Also, V3A shown to have preference to real motion over retinal motion (Fischer et al., 2012). Moreover, the human area V6 is a motion area that responds to unidirectional motion with strong preference for coherent motion and is highly sensitive to optic flow signals (Pitzalis et al., 2012). In a recent fMRI study Nau and colleagues (2018) tested which regions in the human brain

were involved in estimation of objective motion velocity while participants performed a circular pursuit of a moving target on a moving background (Nau et al., 2018). The speed and the trajectory of the moving target was kept constant and they varied the background motion speed, which was induced by coherently moving dots in the same trajectory (circularly) as the moving target. They have found that motion responsive regions V3A, VIP and Pc showed preference for faster objective motion than pursuit compare to objective motion slower than pursuit, while V5/MT+, MST and CSv did not show significant modulation for any of their contrasts. More interestingly, they found early visual cortex responses to objective motion and also that the responses are modulated by motion velocity. Given that neurons need to integrate eye movements with visual input to respond to objective motion, the authors suggested it is more likely that early visual responses reflect that V1 receives extra-retinal signals related to eye movements. Moreover, they argued that given the predictability was matched across their experimental conditions the results are unlikely to be accounted by predictive coding framework. Nevertheless, these results show that early visual areas are involved in real objective motion processing and process signals beyond mere retinal input.

1.3.5 "Looming" bias for expanding motion

When stimuli are biologically relevant and critical for organisms' survival they are considered more salient by the sensory systems. Therefore, perceptual representations may not always reflect the statistical structure of the world, but asymmetries can be observed when there is a bias in processing of such salient stimuli. For example, sensitivity to optical expansion (i.e. looming) is crucial for selecting a defensive response to avoid a collision (e.g. when crossing street). According to the behavioural-urgency hypothesis dynamic visual properties capture visual attention of humans if they signal the need for immediate or urgent action (Franconeri and Simons, 2003). For instance, the human visual system may be biased to attending to the objects that are approaching and encoding motion directions that are toward to the observer. Such sensitivity was observed behaviourally for expanding motion (i.e. looming) in contrast to contracting (i.e. receding) motion stimuli in human infants (Ball and Tronick, 1971; Nanez, 1988), and infant and adult rhesus monkeys (Schiff et al., 1962). Direct comparison of these two motion directions was done with binocular rivalry paradigm to test if expanding motion is a more salient visual stimulation. It was shown that looming/expanding stimuli predominates receding/contracting stimuli (Parker and Alais, 2007). Besides that, the perceptual asymmetry for looming signals was shown to be correlated with faster response time and underestimation of time of arrival of looming sounds (Schiff and Oldak, 1990). The adaptive bias for perceiving auditory looming is not only observed in humans (Neuhoff, 1998), but also in rhesus monkeys (Ghazanfar et al., 2002). The neuronal correlation of the looming versus receding signal bias was

observed in macaque in auditory lateral belt cortical activity as enhanced single cell firing (Maier and Ghazanfar, 2007).

Interestingly, looming signals of 2-D stimuli (i.e. discs expand in diameter) were shown to be associated with subjective time dilation and receding signals (i.e. discs that contract in size) were not. Wittmann and colleagues (2010) conducted an fMRI study to investigate brain structures involved in temporal dilation illusion in humans. They showed the participants stream of visual events of a 2D target for a fixed duration and asked them to indicate whether when the object size was bigger or smaller (compare to the standard stimulus that was presented before and after) the perceived duration of the stimulus appearance was longer or shorter than the standard stimulus. They found that participants reported longer perception of duration when the test stimuli were loomed (i.e. bigger in size) than when it was smaller or the same size. The fMRI signals in a contrast between looming and receding conditions revealed significantly stronger activity for looming in left medial frontal, the posterior cingulate and precuneus regions (Wittmann et al., 2010). However, there is no adult human fMRI research showing any neuronal correlations for looming bias in visual domain when stimuli sizes are controlled. The stimuli I used as Forward and Backward real motion were matching with each other in every aspect except for their motion directions. Therefore, it gave us a chance to investigate whether one of these stimuli correlated with higher BOLD responses in the regions of interest.

1.4 Predictive coding in vision

At any awake moment the brain is confronted with abundant sensory information that need to be processed very quickly and efficiently to both perceive its environment and to guide body movements. Dealing with all the sensory information in an efficient way requires information processing strategies that are optimized to the statistics of the perceivable environment. Understanding how the brain does process sensory information and attributes meaning to somethings while disregards some others is still a mystery to be solved. In the last decade there has been increasing interest in the predictive coding framework for understanding neural computations across different brain regions and modalities. According to the predictive coding framework, the visual system tries to learn an internal model of the external environment to actively predict incoming signals (Rao and Ballard, 1999). Meaning that top-down information influences lower-level estimates, i.e. early visual cortex receives predictive feedback from higher-level regions, and bottom-up/feed forward information influences higher-level estimates of the input signal, i.e. signalling mismatches (prediction errors) with respect to the sensory input (see the illustration in Figure 2). Thus, predictive coding allows neural activity to be guided by prior information. Several studies found experimental evidence for predictive coding in the visual system, and I will review some of them in the next section.

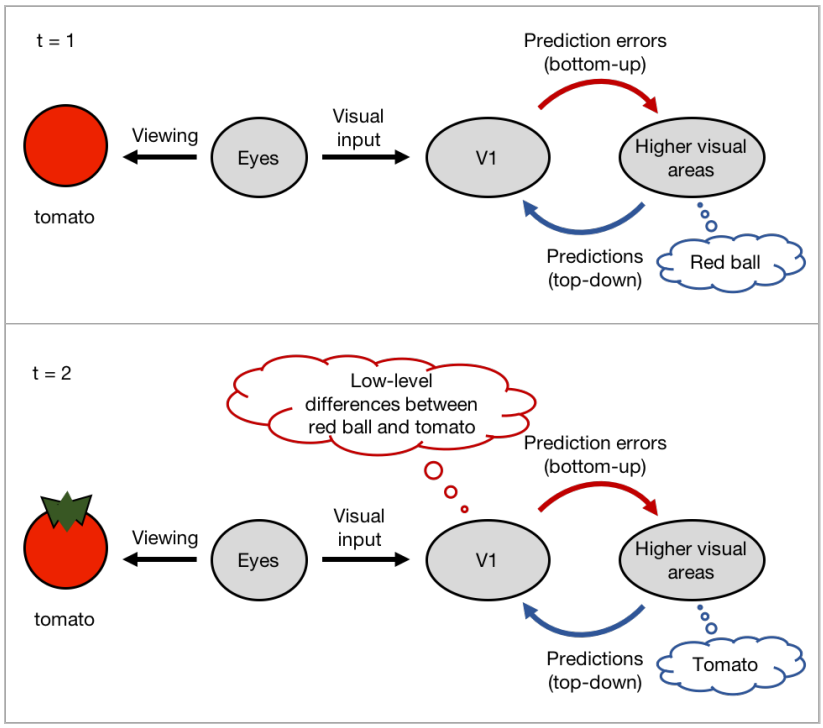

Figure 2: Illustration of predictive coding in vision. The top row illustrates the initial prediction of the higher level visual areas according to the prior knowledge (t = 1), the bottom row illustrates how the new information (seeing the same object from a different angle) is used to update the brain states (t = 2).

1.5 Experimental evidence for predictive coding

According to the predictive coding framework the visual cortices learn statistical regularities of the natural world and instead of transmitting all the incoming sensory input they only signal the unpredictable components of their sensory input to higher visual areas (Rao and Ballard, 1999). Since the proposition of this framework its implications were investigated by many researchers. In the following subchapters I will review some of the findings.

1.5.1 Motion prediction

For example, Alink and colleagues (2010) investigated whether predictable stimuli evoke smaller BOLD fMRI responses in V1 and V5/MT+. They used upward and downward apparent motion as visual stimuli and had predictable and unpredictable conditions for stimulus onset and motion direction. They found that stimulus onset predictability reduces activity levels in V1, but not in V5/MT+. Whereas predictability of motion direction resulted in reduced responses in both V1 and V5/MT+ (Alink et al., 2010). Later on, Schellekens and colleagues (2016) used moving-random-dot stimuli to look for a similar evidence in early visual areas. They used high-field fMRI and recorded activation during predictable versus unpreceded motion induced contrast changes. Their results show a reduced BOLD response to predictable contrast changes in moving stimuli relative to unpredictable changes (Schellekens et al., 2016). These results suggest that predictability of stimuli is reflected in BOLD signal reduction and that predictive coding mechanisms are present in early visual areas and V5/MT+ for visual motion processing.

1.5.2 Size prediction

Size constancy in the visual system is a well-known phenomenon. That is, we perceive the size of an object as constant, irrespective of viewing distance. If our perception of the world would only depend on the retinal images, then the perceived size of an object would increase if we are closer to it and decrease when we move further away from it. It has been shown that the primary visual cortex (V1) activation correlates with perception, rather than direct mapping of the physical stimuli. Murray and colleagues (2006) looked at how perceived diameter would be represented in V1 with a size-depth illusion with an fMRI experiment. They presented equally sized spheres in 3D background that elongated in depth, this induced participants to perceive the sphere that was in the back of the background to appear larger than the front one. When they looked at the cortical representation of these objects in V1, they found that the size of activation for each sphere matched the perceived size of the objects, rather than their actual size (Murray et al., 2006). Similar results were obtained by Sperandio and colleagues (2012) when

they experimentally manipulated the actual distance of an afterimage in an fMRI experiment. They induced afterimages while asking participants to fixate on a light for 4 s and manipulated the size of the afterimages while placing a back screen at one of five viewing distances at a time after turning off the light. Participants reported their perceptual judgements of afterimage size after every trial and the responses positively linearly correlated with their viewing distances to the back screen (i.e. as in Emmert's law: the greater the distance, the bigger the afterimage). When they looked at the BOLD response they found that the sizes of the afterimages were represented in V1 activation: more eccentric V1 activation corresponded to bigger afterimage perception (Sperandio et al., 2012). Given that one of the most fundamental properties of V1 is its precise mapping of visual field onto the cortex, these results indicate that feedback from higher visual areas can even modulate this topological mapping. Following up these findings, recently with an EEG study Chen and colleagues (2019) investigated the influence of real distance on size coding and its temporal correlations in V1. They manipulated the retinal size of two physically distinct sized objects (solid black circles) by presenting them in near and far viewing distances while recoding the event related potentials (ERPs). They found that the first (early) visually evoked component (C1) that reflects feed-forward signals in V1 reflects the retinal image size and not modulated by the perceived or physical size of the stimulus. More interestingly, when they looked at the time course of the ERP amplitude differences they found that waveforms of the same retinal image size overlapped until 148 ms after stimulus onset and later they began to separate. Whereas, the waveform responses to the same physical size began to overlap approximately at 148 ms, when the retinal image size responses start separation (Chen et al., 2019). Overall, these results suggest that retinal images sizes are processed at the very early stages of visual processing in V1 and later processes (yet as early as 150 ms after stimulus onset), probably due to the received feedback, reflect the real-world size of visual stimuli.

1.5.3 Colour prediction

More supporting evidence for predictive coding in visual processing comes from active involvement of visual memory colours in visual perception. In a behavioural study Hansen and colleagues (2006) investigated whether the known colour of objects affects colour appearance while using images of natural fruit objects as visual stimuli. When human observers were asked to adjust the colour of these fruits to match a grey background, they did not stop when the actual grey was reached but rather over-corrected to reach grey. This means that human perception showed a systematic bias toward the actual colour of the object even when the objects were achromatically presented. The authors concluded that prior knowledge about the natural colour of fruits affected low-level perceptual mechanisms and therefore the perception of colour

(Hansen et al., 2006). Following this finding, Bannert and Bartels (2013) hypothesized that the upon viewing colour-diagnostic objects such as bananas, coke-cans etc., top-down signals may send predictive colour signals to earlier processing stages in order to compare incoming with predicted colour signal. They conducted an fMRI experiment to test this hypothesis, in which human participants were shown achromatic images of colour-diagnostic objects and real chromatic ring-shapes as visual stimuli. In order to test for neural representation commonality (i.e. generalization), they used multivariate pattern classification technique and used responses to the chromatic ring stimuli as training dataset for the classifier to distinguish four distinct colours, and responses to the achromatic object stimuli as test dataset. Their results showed that the classifier that learnt to distinguish colours from ring-shaped stimuli could predict the true colour of achromatic objects from fMRI activity in V1 (Bannert and Bartels, 2013). Their results provide direct neurobiological evidence for predictive signals in the earliest cortex, V1.

1.6 The relation between form and motion in the human brain

Traditionally, form processing and motion processing have been considered to be done in parallel and attributed to anatomically and functionally separate neural pathways. Visual information processing starts at the retina, proceeds to the Lateral Geniculate Nucleus (LGN) and then to V1, and V2. Afterwards, according to the two stream of processing hypothesis, visual information goes through different pathways: for shape and object processing to V4 (ventral – "what" - stream) and for spatial and motion processing to V3 and to V5/MT (dorsal –"where"-stream) (Mishkin et al., 1983; Haxby et al., 1991). The temporal lobe, for instance, is part of the ventral stream, whereas parietal cortex is part of the dorsal stream. Single-unit recordings of neurons in areas part of the ventral stream show selectivity for colour, shape and texture while neurons in areas part of the dorsal stream show selectivity for the direction and speed of visual motion – these results are in line with the two streams hypothesis (Maunsell and Newsome, 1987; Ungerleider and Haxby, 1994). However, more recent studies show accumulating evidence that these pathways do not work as separately as it was first proposed. Indeed, these pathways interact with one another and therefore neither form nor motion processing does occur independent from each other, as briefly reviewed below.

1.6.1 Motion from Form

Motion from form is a term that is being used to indicate mechanisms that form information affects motion processing. For instance, it is known that orientation information can affect motion processing in V1 (Geisler, 1999). In his proposal Geisler suggested that the brain could use motion streaks to improve detection of moving objects and to determine direction of motion. Motion streaks, (also called as motion smear or speed lines), are the blurred lines along the trajectory of a moving object. In art and photography motion streaks have long been used to imply motion. Although we perceive as if our visual experiences are created instantly by the visual input we receive through our eyes, the brain has a temporal integration period to accumulate the visual information. Due to this temporal integration in the visual system, moving objects generate static, oriented motion streaks. It has been suggested that these trails are neural homologue of the speed lines used by artists to imply motion (Burr, 1980, 2000). Moreover, it was demonstrated with psychophysical and physiological analyses that the human visual system estimates motion direction by performing a spatial analysis of motion streaks (Geisler, 1999). However, these were only considered for V1 neurons and not for other areas.

Another case for motion from form is the case of implied motion, where there is no explicit motion information, but where (object) form information aids motion perception. Well known human motion responsive area V5/MT+ activation has been found repeatedly in response to static images with implied motion. It was suggested that the involvement of V5/MT+ in implied motion processing, where there is no physical motion, occurs automatically in a top-down modulated fashion (Kourtzi and Kanwisher, 2000). Nevertheless, this is a finding showing interaction between form and motion processing. Furthermore, psychophysics showed a transfer of adaptation from implied motion to real motion provides further evidence for form and motion processing interactions (Winawer et al., 2008).

Static Glass patterns (random dot patterns oriented along a common path), when presented in sequences are also shown to give a rise to coherent global motion although they do not contain any dynamic structure (Ross et al., 2000). Krekelberg and colleagues consider motion perception in response to Glass patterns as implied motion because there is ambiguity in motion direction (Krekelberg et al., 2003). Although this definition of implied motion is not consistent with our and other definitions of implied motion, we consider the percept in response to Glass patterns as an example to motion from form.

1.6.2 Form from Motion

Form from motion is a term that is being used to describe ability to extract the forms of objects defined entirely by visual motion cues. The most impressive case of it comes from perception of form from biological motion. Johansson demonstrated that humans can recognize human actions (e.g. walking, running, cycling, dancing) from the movement patterns of small bright spots (point lights) attached to the joints of an otherwise invisible human actor (Johansson, 1973). Point-light animations later were studied further and it has been revealed that humans can also extract gender and emotional states from these motion patterns (Blake and Shiffrar, 2007).

The other cases are sometimes also called structure from motion (Wallach and O'Connell, 1953) and more specifically refers to perception of three-dimensional shape of an object when observing its two-dimensional motion patterns. In this case visual motion is being used as a depth cue. For instance, with coherently formed smoothly moving dots on a background of random dot displays it is possible to induce perception of moving cylinder (Treue et al., 1991), globe or some other shapes. Interestingly, it was shown that adaptation using unambiguous, stereoptically defined object rotation affected rotation direction of subsequently presented non-stereoptically defined motion cylinders, demonstrating a neural interaction

between stereopsis and structure from motion (Nawrot and Blake, 1991). Perceived rotation of a rotating ambiguous structure from form was predicted in BOLD response patterns of V5/MT+, V3A, V4D and V7 in an fMRI study that used MVPA (Brouwer and van Ee, 2007).

1.6.3 Conclusion

Taken together, the area V5/MT+ has been repeatedly found to be involved in both in perception of motion from form and form from motion. This adds to the evidence for representation of objects and shapes in dorsal pathway. However, it is not known so far whether areas in the ventral pathway are also involved in processing of implied motion. The areas in the ventral pathway have been overlooked in the past for such involvement and this is one of the questions I aimed to answer in this thesis. In the end, including the parietal cortex areas, higher visual areas and early visual areas, I had 27 regions of interest. In this way I had the most extensive direction information search for real and implied motion in the human brain, to my knowledge.

2 RESEARCH GOALS

In this thesis I aimed to investigate neural mechanisms involved in real and implied motion processing. In particular, one main aim was to determine whether and where neural coding of directional information shared neural representations between implied and real motion. Achieving the main aim hence implied achieving several other insights first, such as identifying neural representations of directional information for implied motion, separately from that of real motion, in the human brain.

In the first experiment I tested whether MVPA can be used to discriminate motion directions when the stimuli are texture based. I asked this question for two distinct motion axes: *forward (expansion) versus backwards (contraction)*, and *right versus left*, yielding a total of four different motion directions. One novelty that distinguishes our data from all other prior studies using MVPA to distinguish motion direction was that we used more naturalistic visual stimuli, designed to optimally stimulate visual motion processing channels: for left-right motion, we used 1/f Fourier noise, i.e. visual stimuli that matched in their frequencies those occurring in the natural world. For forward-backward motion, we used continuously expanding fractal-like stimuli with similarly naturalistic image statistics. Finally, to our knowledge, no prior study compared multivariate voxel responses for two distinct motion axes. A reasonable subordinate research question was hence to compare the decoding performance of the specified areas for their preference for either type of motion direction: do some brain regions encode forward-backward motion better than left-right motion in terms of MVPA distinguishability?

For analysis, I took great care to localize a variety of different brain regions, including early visual (V1, V2, V3) and other retinotopic areas (V4, V3B, LO1, LO2), numerous motion responsive regions (V5/MT, MST, V3A, V6, Pc, CSv, VIP), as well as object responsive regions in the ventral stream (VO1, VO2, PHC1, PHC2) and parietal cortex areas (IPS0, IPS1, IPS2, IPS3. IPS4, IPS5, SPL1). Overall, several of the areas I looked at were not previously investigated for their encoding of real motion directions.

In the second experiment I looked at the same brain areas, this time to investigate whether they encode information about implied motion directions. The directions and classification pairs were the same as in the first experiment: forward versus backward and left versus right. Instead of using dynamic stimuli I used static stimuli which contained directional implied motion as visual stimuli. In the Right versus Left condition all stimuli had blurred background and sharp foreground objects (simulating smooth pursuit of the foreground object), in the Forward versus Backward condition blur was applied only to the foreground objects

(simulating fixation on the foreground object while it moves across the retina). A key research question was which brain regions encode implied motion directions. One particularly interesting question was whether eccentric visual representations in early visual cortex (V1-V3) also encoded implied motion directions, even though the *information of directionality* was given by the foreground object represented only foveally. In other words, this question regarded whether information of implied motion could reach early visual eccentric representations via feedback from higher-level regions.

In the third experiment I tested whether the brain generalizes motion direction information between real and implied motion. If the processing of real and implied motion shares common neural representations in a given brain region, then the directional information encoded by one motion type (e.g. implied motion) should be encoded in a similar way as the direction information by the other motion type (e.g. real motion), and a classifier trained to distinguish motion directions for one type should be able to decode directions for the other type (cross-decoding).

In the last experiment I tested whether there is significant difference in BOLD response to real Forward and Backward motion directions, given that they do not only differ in direction, but also in ecological salience (approaching versus receding objects). Moreover, I checked for the difference between Right and Left real motion directions in BOLD response while not expecting to find any.

3 MATERIALS AND METHODS

3.1 Subjects

20 healthy adults (11 female, 9 male, 1 left-handed, age between 24 and 39 (mean age: 27.5)) voluntarily participated in the study. All of them had normal or corrected-to-normal vision, gave written informed consent before the experiments and received monetary compensation for their participation. There was no dietary or language based exclusion criteria for subject selection (i.e. smoker vs. non-smoker, native speaker or not), the only exclusion criteria were regarding MRI safety. Due to unknown technical problems with the MRI machine the data of one of the participants were incomplete therefore this participant was excluded from analysis. The study was conducted according to the Declaration of Helsinki and was approved by the local ethics committee of the University Hospital of Tübingen.

3.2 Experimental Design

The data for all the experiments were acquired in two separate sessions from the same subjects. In both sessions the functional brain images of the subjects were collected with a 3 Tesla MRI machine. The first session contained 1) retinotopic data collection, 2) motion area localizer, 3) early visual eccentricity localizer, 4) structural imaging. The second session contained the runs of main experiments and the details of them will be described under relevant titles.

3.3 Localizer Experiment

3.3.1 Retinotopic Mapping

We used a standard (i.e. traveling-wave method) polar angle retinotopic mapping stimulus (see the Figure 3) to acquire data from 11 of the participants (Wandell et al., 2007). The stimulus consisted of a grey background with a superimposed wedge of 90° angle that extended to the edges of the screen the wedge flickered (luminance inversion) clockwise in half of the runs and counter-clockwise in the other half. In a run, participants observed 10 wedge cycles, each cycle lasting 55 sec. During the mapping, participants fixated the centre of the screen and pressed a button whenever a red circle appeared on the screen. Participants performed a task on central fixation at all times (see Tasks below). Data were pre-processed and analysed using cortical surface-based methods using Freesurfer software. The retinotopy data were motion corrected and spatially smoothed with a Gaussian Kernel of 6 mm FWHM.

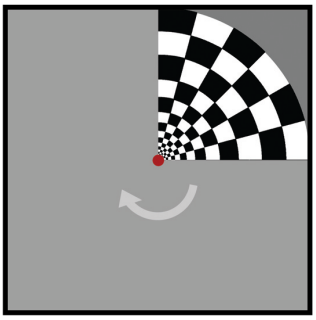

Figure 3: Illustration of the rotating wedge, the standard polar angle retinotopic mapping stimulus, that was used in the localizer experiment.

3.3.2 Human Motion Areas Localizer

The human motion complex V5+/MT+ was defined using two conditions of a motion localizer: 3D optic flow and a static condition. In the 3D optic flow condition, participants were presented with full-field coherent motion of a random dot pattern with 3D flow (e.g. expansion/contraction). The static stimulus contained stationary dots taken from a snapshot of optic flow condition, but every frame 4% of the dots were redrawn at random positions to match the rate of appearance/disappearance of dots of the 3D flow stimulus (Fischer et al., 2012). The human visual responsive area V3A was defined using another two conditions of a motion localizer: 2D Planar Motion and 2D Static. Both of these contrasts had moving fixation circle that subjects were instructed to pursuit with their gaze. The details of this functional localizer can be found in a previous paper from our lab (Fischer et al., 2012). Conditions lasted 12 s and had been presented in a random sequence along with three additional motion flow conditions not used here. Participants performed a task on central fixation at all times (see Tasks below).

3.3.3 Early Visual Eccentricity Localizer

The early visual eccentricity localizer stimuli had a counterbalanced design involving three conditions: foveal, peripheral and baseline, as illustrated in Figure 4. This localizer functionally defined the parts of the early visual cortex that were stimulated by background and foreground parts of the implied motion stimuli. The foveal condition contained a central, circular checkerboard (100% contrast) whose radius covered the maximal stimulus extent of the foreground objects of the Right and Left implied motion stimuli, displayed on an isoluminant grey background. The peripheral condition was the inverse of the foveal stimulus, i.e. a checkerboard reaching into the periphery, with the central circular aperture covered in isoluminant grey. The baseline condition consisted of a full-screen grey background. During the localizer run each of the 3 conditions was presented 3 times in a block-design (each block lasted 12 seconds). The condition sequence was pseudo-randomized to control for order effects. Participants performed a task on central fixation at all times.

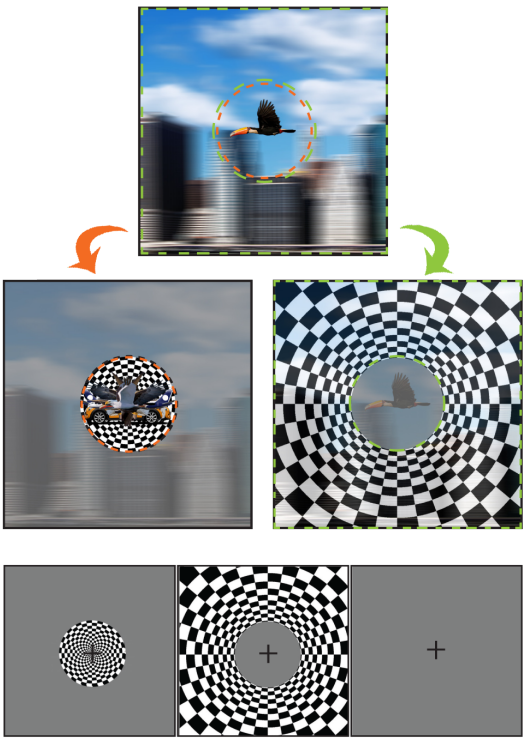

Figure 4: First two rows illustrate how the foveal and peripheral areas were identified by overlapping the foreground objects and circularly separating the area from the rest of the image. The bottom row shows the stimuli that were used in the localizer. Foveal, peripheral and baseline conditions, respectively.

3.3.4 Structural Imaging

At the end of the first fMRI session the subjects went through a structural imaging scan (T1). Having their anatomical brain scan was necessary for the analysis of their functional data. This scan lasted approximately 10 minutes.

3.3.5 Fixation Tasks

During all trials of all experiments, subjects performed a central task that ensured central fixation and balanced attentional load across conditions. During the **motion localizer** runs, subjects were asked to indicate character repeats during a continuous serial display of randomly assembled alphabetical characters (n = 26) by pressing a key on a button box. The character repeat occurred between every 5 to 10 character presentations. During the **retinotopic mapping** and **early visual cortex localizer** runs participants were instructed to maintain fixation to the fixation cross and press a key when a red circle appeared on the screen. The event (red circle appearing) lasted 0.2 s and its frequency was determined probabilistically (for each TR there was a 15% probability of event occurring). During the main experiment with **implied motion** stimuli, the fixation cross remained visible throughout the runs, and the participants were instructed to maintain fixation while attending to the entire stimulus. They performed a 1-back task to maintain attention on the images and pressed a key when the same image (matching both fore- and background) was presented the second time in a row, which occurred randomly once per block. During the presentation of **real motion** stimuli, the task was to press a key when the velocity of the motion increased. The velocity change occurred after most of the trials (i.e. textures were presented with pseudorandomized velocities from eight different velocities). Increase of velocity occurred at least once in a block.

3.4 Experimental Stimuli

For our experimental questions, it was crucial to have stimuli that 1) induced broad directional motion perception, 2) induced strong implied motion perception. For this purpose, I created the visual stimuli for both real and implied motion while considering image statistics to be matching across experimental conditions.

The stimuli were implemented in MATLAB 2015a (MathWorks, Natick, MA) using the Psychophysics Toolbox 3 extensions and were presented trough a linearized projector with a resolution of 1280x1024 at 60 Hz. Participants viewed the projected stimuli while they laid in the scanner from the mirror that was mounted on the head-coil.

3.4.1 Left and Right Real Motion

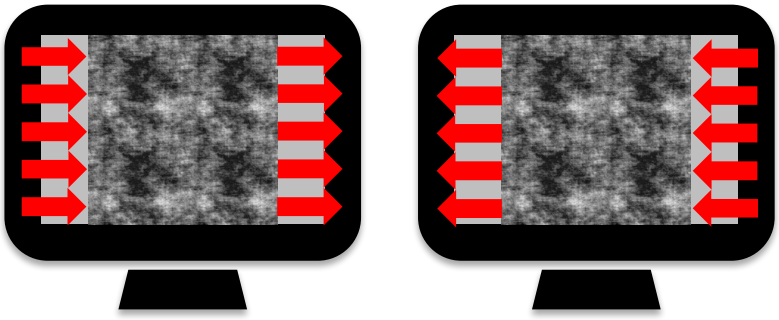

Figure 5: Illustrations of the Right and the Left real motion stimuli. Left: Rightward moving rectangular texture. Right: Leftward moving rectangular texture.

The real motion stimuli for left and right conditions were rectangular grey-scaled textures that moved horizontally in alternating speeds, as illustrated in Figure 5. In total of 30 different phase scrambled images of natural scenes were created with application of Fourier transformation. In this way, the statistics of the natural images were maintained (Simoncelli and Olshausen, 2001) and more naturalistic stimulation (in contrast to random dot stimuli) was achieved. In each block 8 textures were presented in a randomized order, each texture was presented for 1.5 s and the speed changes occurred at the time of texture change (850x850 pixels; 14 x 14 visual degrees). In total there were 8 different velocities (4, 8, 12, 16, 20, 24, 28, 32 sec/degree) for each direction and the alternation occurred in pseudorandom order. After each 12 s long block there was a block interval that lasted for 5 s. During the block interval normally distributed dynamic white noise was presented. Importantly, the direction of motion did not change within a block. In total, each condition was presented 4 times in a run and there were in total of 8 runs.

3.4.2 Forward and Backward Real Motion

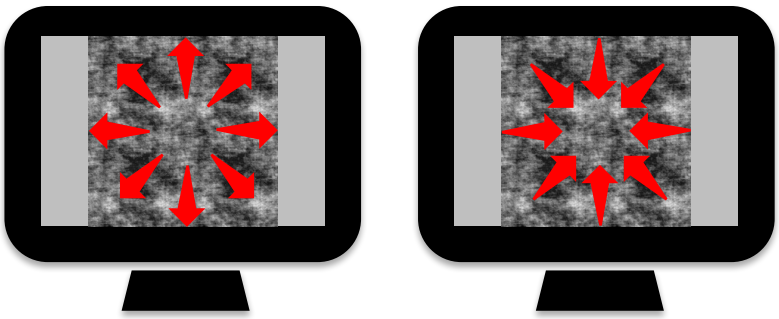

Figure 6: Illustrations of the Forward and Backward real motion stimuli. Left: Forward moving rectangular texture; Right: Backward moving rectangular texture.

The real motion stimuli for forward and backward conditions were the same gray scaled textures that were used for left and right real motion conditions, as illustrated in Figure 6. In the forward condition the stimuli appeared to expand (i.e. zoom in effect), while in the backward condition the stimuli appeared to contract (i.e. zoom out effect). However, the size of the presented textures actually did not change. To achieve this, I adapted the blending technique that was implemented in ShepardZoomDemo in Psychtoolbox (Berger, 2003). In short, the Shepard zoom blending technique overlays several textures while continuously varying their spectral composition as well as their transparency. This way, an impression of infinite zoom (or expansion) can be created using only few textures and little actual magnification. During a 12 s long block, the same set of textures were used and the motion direction did not change while the speed alternated every 1.5 s. The block interval lasted for 5 s and during it normally distributed dynamic white noise was shown. The stimulation was repeated within 8 runs and within each run for each condition there were 4 repetitions.

3.4.3 Right and Left Implied Motion

The experimental stimuli were implied motion stimuli and consisted of Right and Left conditions of 64 images in square format (850x850 pixels; 14 x 14 visual degrees) and were manually created with Adobe Photoshop CS5. Each image consisted of a background image (i.e. landscape) that had been modified by applying a horizontal motion blur filter, and an ecologically sensible foreground object placed at the centre (see Figure 7 for examples). In this way, the images appeared as if they had been taken while moving the camera at the same speed as the foreground object (panning technique), mimicking a snapshot taken during *smooth pursuit* of the foreground object. Importantly, the background alone did not contain any directional information (merely the right-left axial information due to axial smoothing). There were 16 images of unique foreground objects (real images of birds, airplanes or cars captured from a side view), centrally overlaid on 16 unique background images (landscapes or cityscapes). Another set of 16 images were created using the same foreground objects yet with right-left flipped background images in order to balance out potential differences in the horizontal plane. The remaining 32 images were right-left flipped duplicates of the above-mentioned 32 images. In this way, we had two sets of directional implied motion stimuli: rightward and leftward implied motion that differed only in the facing-direction of the foreground objects.

Figure 7: Examples of the experimental stimuli for Right (left column) and Left (right column) implied motion conditions.

3.4.4 Forward and Backward Implied Motion

Forward and Backward conditions were analogue to the Right and Left conditions, with the following differences. A different set of ecologically sensible background images were used, and they were not blurred in order to simulate fixation on approaching / receding foreground objects. Foreground images were correspondingly blurred by application of a radial (zoom) blur filter. Foreground objects were images of cyclists on bikes, motorcyclists on motorbikes, cars and running humans captured from front- and back-view (see Figure 8 for examples). The same background images were used for both Forward and Backward implied motion stimuli in order to match background images across conditions. However, some of the foreground objects did not have both front- and back-view configurations of the identical object available, such that e.g. motorcyclists, bikers and humans might differ across forward and backward conditions. A total of 32 unique forward, 32 backward images were used.

Figure 8: Examples of the experimental stimuli for Forward (left column) and Backward (right column) implied motion conditions.

3.5 Image Acquisition

Imaging data were acquired with a 3 Tesla MRI scanner with a 64-channel head coil (Magnetom Prisma, Siemens, Erlangen, Germany). For the main experiment **T2* weighted** functional images were recorded using a multi-band EPI sequence with a multi-band factor of 2. The sequence had a **TR** of 1.2 s, **TE** of 30 ms and a **flip angle** of 68°. Each brain volume consisted of 36 **slices** with a **voxel size** of 3 x 3 x 3 mm^3. Functional runs had 260, 297, 477 and 517 **volumes** for the main experimental runs, early visual eccentricity localizer, retinotopic mapping and motion localizer runs, respectively. The first 8 volumes of each run were discarded to allow for T1 equilibrium effects. **T1-weighted** high-resolution structural images were obtained with a resolution of 1 x 1 x 1 mm^3.

3.6 fMRI Data Processing

All the fMRI data (except for retinotopy) were pre-processed with SPM12 (http://www.fil.ion.ucl.ac.uk/spm/) and MATLAB 2015a. Functional images were corrected for slice acquisition time, realigned to the first image using an affine transformation to correct for small head movements and EPI distortions; data were un-warped, co-registered to the structural data and spatially smoothed using an isotropic kernel of 3-mm full width at half-maximum (FWHM) for the main experiment data and 4-mm FWHM for the localizer data. All analyses were performed within individual subjects' space and all the time-series were high-pass filtered with a cut off of 128 s to eliminate the low-frequency drifts in the BOLD signal. In order to estimate the fMRI response patterns to directional implied motion stimuli we performed GLM analyses with SPM12. The voxel time series of each run were modelled differently for each condition with 4 selectively expanded GLMs and later combined into one expanded GLM that had one beta estimate for each stimulus block of each condition (see the subsection below for details). Each stimulus block was modelled separately as a boxcar function shifted forward in time by 5 s to account for the hemodynamic lag. Additional regressors modelled were the estimated motion parameters. We z-scored the beta estimates for each voxel and replaced values above 2 with 2s and values below -2 with -2s to handle outliers as recommended by the LIBLINEAR authors (Fan et al., 2008).

3.6.1 Comparison of Directional Real Motion Decoding with Different GLMs

In this subchapter I describe and report the effect of varying parameters for first level general linear model (GLM) analysis on decoding performance for real motion direction classification. At the beginning of my analyses I followed the conventional ways to perform first level GLM analysis. Meaning that given that within a run I had four repetitions of a direction I modelled my first GLM while creating one regressor for each direction (i.e. grouping four blocks that belonged to each direction). Plus, I used canonical HRF convolution for each block (see the first design matrix in Figure 9). The results I got for decoding with these parameters were unexpectedly high in variance. Then we had an idea to model the conditions as following: instead of performing a single first level GLM analysis, I did perform four (total number of directions) GLM analysis and each one I expanded one of the directions by means of having one regressor for each block for that one direction, and for the rest of the directions I kept using one regressor per direction. In the end, I gathered the betas of expanded directions from each GLM analysis and performed the decoding on these betas (see the second design matrix in Figure 9). In addition to this, I used boxcar convolution instead of using canonical HRF. In comparison to modelling each block as a separate regressor and performing a single GLM analysis, this way of combining betas have advantage for minimalizing the noise and the effects of other three conditions on the one that was expanded.

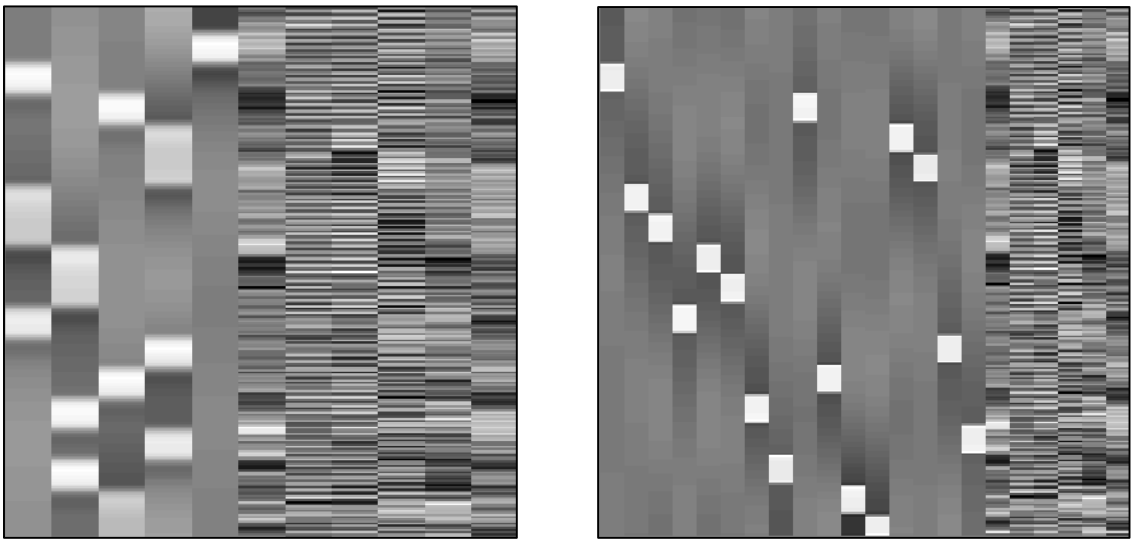

Figure 9: Design matrices obtained from SPM for first level GLM analysis. Left: the compact design matrix. Right: Selective Expanded and custom combined design matrix.

The decoding results from a set of ROIs for real motion directions on different GLM analysis are shown in Figure 10(A) for the Right versus Left condition, and in Figure 10(B) for the Forward versus Backward condition. The main difference in outcome of differently modelling the directions was the number of beta images. When all the blocks for each condition was combined in one regressor I had only eight beta images per direction (i.e. number of runs), however, when I separately modelled each block to then I had 32 beta images per condition. There is a known trade-off associated with number of examples (i.e. number of beta images) used for decoding, such that having more examples for each condition while using each trial as an example may result in having more noise compare to averaging trials and having less examples in return (Pereira et al., 2009). However, having more examples is better to train the classifier in general. Since we expected more robust decoding of real motion directions compare to the implied ones, we decided to compare the results of real motion decoding with different number of examples to decide which way is better for our dataset.

Statistical comparison of the mean accuracy results on ROI level showed significant difference between expanded and compact way of modelling for the Forward versus Backward condition, favouring the expanded version to have higher accuracies, but not for the Right versus Left condition (Right versus Left: $t(15) = 1.35$, $p = 0.10$, one-sided t-test; Forward versus Backward: $t(15) = 2.39$, $p = 0.01$, one-sided t-test). Comparison of the variances with two-sample F-test showed that for the Right versus Left condition 75% of the ROIs had higher variance in compact version than in expanded version. For the Forward versus Backward condition the variances for all ROIs were higher in the compact version. Therefore, we decided to continue the analyses on the expanded version, with more examples per condition.

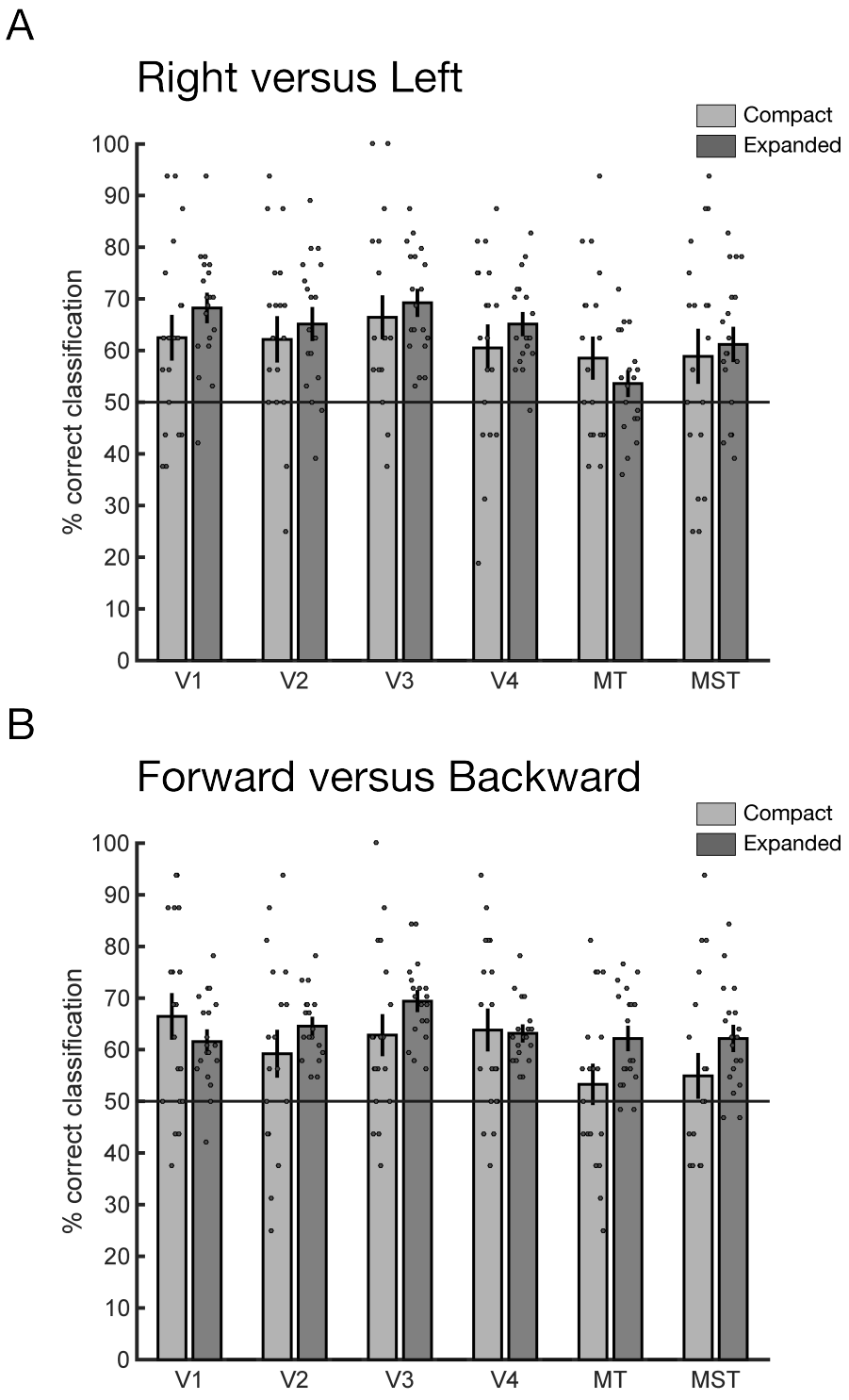

Figure 10: Decoding performances of the classifier for (A) Right versus Left and (B) Forward versus Backward real motion in V1-V4, MT and MST. Dark gray bars show the results obtained from Selectively Expanded design matrix, light gray bars show the results obtained from compact design matrix. Error bars show the group average (n =19) with the SEM and the scattered dots over each bar show the individual results. The horizontal line highlights the chance level (50%) of decoding.

3.6.2 Multivoxel Pattern Analysis (MVPA) & Statistical inference

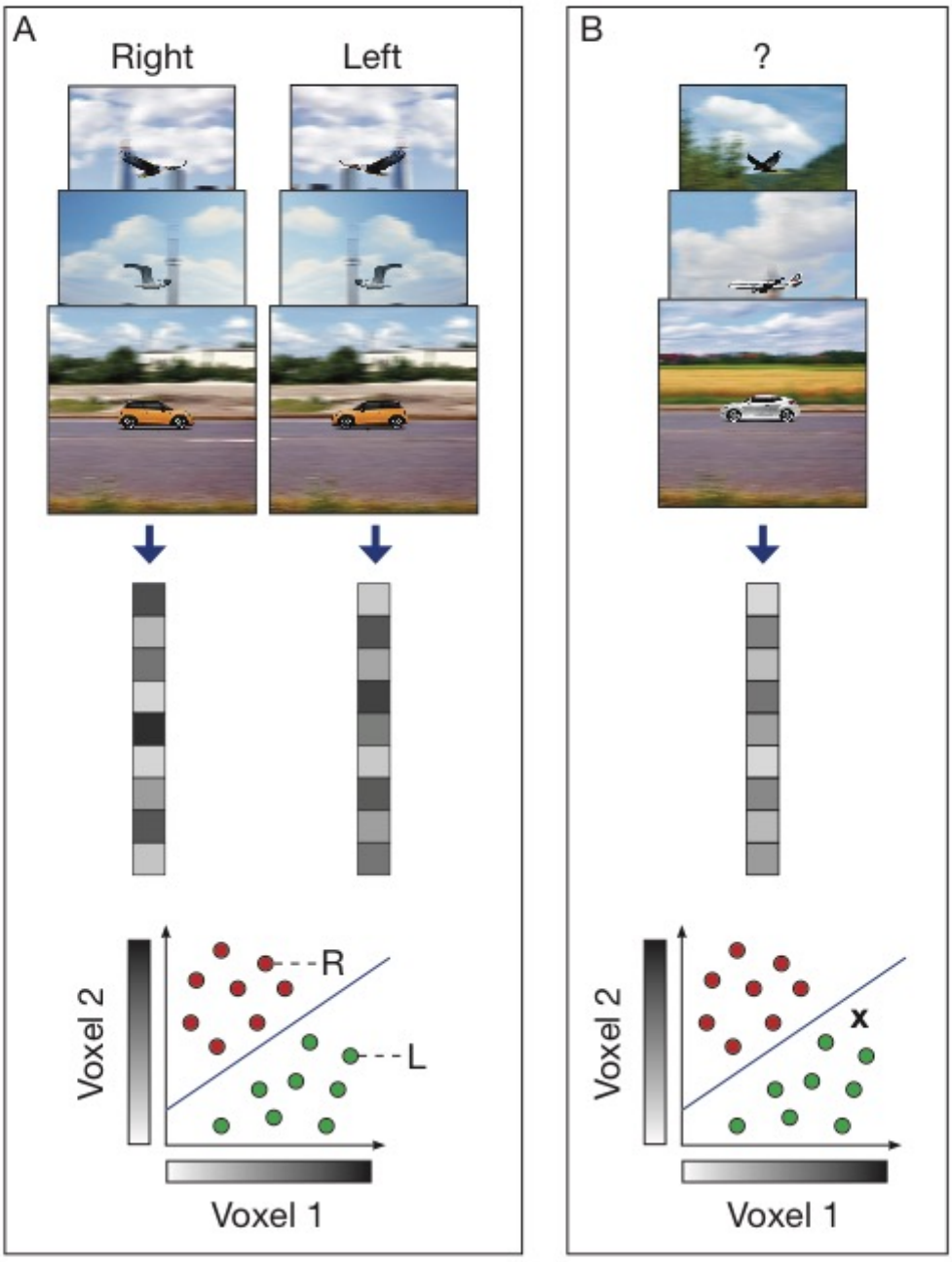

Figure 11: Illustration of MVPA for implied motion direction classification. (A) The visual stimuli were presented to the participants while measuring their brain activities. From each region of interest of each participant the pattern vectors were extracted to train the linear classifier. The classifier was then trained on activity patterns in response to right and left implied motion directions to differentiate right from left (and vice versa) on the patterns of activation in each ROI. (B) After training the classifier was given unlabeled data (indicated by 'X') which was not used during the training and did predict the label of the given data based on what it learnt from the training set (indicated by colored dots). In the end, accuracy values were obtained that were comparison of the predicted labels to true labels of the test data.

MVPA training and testing procedures. MVPA was performed on beta-images of the main experiment using a linear classifier (LIBLINEAR software) that was implemented in The Decoding Toolbox (Hebart et al., 2014). The beta images were labelled according to the motion type (i.e. real or implied) and the corresponding motion direction (i.e. leftward, rightward, forward, backward). For experiment I and II cross-validation analyses were performed (see Figure 11 for illustration) to test whether a linear classifier could discriminate between voxel-activity patterns within each ROI evoked by stimuli containing 1) rightward- vs. leftward- real motion, 2) forward- vs. backward- real motion, 3) rightward- vs. leftward- implied motion 4) forward- vs. backward- implied motion. I used a 8-fold leave-one-run-out strategy in which the classifier was trained on voxel-activity patterns from 7 runs and tested on the remaining run, while the test run was changing during each fold. This was performed separately for each ROI of each subject. For experiment III, a cross-classification analysis was performed to test whether a linear classifier that was trained on directional real motion data could discriminate between voxel-activity patterns evoked by stimuli containing directional implied motion data. This test was to assess generalization of motion direction information in each ROI. For testing right and left motion directions the classifier was trained on right and left real motion data and the right and left implied motion data was used to test the performance of the classifier. The same was done for forward and backward conditions. At the end I acquired one classification accuracy value for each ROI decoding per subject. I continued the analysis on group level, meaning that for each ROI I looked at the group average decoding accuracy. As we had only two directions per condition the chance level was 50%.

Statistical inference. For statistical inference I performed non-parametric permutation tests while calculating classification accuracy for randomly shuffled labels 1000 times for every ROI of each subject, separately for each analysis. I took great care that the same label permutations were applied in the same analysis for each subject. In this way I acquired a distribution of mean classification accuracies at the group level that would be expected if no relationship existed between the multivariate data and the class labels by averaging permuted classification accuracies across subjects for each ROI. The p values were calculated by dividing the total number of mean accuracy values for each ROI that is equal or bigger than the group level mean accuracy with total number of permutations (i.e. 1000).

Correction for multiple comparisons. In order to correct for multiple comparisons errors due to the number of ROIs tested, I applied the family-wise error (FWE) correction the following way (Nichols and Holmes, 2002; Fan et al., 2008; Bannert and Bartels, 2017): after calculating the group mean ROI classification values from randomized label assignments, only the maximum group mean value across all ROIs in the same ROI group (i.e. for MST the null

distribution was calculated as the highest values across all seven ROIs that were in the motion areas group) was used for the null distribution. This allowed to control the error probability of at least one null hypothesis being falsely rejected.

3.6.3 Univariate Analysis & Statistical inference

The analysis for the fourth experiment was a straight-forward univariate analysis. During the first level SPM analysis the conditions were modelled to have one regressor for each run. For each ROI the average beta values from each run per participant was calculated and then averaged again across total number of runs, this was done separately for each condition. In the end, for each condition one value per participant was obtained for each ROI. The outliers were defined as data points that are more than 1.5 interquartile ranges above the upper quartile (75 percent) and below the lower quartile (25 percent). These data points were removed with 'rmoutliers' function of Matlab. This resulted in removal of five subjects from the further analysis for the Right versus Left and the Forward versus Backward mean BOLD difference. For the analysis of difference in response to motion in different axes (i.e. Forward and Backward directions combined as one axis and compared to the combination of Right and Left directions) in total of two subjects were removed with 'rmoutliers' function with 'mean' method. For statistical inference, the difference between the conditions were calculated for each ROI and tested with paired t-test against zero. In order to correct for multiple comparisons errors due to the number of ROIs tested, Finally, I applied Bonferroni-Holm correction (Holm, 1979) to the p values of all ROIs to account for multiple comparisons (twenty-seven comparisons).

3.7 Eye Tracking Recording & Analysis

To examine whether our fMRI results can be explained by the differences in fixation accuracy across conditions we recorded monocular eye positions of 10 of the participants during the Experiment I and of 9 of the participants during the Experiment II. The eye tracking was done at a sampling rate of 60 Hz using an infrared camera based eye-tracker with long range optics (ASL EyeTrac 6 Eye Tracking System, Applied Science Laboratories, recorded using ViewPoint Eyetracking Software; Arrington Research, Scottsdale, USA). As raw data vertical and horizontal eye positions of the participants with the label of the condition that was viewed was collected. The pre-processing of the raw eye-tracking data included high-pass filtering, temporal smoothing with a 200 ms running average window, detection of blinks and linear interpolation. The values were transformed from eye-tracker unit to visual degrees. The distances between the gaze position and the centre of fixation were calculated. All values were sorted according to the conditions that they were collected from and tested for differences using one-way repeated measurements ANOVA with factors of experimental conditions (i.e. right, left, forward, backward). All of the data that were collected during the implied motion runs were included in the analysis. However, because of some technical problems while data recoding during the Experiment I analysing all the data was not possible (three participants had data from only seven runs, one participants had data from only three runs).

3.8 Definition of Regions of Interest (ROIs)

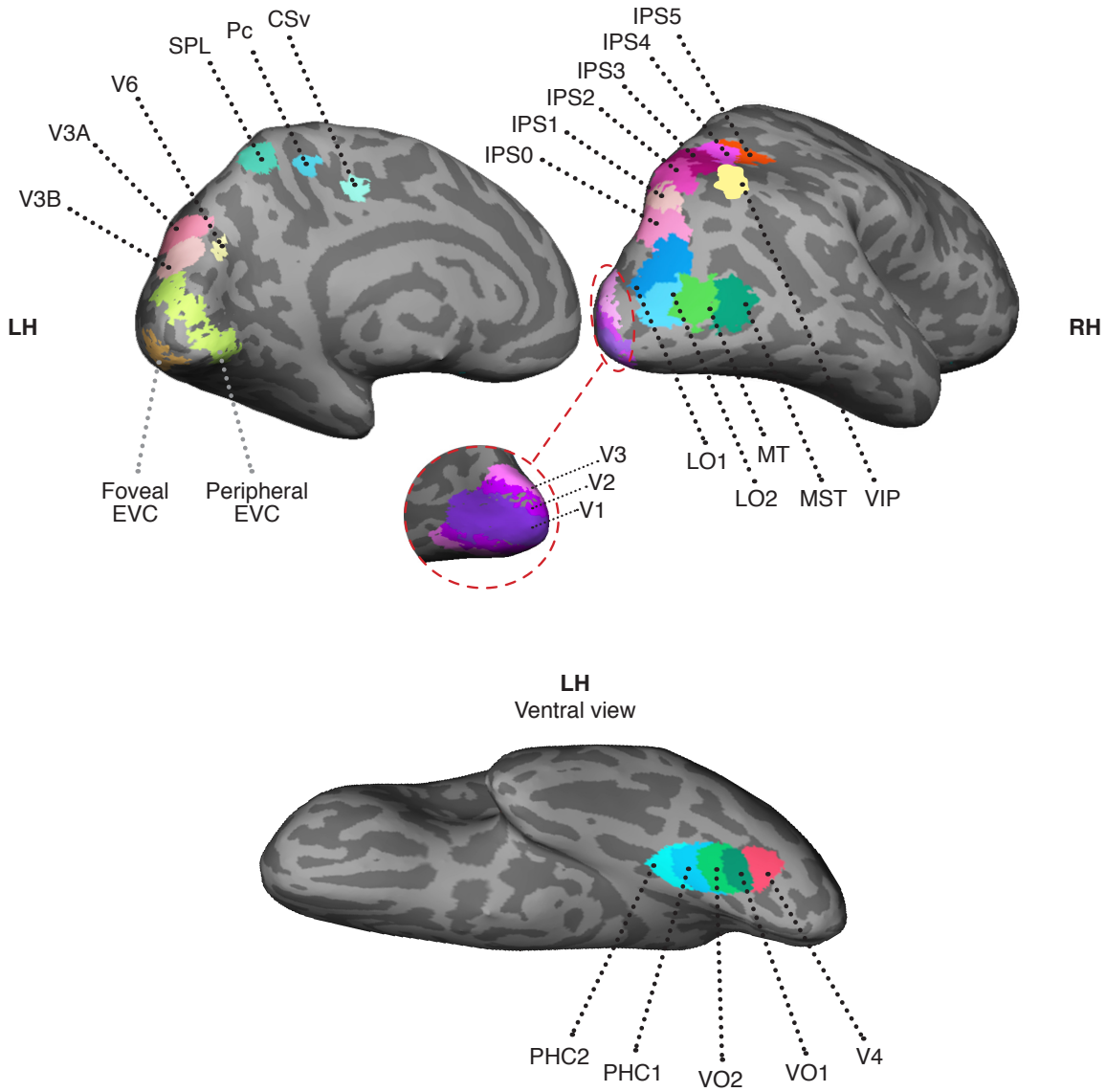

Figure 12: Illustration of all the regions of interest (ROIs) on an inflated brain of a single subject. LH: Left hemisphere, RH: right hemisphere.

For each subject the regions of interests were identified on native subject space, rather than on a normalized space. Except for three motion areas (Pc, CSv, VIP) that were not identified in all of the subjects, all the other areas were defined for all the subjects. The locations of the ROIs for a single subject are shown in Figure 12.

3.8.1 Early Visual Cortex Areas

For the subjects which I had acquired their polar retinotopy data (n = 11) I used FreeSurfer to localize their V1, V2, V3. For the subjects lacking retinotopic data (n = 8) I used anatomical retinotopic surface templates for FreeSurfer from the Aguirre Lab (Benson et al., 2012).

3.8.2 Foveal and Peripheral EVC

The data I collected with the Early Visual Cortex Eccentricity localizer allowed me to separately define the visual field maps for foveal and peripheral parts of the early visual cortex for each subject. After defining V1, V2 and V3 for all subjects I combined these ROIs and created individual EVC masks. To define the foveal ROIs, I took the voxels that were within the EVC masks and active in the central condition of the localizer in contrast to the peripheral and the baseline conditions. To define the peripheral ROIs, I took the voxels that were within the EVC masks and active in the peripheral condition of the localizer, in contrast to the central and the baseline conditions. Eventually, I had the foveal and peripheral representations of the EVC for each subject that correspond to the cortical areas that received direct visual stimulation from the foreground object including and background including parts of the implied motion stimuli.

3.8.3 Ventral-temporal Areas

When defining ROIs using surface-based mapping is better than volume-based mapping (Oosterhof et al., 2011). The definition of V4, VO1, VO2, PHC1 and PHC2 were done with FreeSurfer while using the probabilistic maps of visual topographic areas by Wang and colleagues (Wang et al., 2015). For all these areas thresholding at 20% was applied to exclude the voxels with equal and lower probabilities.

3.8.4 Dorso-lateral Areas

The definition of V3B, LO1 and LO2 were done with FreeSurfer while using the probabilistic maps of visual topographic areas by Wang and colleagues (Wang et al., 2015). For V3B thresholding at 30% was applied to exclude the voxels with equal and lower probabilities, for LO1 and LO2 no thresholding was applied.

3.8.5 Motion Areas

The motion area V6 was defined using Flow and Random motion conditions of the motion localizer. The other motion responsive areas CSv, Pc and VIP were defined while contrasting Flow, 2D Planar Motion and 2D No Planar motion conditions with Random and Static motion conditions of the motion localizer. In addition to these functionally defined motion areas, area MST, V5/MT and V3A were defined while using the probabilistic maps of visual topographic areas (thresholding at 30% was applied to exclude the voxels with equal and lower probability) by Wang and colleagues (Wang et al., 2015).

3.8.6 Parietal Cortex Areas

The definition of IPS0, IPS1, IPS2, IPS3, IPS4, IPS5 and SPL1 were done with the FreeSurfer while using the probabilistic maps of visual topographic areas by Wang and colleagues (Wang et al., 2015). For IPS0 and IPS1 thresholding at 30% was applied, for IPS2, IPS3, IPS4, IPS5 and SPL1 thresholding at 20% was applied to exclude the voxels with equal and lower probabilities.

3.8.7 Sizes of the ROIs

Table 1 shows the sizes of ROIs that were investigated within this thesis. Except for the 'n' column which corresponds to the total number of subjects that the corresponding ROIs were identified, all the other column values correspond to number of voxels.

ROI names	n	mean	std	max	min
Foveal	19	162	72	293	57
Peripheral	19	518	146	867	270
V1	19	964	363	1666	535
V2	19	1067	266	1420	657
V3	19	1114	351	1641	642
V4	19	247	35	317	198
VO1	19	98	20	127	63
VO2	19	186	29	230	138
PHC1	19	187	27	230	138
PHC2	19	170	24	210	135
LO1	19	175	22	215	137
LO2	19	199	29	245	148
V3B	19	280	33	340	216
V3A	19	51	42	124	4
MST	19	205	25	247	154
MT	19	136	21	167	84
V6	19	93	42	169	12
CSv	14	25	17	69	4
Pc	17	61	29	114	16
VIP	15	74	40	163	23
SPL	19	304	41	396	249
IPS0	19	375	47	467	305
IPS1	19	257	41	359	185
IPS2	19	308	33	385	253
IPS3	19	280	32	345	220
IPS4	19	210	29	271	158
IPS5	19	202	40	266	128

Table 1: The final ROI sizes. Note that some ROIs were not possible to be defined for every subject, as noted within the n column. Mean, standard deviation and, max and min values correspond to number of voxels.

4 CHAPTER I: Decoding of real motion directions

4.1 Summary

Which early visual and other retinotopic areas do encode selective motion direction information? Is there a preference for encoding lateral motion information over motion in depth information in motion areas? Previous studies have shown that decoding motion direction from fMRI BOLD pattern activity is possible in early visual areas and from V5/MT+. However, these studies either used moving dots as visual stimuli or only used rotational motion. Moreover, they only looked at a few regions in visual cortex. Here I provide results for more extensive real visual motion direction classification. In this experiment, I tested the decoding performance across early visual areas, ventral-temporal areas, dorso-lateral areas, visual motion areas and parietal areas for Right versus Left (R vs. L) directional real motion and Forward versus Backward (F vs. B) directional real motion. In total I looked at 27 brain areas for their encoding of motion directions and tested their directional motion decoding performances with nonparametric permutation tests. All p values reported in the results were family-wise error (FWE) corrected according to the groups that the ROIs belonged. The results show that classification of F vs. B real motion directions from BOLD activity patterns was possible in all early visual areas (V1-V3, Foveal, Peripheral), ventral areas (V4, VO1, VO2, PHC1), higher visual areas (V3B, LO1, LO2), motion areas (MST, MT, V3A, V6, Pc, VIP) and parietal areas (IPS0-IPS4, SPL1). The classification of R vs. L real motion directions was also possible in all the aforementioned areas except for VO2, PHC1, MST, Pc and VIP. Second, I examined whether any of the above regions differed in terms of decoding success between the right-left and forward-backward axes. I found that the primary visual area (V1) and the peripheral representation of early visual cortex (Peripheral EVC) have a preference for encoding right and left motion directions, whereas motion area MST has a preference for encoding forward and backward motion directions. These results show that real motion processing is a very distributed process across the cortex and not limited to the dorsal areas. Moreover, while these results add to the evidence that decoding motion directions with MVPA is possible, they also extend our knowledge in that decoding does not depend using moving dots as stimuli nor on rotational motion, and in demonstrating preferences for motion axes in distinct cortical regions.

4.2 Results

The results of the decoding of real motion directions revealed that it is indeed possible to decode both **Right versus Left (R vs. L)** and **Forward versus Backward (F vs. B)** motion directions from fMRI BOLD activity patterns. That means the response patterns in most of our ROIs coded for the direction of the real motion stimuli. For some areas decoding in one condition worked significantly better than the other. Statistical inference was performed on 1000 permuted direction labels for each condition per ROI, and the corrected p values were acquired via applying FWE correction for multiple comparisons (described with more details in the Methods section). Below I will present the results in detail while considering the ROI groupings.

For the R vs. L real motion condition the best decoding performance was obtained from the Peripheral early visual cortex (EVC) and the result was highly significant even after correction for multiple comparisons (71%, p = 0.001, corrected). The Foveal EVC also had response patterns that coded for the direction of real motion stimuli (59%, p = 0.001, corrected) (Figure 13). For the F vs. B real motion condition the decoding performance was comparable in Foveal (60%, p = 0.001, corrected) and Peripheral (64%, p = 0.001, corrected) parts of the early visual cortex (Figure 13). Comparison of the decoding performances between the R vs. L and F vs. B real motion conditions revealed a significant difference in Peripheral EVC (t (18) = 3.54, p = 0.002, two-sided t-test).

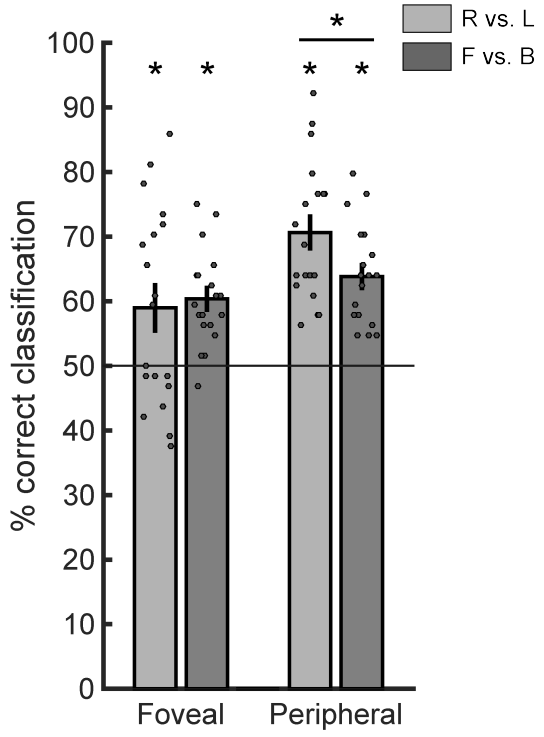

Figure 13: Decoding performance for directional real motion in Foveal and Peripheral parts of the early visual cortex (EVC). Error bars show the group average (n = 19) with the SEM and the scattered dots over each bar show the individual results. The horizontal line highlights the chance level (50%) of decoding. Asterisks are presented over the ROIs that have significant corrected p values. Asterisk over the line corresponds to the significant difference between the conditions for the relevant ROI.

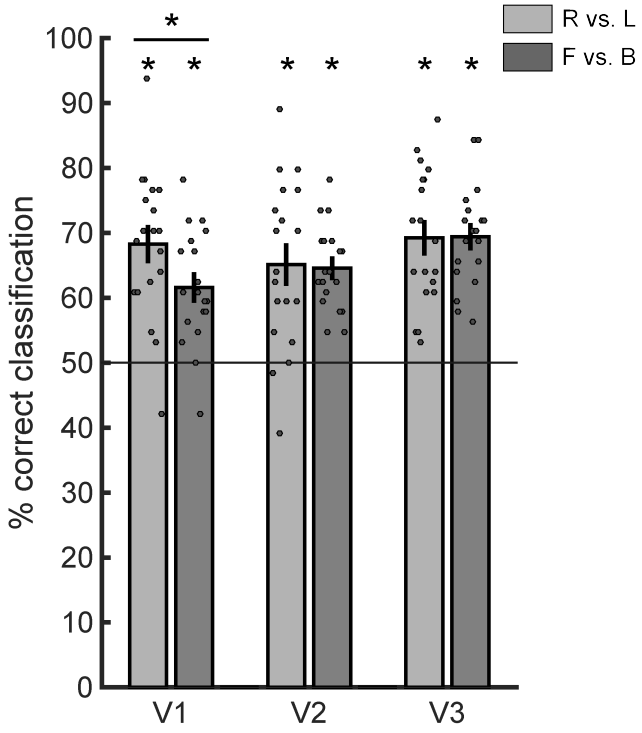

Figure 14: Decoding performance for directional real motion in the early visual cortex (V1-V3). Error bars show the group average (n = 19) with the SEM and the scattered dots over each bar show the individual results. The horizontal line highlights the chance level (50%) of decoding. Asterisks are presented over the ROIs that have significant corrected p values. Asterisk over the line corresponds to the significant difference between the conditions for the relevant ROI.

Separate examination of EVC areas revealed that for the R vs. L real motion condition the decoding of the motion directions was possible at different rates for each area: V1 (accuracy = 68%, p = 0.001, corrected), V2 (accuracy = 65%, p = 0.001, corrected), V3 (accuracy = 69%, p = 0.001, corrected) (Figure 14). For the F vs. B real motion condition the decoding results showed linear increase from V1 to V3: V1 (accuracy = 62%, p = 0.001, corrected), V2 (accuracy = 65%, p = 0.001, corrected), V3 (accuracy = 69%, p = 0.001, corrected) (Figure 14). Comparison of the decoding performances between the R vs. L and F vs. B real motion conditions revealed a significant difference in V1 (t (18) = 2.83, p = 0.01, two-sided t-test).

In the ventral-temporal ROIs group the decoding performance was significant and highest in visual area V4 compare to the other areas for both the R vs. L (accuracy = 65%, p = 0.001, corrected) and the F vs. B (accuracy = 63%, p = 0.001, corrected) real motion conditions (Figure 15). Among the rest of the areas in this group only ventral visual area VO1 (accuracy = 56%, p = 0.003, corrected) had significant decoding performance for the R vs. L real motion condition, while decoding from the ventral visual area VO2, and parahippocampal areas PHC1 and PHC2 were at the chance level (see Table 2 for the values). For the F vs. B real motion condition the ventral visual areas VO1 (accuracy = 57%, p = 0.001, corrected) and VO2 (accuracy = 56%, p = 0.003, corrected) and parahippocampal area PHC1 (accuracy = 56%, p = 0.001, corrected) had response activity patterns that allowed decoding significantly over chance, however the parahippocampal area PHC2 did not (see Table 2 for the values) (Figure 15).

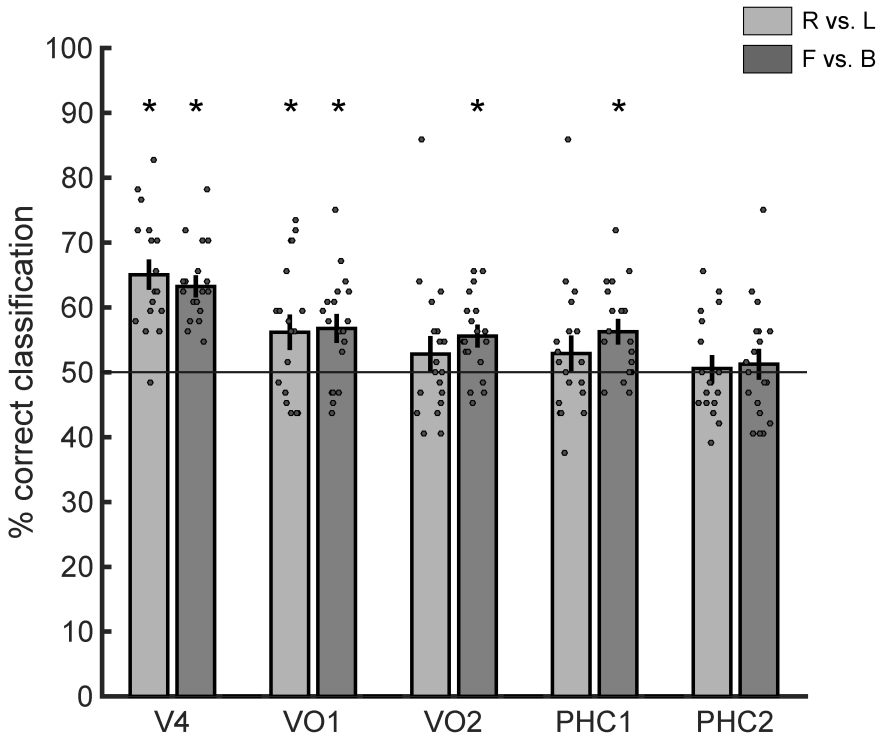

Figure 15: Decoding performance for directional real motion in the ventral – temporal cortex (V4, VO1, VO2, PHC1, PHC2). Error bars show the group average (n = 19) with the SEM and the scattered dots over each bar show the individual results. The horizontal line highlights the chance level (50%) of decoding. Asterisks are presented over the ROIs that have significant corrected p values.

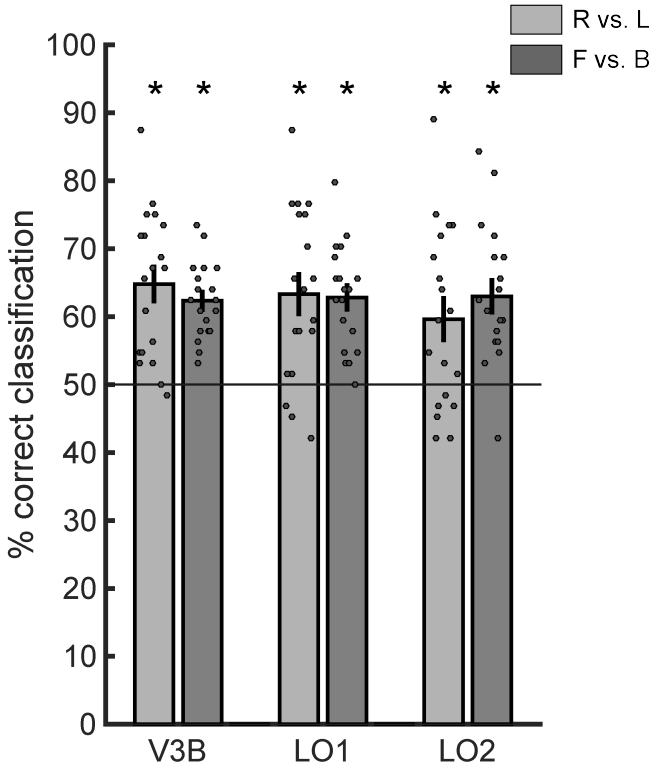

Figure 16: Decoding performance for directional real motion in the dorso-lateral visual areas (V3B, LO1, LO2). Error bars show the group average (n = 19) with the SEM and the scattered dots over each bar show the individual results. The horizontal line highlights the chance level (50%) of decoding. Asterisks are presented over the ROIs that have significant corrected p values.

In the dorso-lateral ROIs group decoding performances for both R vs. L and F vs. B real motion conditions in all ROIs (visual area V3B, lateral visual areas LO1 and LO2) were significantly above chance. The results for the R vs. L condition were: V3B (accuracy = 64%, p = 0.001, corrected), LO1 (accuracy = 63%, p = 0.001, corrected), LO2 (accuracy = 60%, p = 0.001, corrected) (Figure 16). For the F vs. B condition the results were: V3B (accuracy = 62%, p = 0.001, corrected), LO1 (accuracy = 63%, p = 0.001, corrected), LO2 (accuracy = 63%, p = 0.001, corrected) (Figure 16).

Among the motion responsive areas, for the R vs. L condition, V5/MT (accuracy = 61%, p = 0.001, corrected), V3A (accuracy = 57%, p = 0.005, corrected), and V6 (accuracy = 58%, p = 0.001, corrected) contained response patterns that coded for the real motion directions significantly better than chance (Figure 17). Whereas decoding in MST (accuracy = 54%, uncorrected p = 0.02, corrected p = 0.19) and CSv (accuracy = 53%, uncorrected p = 0.047, corrected p = 0.33) was significant only before applying multiple comparisons correction. For

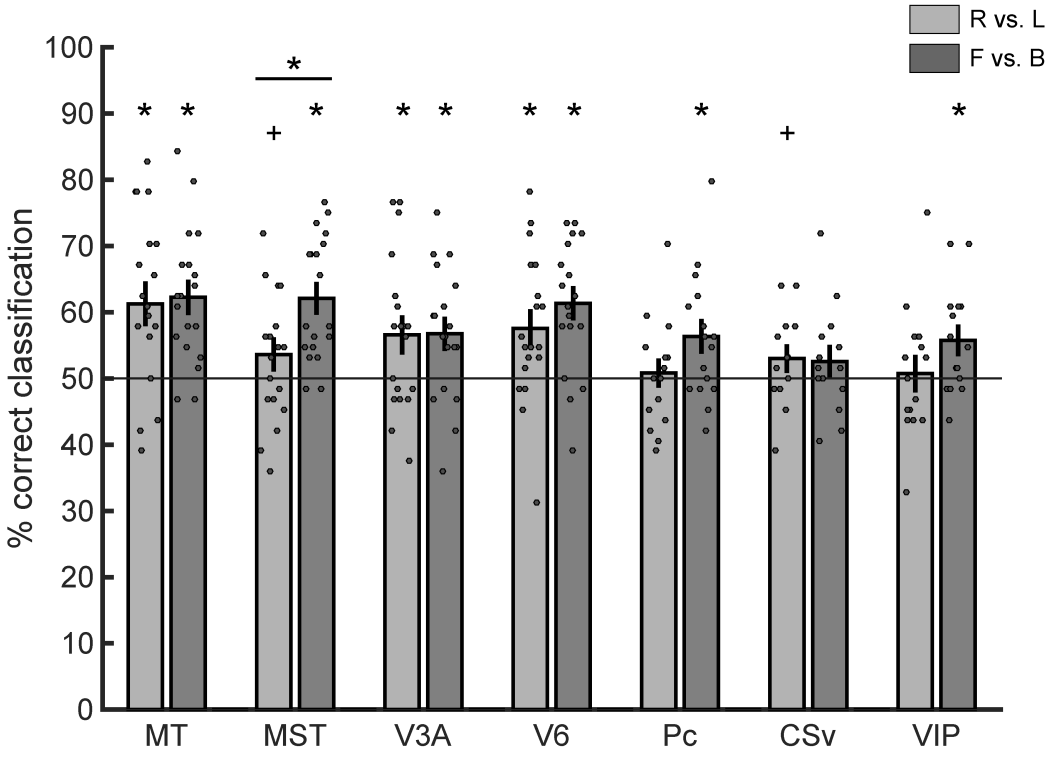

Figure 17: Decoding performance for directional real motion in the visual motion areas MT, MST, V3A, V3B, V6, Pc, CSv and VIP. Error bars show the group average (n = 19 for the first 4 of them, n =14 for CSv, n = 17 for Pc and n = 15 for VIP) with the SEM and the scattered dots over each bar show the individual results. The horizontal line highlights the chance level (50%) of decoding. Asterisks are presented over the ROIs that have significant corrected p values. Plus signs (+) are presented over the ROIs that have significant uncorrected p values. Asterisk over the line corresponds to the significant difference between the conditions for the relevant ROI.

this condition the decoding was at the chance level in Pc and VIP (see Table 2 for the values). For the F vs. B condition V5/MT (accuracy = 62%, p = 0.001, corrected), MST (accuracy = 62%, p = 0.001, corrected), V3A (accuracy = 57%, p = 0.004, corrected), V6 (accuracy = 61%, p = 0.001, corrected) and VIP (accuracy = 56%, p = 0.01, corrected) showed significantly better than chance level of decoding of the motion directions. For this condition, decoding was at the chance level in CSv (see Table 2 for the values). Comparison of the decoding performances between the R vs. L and F vs. B real motion conditions revealed a significant difference in MST (t (18) = -3.28, p = 0.004, two-sided t-test) (Figure 17).

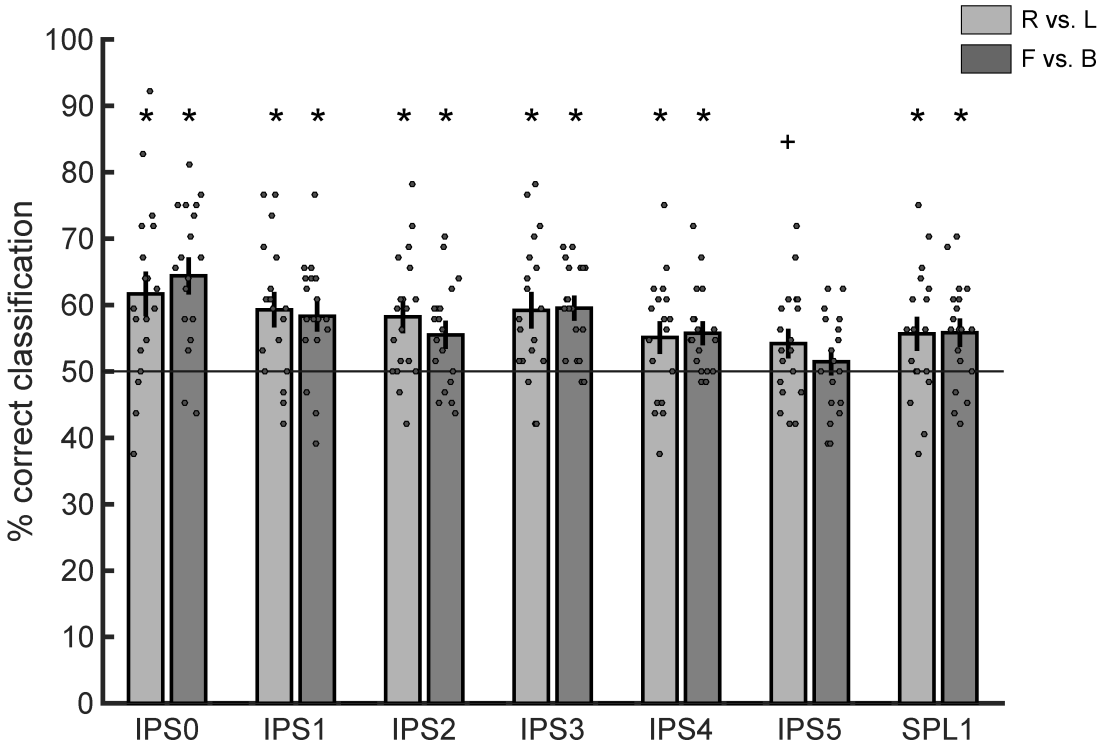

Figure 18: Decoding performance for directional real motion in the parietal cortex (IPS0 – IPS5, SPL1). Error bars show the group average (n = 19) with the SEM and the scattered dots over each bar show the individual results. The horizontal line highlights the chance level (50%) of decoding. Asterisks are presented over the ROIs that have significant corrected p values. Plus sign (+) is presented over the ROI that has significant uncorrected p value.

In the parietal cortex ROIs group, except for the intraparietal sulcus area IPS5 that allowed decoding only of R vs. L directions to some degree and not of F vs. B (see Table 2 for the values), all the other areas allowed decoding of both R vs. L and F vs. B real motion directions significantly better than chance (Figure 18). For the R vs. L condition the decoding performances were: IPS0 (accuracy = 62%, p = 0.001, corrected), IPS1 (accuracy = 59%, p = 0.001, corrected), IPS2 (accuracy = 58%, p = 0.001, corrected), IPS3 (accuracy = 59%, p = 0.001, corrected), IPS4

(accuracy = 55%, p = 0.03, corrected), SPL1 (accuracy = 56%, p = 0.009, corrected). For the F vs. B condition the decoding performances were: IPS0 (accuracy = 64%, p = 0.001, corrected), IPS1 (accuracy = 58%, p = 0.001, corrected), IPS2 (accuracy = 56%, p = 0.01, corrected), IPS3 (accuracy = 60%, p = 0.001, corrected), IPS4 (accuracy = 56%, p = 0.01, corrected), SPL1 (accuracy = 56%, p = 0.01, corrected) (Figure 18).

Real motion decoding results

ROI	Right vs. Left			Forward vs. Backward		
	accuracy	uncor. p	cor. p	accuracy	uncor. p	cor. p
Foveal	58.96	0.001	0.001	60.36	0.001	0.001
Peripheral	70.64	0.001	0.001	63.81	0.001	0.001
V1	68.25	0.001	0.001	61.59	0.001	0.001
V2	65.13	0.001	0.001	64.55	0.001	0.001
V3	69.24	0.001	0.001	69.4	0.001	0.001
V4	65.04	0.001	0.001	63.24	0.001	0.001
VO1	56.16	0.001	0.003	56.74	0.001	0.001
VO2	52.79	0.067	0.244	55.59	0.001	0.003
PHC1	52.87	0.06	0.223	56.25	0.001	0.001
PHC2	50.57	0.376	0.774	51.23	0.28	0.635
V3B	64.8	0.001	0.001	62.33	0.001	0.001
LO1	63.32	0.001	0.001	62.82	0.001	0.001
LO2	59.62	0.001	0.001	62.99	0.001	0.001
MT	61.26	0.001	0.001	62.25	0.001	0.001
MST	53.61	0.024	0.197	62.08	0.001	0.001
V3A	56.57	0.001	0.005	56.74	0.001	0.004
V6	57.56	0.001	0.001	61.34	0.001	0.001
Pc	50.82	0.336	0.878	56.34	0.001	0.008
CSv	53.01	0.047	0.33	52.56	0.091	0.459
VIP	50.72	0.386	0.903	55.72	0.008	0.016
IPS0	61.67	0.001	0.001	64.39	0.001	0.001
IPS1	59.29	0.001	0.001	58.3	0.001	0.001
IPS2	58.22	0.001	0.001	55.5	0.003	0.014
IPS3	59.21	0.001	0.001	59.53	0.001	0.001
IPS4	55.09	0.009	0.031	55.75	0.001	0.011
IPS5	54.19	0.017	0.101	51.48	0.222	0.686
SPL1	55.67	0.001	0.009	55.83	0.001	0.011

Table 2: The results of the decoding real motion directions. Accuracy values correspond to percentages. Uncor p stands for uncorrected p values and cor. p stands for family-wise error corrected p values.

4.2.1 Eye – Tracking Results

The analysis of the eye-tracking data showed a high fixation accuracy across all tested subjects (n = 10) in all conditions (mean deviation in real motion runs over all subjects: 0.7904 ± 0.4156). Between the experimental conditions there were no differences in fixation position (one-way ANOVA with four factors [experimental conditions]: $F_{3,27} = 2.14$, $p = 0.11$). Mauchly's test indicated that the assumption of sphericity had been violated ($X^2(5) = 34.68$, $p = 0.17 * 10^{-5}$). Therefore, degrees of freedom were corrected using Greenhouse-Geisser estimates of sphericity ($\varepsilon = 0.42$, corrected $F_{1.26,\ 11,40} = 2.14$, $p = 0.17$). Below there are two figures showing one subjects (Figure 19) and all subjects (Figure 20) fixation during all different experimental conditions.

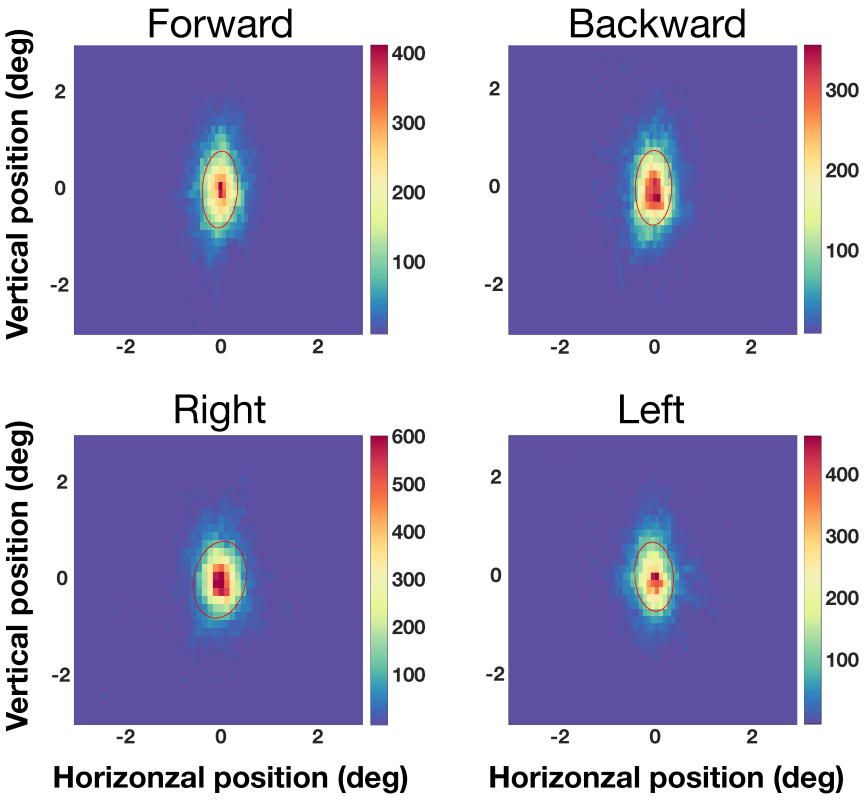

Figure 19: Histograms of the eye position (in visual degrees) of a subject for each directional real motion condition is shown to visualize fixation position. The red lines depict the 50% confidence ellipse.

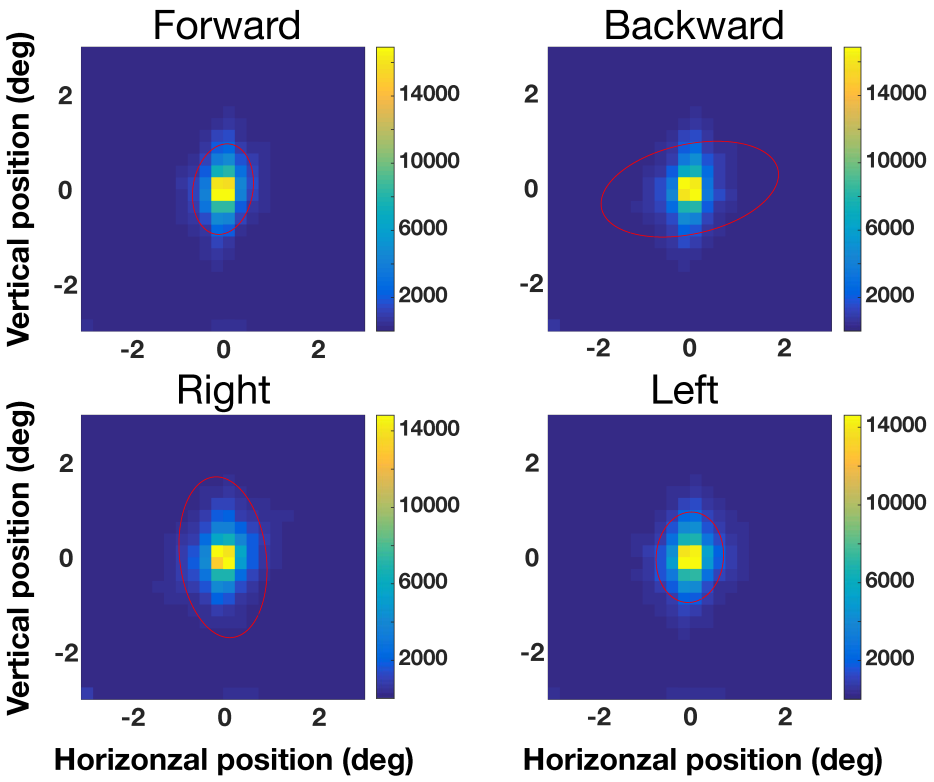

Figure 20: Histograms of the eye positions (in visual degrees) of all measured subjects (n = 10) for each real motion condition is shown to visualize fixation position. The red lines depict the 50% confidence ellipse.

4.3 Discussion

The results of the decoding of real motion directions revealed that it is indeed possible to decode both Right versus Left (R vs. L) and Forward versus Backward (F vs. B) motion directions from fMRI BOLD activity patterns. That means the response patterns in most of our ROIs coded for the direction of the real motion stimuli. For some areas decoding in one condition worked significantly better than the other. Below I will discuss the results while considering the ROI groupings.

4.3.1 Real motion direction encoding in early visual cortex

The results showed that response patterns in early visual areas V1, V2 and V3 contain motion direction information that allowed the linear machine classifier to learn and to classify both R vs. L and F vs. B real motion directions. Given that these areas are known to have high-density of direction-selective neurons these results are not surprising, although containing direction-selective neurons does not guarantee that highly significant motion direction decoding performance would be obtained from that area (see the results for V5/MT and (Bartels et al., 2008)). The decoding performance in V1 was significantly different between the R vs. L and F vs. B conditions, and was better for R vs. L directions. Such preference for a motion axis was not present in V2 or V3; these areas had very similar results for both R vs. L and F vs. B conditions. Among early visual areas the decoding performance was lowest in V1 and highest in V3 for both conditions. Previous studies (Kamitani and Tong, 2006; Seymour et al., 2009; Beckett et al., 2012; Wang et al., 2014) that reported significantly over chance decoding in these areas only used random dots as stimuli, had smaller number of subjects and did not have comparable condition to the F vs. B condition. Moving textures are categorically different than moving dot displays and the former are ecologically more relevant to the visual system. Until now it was not known if the previous findings of decoding motion direction of random dot kinetograms are comparable to natural motion direction stimulation. One important aspect of the different stimulation is related to the findings of Wang and colleagues (2014) that showed in V1, V2 and V3 (but not in higher visual areas) the decoding of direction-selective response corresponds to the shape of the stimulus aperture rather than the true direction of motion (Wang et al., 2014). In our experiment, the stimuli were Fourier-scrambled natural images (covered 14 x 14 visual degrees) that moved towards right, left, backward and forward directions in separate blocks. The textures covered 14 x 14 visual degrees and started to move after initial presentation (i.e. the stimuli did not enter or exit the visual field at the beginning and at the end of the presentation). If we consider the reported ‘aperture-inward’ response bias for the Right versus Left condition, then only the right or left edge of the screen (our stimulus aperture) would be subject to this; for

the Forward-Backward condition, however, all the edges of the screen would be subject to this bias, especially for backward motion stimulation. While this may raise a question regarding what we decoded from Peripheral EVC, V1, V2 and V3 may correspond to the reported bias, we note that our results show significantly above chance decoding also in Foveal EVC which is not directly stimulated by the visual field that covers the screen edges. One might argue that the higher decoding accuracies obtained from Peripheral EVC in comparison to Foveal EVC can be explained by the aperture-inward bias. However, this does not explain why decoding from Peripheral EVC and V1 worked better for the Right versus Left condition in comparison to the Forward versus Backward condition. Overall, while our results confirm that decoding motion directions from early visual areas is possible, they also further show that the decoding does not depend on using moving dots as stimuli or within a certain speed range. Furthermore, decoding motion directions across two different motion axes allowed us to show that Peripheral EVC and V1 have a preference for encoding R vs. L motion directions compare to F vs. B motion directions, which was not shown before.

4.3.2 Real motion direction encoding in motion areas

Our results confirm that V5/MT encodes directional real motion information (Kamitani and Tong, 2006; Seymour et al., 2009; Beckett et al., 2012; Wang et al., 2014). However, the previous studies investigated V5/MT+ as complex and did not investigate MST and V5/MT separately. I found that V5/MT does encode both real right-left and forward-backward motion directions equivalently, and in this manner shows difference to MST. The response activity patterns in MST allowed the classification of forward-backward real motion directions robustly, however for right-left real motion directions the decoding was at the chance level. As mentioned in the previously, a previous MVPA study which investigated encoding of rotational random dot motion directions reported successful decoding from V3A/V3B as a combined area (Seymour et al., 2009). In our study we looked at V3A and V3B separately and showed that area V3A encodes both right-left and forward-backward real motion directions equally well. The other visual motion areas that are relatively less investigated are precuneus (Pc), cingulate sulcus area (CSv), and ventral intraparietal area (VIP). Our results show that directional information for forward-backward real motion are encoded in Pc and VIP, but not in CSv. Moreover, decoding of right-left real motion directions from these three areas was at the chance level. Here we showed for the first time that the decoding of real motion directions is possible from human area V6. Although, the human V6 was previously shown to have preference for flow fields over drifting edges (Pitzalis et al., 2010; Pitzalis et al., 2012), we did not observe any significant difference between the F vs. B and R vs. L real motion conditions. Thus, we report that this area encodes direction information of both right-left and forward-backward motion axes.

4.3.3 Real motion direction encoding in the ventral pathway

We found that BOLD activity patterns in the ventral pathway contain information allowing for correct predictions of the real motion directions. Previously V4 was reported to have direction selective neurons (Tolias et al., 2005) and significantly above chance level of decoding in V4 for was shown before only for the directions of random dots (Kamitani and Tong, 2006; Seymour et al., 2009). Our results of decoding texture based right, left, forward and backward directional motion information from V4 confirms the directional information presence in this higher visual area. Interestingly, decoding of the real motion directions was also possible from ventral occipital areas VO1 and VO2 and parahippocampal cortex area PHC1. For VO2 and PHC1 only the decoding of F vs. B motion directions worked, while for V4 and VO1 decoding of both R vs. L and F vs. B real motion directions was possible. As these areas are part of the ventral stream investigation of motion direction encoding of these areas were overlooked. Although our experiment cannot directly assess presence of direction selective neurons in a given area, the results obtained from VO1, VO2 and PHC1 may signal the presence of directions selective units in these areas. Therefore, I encourage future studies to investigate this. Overall, our results support the view that motion processing is not exclusively done in dorsal stream and that areas that are known to be involved in object processing also take a part in motion processing.

4.3.4 Real motion direction encoding in higher visual and object-processing areas

Dorsal visual area V3B is a rather controversial area and it is sometimes noted as KO (kinetic occipital) region (Orban et al., 1995; Smith et al., 1998). Previously the area V3B (KO) was shown to process motion and shape information (Dupont et al., 1997) and kinetic boundaries (Van Oostende et al., 1997). A previous MVPA study which investigated encoding of rotational random dot motion directions reported successful decoding from V3A/V3B as a combined area (Seymour et al., 2009). Although their results hint for V3B to encode motion direction information, given that they did not look at this area separately it is possible their results are highly confounded by motion direction encoding of V3A. I found that V3B encodes both right-left and forward-backward real motion directions and its performance is better than V3As. I obtained similar results for the lateral occipital areas LO1 and LO2 that are recognized as object processing areas (Malach et al., 1995). Both of these areas are a part of the lateral occipital complex (LOC) and they lay in between V3 and V5/MT+ (Larsson and Heeger, 2006). All of these areas were previously shown to encode some form of shape representation (Erlikhman et al., 2016), rather than low-level representation of object features (Grill-Spector et al., 1999). In a MVPA study where the stimuli were randomly expanding and contracting rings presented in

different colours in separate blocks, LOC was shown to carry information about real colours that allowed linear classifiers to predict the colours of the stimuli (Bannert and Bartels, 2013), which suggests LOC is involved in other processes that do not contain objects. This is supported by the findings of a study that was able to decode the direction of auditory motion (i.e. rightwards vs. leftwards) from the LOC (Alink et al., 2012). Our results of decoding right-left visual motion directions from LO1 and LO2 are compatible with the previous results. Furthermore, we show that the decoding of forward-backward visual motion direction from LO1 and LO2 is also possible.

4.3.5 Real motion direction encoding in posterior parietal cortex

The human posterior parietal cortex (PPC) is traditionally known to be involved in spatial vision and visually guided actions (Goodale and Milner, 1992). The PPC contains topographically organized areas along the intraparietal sulcus, namely IPS1, IPS2, IPS3, IPS4, IPS5 and superior parietal lobule 1 (SPL1) (Silver et al., 2005; Konen and Kastner, 2008). The motion area V5/MT feeds information to the PPC areas and the PPC is the highest level of motion processing pathway (Andersen, 1989). Previous studies suggested that human IPS5 to be equivalent to macaque VIP (Sereno and Huang, 2006; Konen and Kastner, 2008), and macaque VIP is known to be selective for direction and speed of motion and contains high concentration of direction-selective neurons (Colby et al., 1993). An fMR adaptation study found that all of these seven PPC areas show motion-selective responses to planar, circular and radial motion of random dots (Konen and Kastner, 2008). An electrophysiological recording study investigating working memory showed that neuron populations in monkey PPC encode motion directions of random dot stimuli (Sarma et al., 2016; Masse et al., 2017). However, to our knowledge no one looked whether these human brain areas actually encode visual motion directions. Our results showed that except for the IPS5 all the other tested PPC areas robustly encode both real right-left and forward-backward motion directions. One reason for the significant decoding from these areas would be that the activity patterns in these areas reflect the eye-movements of the participants. However, as our eye-tracking results showed no significant difference for fixation position between the conditions, therefore we think that eye movements are unlikely to explain our results. It is more likely that the IPS areas and SPL1 contain high-level information about the visual motion directions that allows the classifier to learn. This would also explain why these areas have better decoding performances than the motion areas. Overall, our results demonstrate that human PPC encodes directions of real motion stimuli.

5 CHAPTER II: Decoding of implied motion directions

5.1 Summary

Can we decode implied motion directions in early visual cortex? Can we decode implied motion direction also from peripheral visual representations that do not receive bottom-up information on directionality? Do the activity patterns in motion responsive areas allow decoding of directional implied motion? Do ventral-temporal regions involved in object-processing encode directional implied motion? Do the higher visual areas in dorso-lateral and parietal areas encode direction of implied motion stimuli? In past studies, implied motion has been studied with univariate methods extensively. All the previous research points out the involvement of V5/MT+ in implied motion processing. However, activity changes in a cortical region in response to implied motion stimuli does not necessarily imply that this region encodes information about the motion direction. Therefore, it is still not known whether V5/MT+ encodes implied motion directions. The results of experiment I showed that real motion directions are encoded in early, ventral and lateral areas. Based on prior studies it is not known whether also object-processing regions or early visual regions are involved in implied motion processing. In experiment II, the aim was to identify the neural sites encoding directional implied motion in static images. For this, I showed human participants static images with rightward, leftward, forward and backward implied motion while recoding their fMRI BOLD responses. For comparison, I included all the ROIs that I tested for real motion direction encoding. All p values reported in the results were family-wise error (FWE) corrected according to the groups that the ROIs belonged. The results show that classification of both Right versus Left and Forward versus Backward implied motion directions was possible in all early visual areas. A key result was that implied motion directions were decodable also the peripheral representations of early visual cortex. However, only the foreground objects in the visual stimuli contained directional information. The peripheral representations only received bottom-up input of the background. Encoding of implied motion in peripheral representations hence means that feedback from higher-level visual representations conveyed the direction information. Among the ventral areas V4 encoded implied directions, and VO1 allowed decoding of Forward versus Backward directions. Among the lateral and object processing regions decoding was possible in LO2 and in LO1, but for the latter only for the Right versus Left directions. Among the motion regions, MST and V5/MT encoded directions, and only for the Forward versus Backward implied motion directions. Overall, the present results demonstrate that feedback conveys directional information of implied motion directions to early visual representations. In addition, the results show that both, motion regions as well as object processing regions encode implied motion directions.

5.2 Results

For the implied motion directions, the decoding results varied for **Right versus Left (R vs. L)** and **Forward versus Backward (F vs. B)** conditions and for each ROI. Yet, overall, decoding implied motion directions from fMRI BOLD activity patterns was possible. Statistical inference was performed on 1000 permuted direction labels for each condition per ROI, and the corrected p values were acquired via applying FWE correction for multiple comparisons (described with more details in the Methods section). Below I will present the results in detail while considering the ROI groupings.

Examination of decoding performances in retinotopically defined foveal and peripheral representations of the early visual cortex revealed that both Foveal (accuracy = 59%, p = 0.001, corrected) and Peripheral (accuracy = 56%, p = 0.001, corrected) representations coded for the R vs. L implied motion directions. Decoding of F vs. B implied motion directions from Foveal (accuracy = 54%, p = 0.001, corrected) and Peripheral (accuracy = 57%, p = 0.001, corrected) representations were possible, as well (Figure 21). Comparison of the decoding performances between the R vs. L and F vs. B implied motion conditions revealed a significant difference in Foveal (t (18) = 2.41, p = 0.02, two-sided t-test) representation (Figure 21).

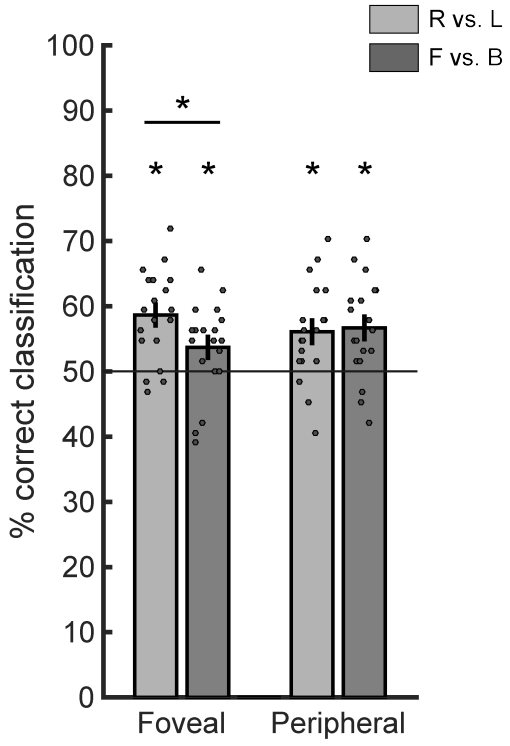

Figure 21: Decoding performance for directional implied motion in Foveal and Peripheral representations of the early visual cortex. Error bars show the group average (n = 19) with the SEM and the scattered dots over each bar show the individual results. The horizontal line highlights the chance level (50%) of decoding. Asterisks are presented over the ROIs that have significant corrected p values. Asterisk over the line corresponds to the significant difference between the conditions for the relevant ROI.

Separate examination of the early visual areas revealed that for both of the implied motion conditions all of the areas allowed significantly better than chance level of decoding. For the R vs. L implied motion condition the decoding performances were very similar in these areas: V1 (accuracy = 61%, p = 0.001, corrected), V2 (accuracy = 61%, p = 0.001, corrected), and V3 (accuracy = 62%, p = 0.001, corrected). For the F vs. B implied motion condition the decoding performances were: V1 (accuracy = 55%, p = 0.01, corrected), V2 (accuracy = 58%, p = 0.001, corrected), V3 (accuracy = 56%, p = 0.001, corrected) (Figure 22). Comparison of the decoding performances between R vs. L and F vs. B implied motion conditions revealed a significant difference in V1 (t (18) = 2.24, p = 0.04, two-sided t-test) (Figure 22).

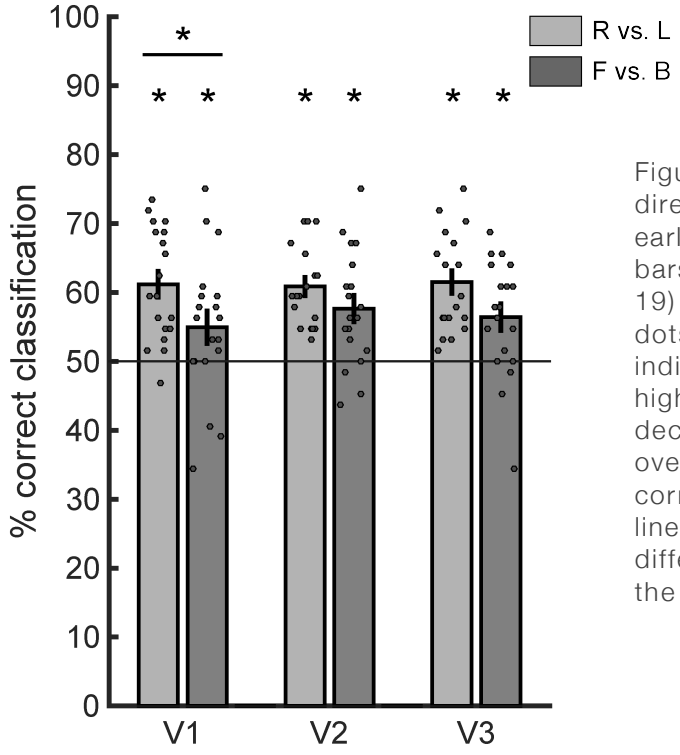

Figure 22: Decoding performance for directional implied motion in the early visual cortex (V1-V3). Error bars show the group average (n = 19) with the SEM and the scattered dots over each bar show the individual results. The horizontal line highlights the chance level (50%) of decoding. Asterisks are presented over the ROIs that have significant corrected p values. Asterisk over the line corresponds to the significant difference between conditions for the relevant ROI.

In the ventral-temporal ROIs group, only the visual area V4 (accuracy = 63%, p = 0.001, corrected) allowed significantly over chance decoding of the R vs. L implied motion directions. Decoding of F vs. B implied motion directions was possible in the ventral visual area VO1 (accuracy = 55%, p = 0.01, corrected) and to some degree in V4 (accuracy = 54 %, uncorrected p = 0.02, corrected p = 0.06) (Figure 23). For both of the implied motion conditions decoding performances were at the chance level for the other areas of this group, namely the ventral visual are VO2 and the parahippocampal areas PHC1 and PHC2 (see Table 3 for the values). There was a significant difference in the decoding performances between the R vs. L and F vs. B implied motion conditions in V4 (t (18) = 4.37, p = 0.0003, two-sided t-test) (Figure 23).

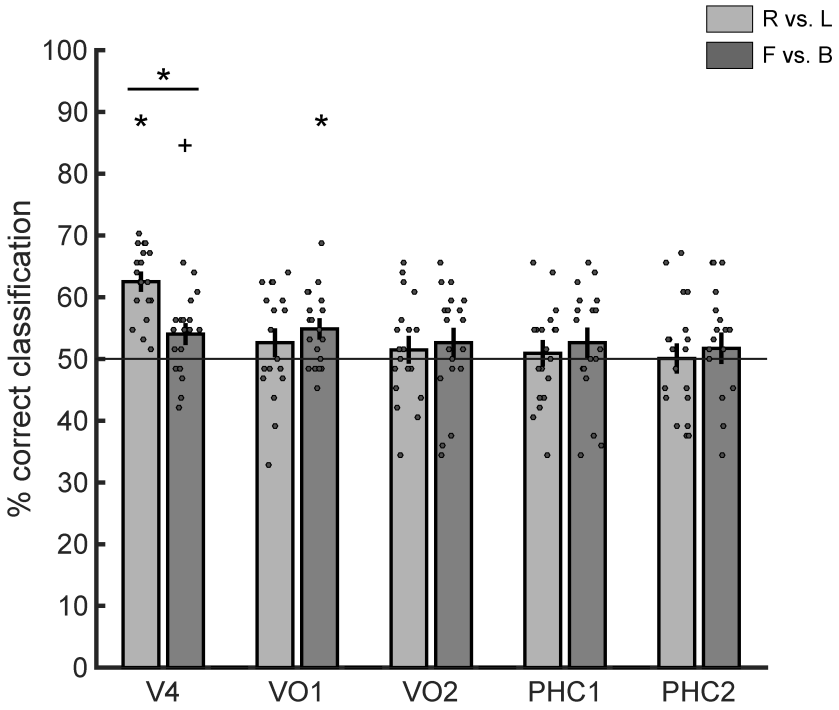

Figure 23: Decoding performance for directional implied motion in the ventral – temporal cortex (V4, VO1, VO2, PHC1, PHC2). Error bars show the group average (n = 19) with the SEM and the scattered dots over each bar show the individual results. The horizontal line highlights the chance level (50%) of decoding. Asterisks are presented over the ROIs that have significant corrected p values. Plus sign (+) is presented over the ROI that has significant uncorrected p value. Asterisk over the line corresponds to the significant difference between conditions for the relevant ROI.

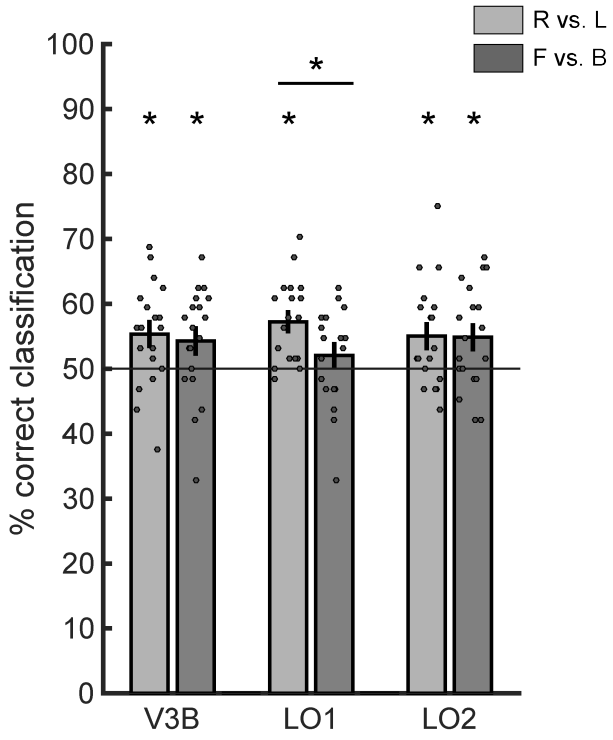

Figure 24: Decoding performance for directional implied motion in the dorso-lateral areas (V3B, LO1, LO2). Error bars show the group average (n = 19) with the SEM and the scattered dots over each bar show the individual results. The horizontal line highlights the chance level (50%) of decoding. Asterisks are presented over the ROIs that have significant corrected p values. Asterisk over the line corresponds to the significant difference between conditions for the relevant ROI.

In the dorso-lateral ROIs group, all of the areas, namely visual area V3B (accuracy = 55%, p = 0.007, corrected), lateral occipital areas LO1 (accuracy = 57%, p = 0.001, corrected), and LO2 (accuracy = 55%, p = 0.004, corrected) had significantly better than chance level of decoding of the R vs. L implied motion directions (Figure 24). For the F vs. B implied motion condition, the decoding performances were significantly better than chance for V3B (accuracy = 54%, p = 0.034, corrected) and LO2 (accuracy = 55%, p = 0.019, corrected), but not for LO1 (see Table 3 for the values). However, there was a significant difference in the decoding performances between R vs. L and F vs. B implied motion conditions in LO1 (t (18) = 2.47, p = 0.02, two-sided t-test) (Figure 24).

Among the motion responsive areas, decoding of the R vs. L implied motion directions was not possible in any of the areas (Figure 25). However, the response activity patterns in V5/MT (accuracy = 55%, p = 0.047, corrected) and MST (accuracy = 55%, p = 0.018, corrected) allowed decoding of F vs. B implied motion directions significantly better than chance. Interestingly, there was a significant difference in the decoding performances between R vs. L and F vs. B implied motion conditions in Pc (t (16) = -2.44, p = 0.026, two-sided t-test) (Figure 25). Nevertheless, the decoding performances for both the R vs. L and the F vs. B implied motion conditions in V3A, V6, Pc, CSv and VIP were at the chance level (see Table 3 for the values).

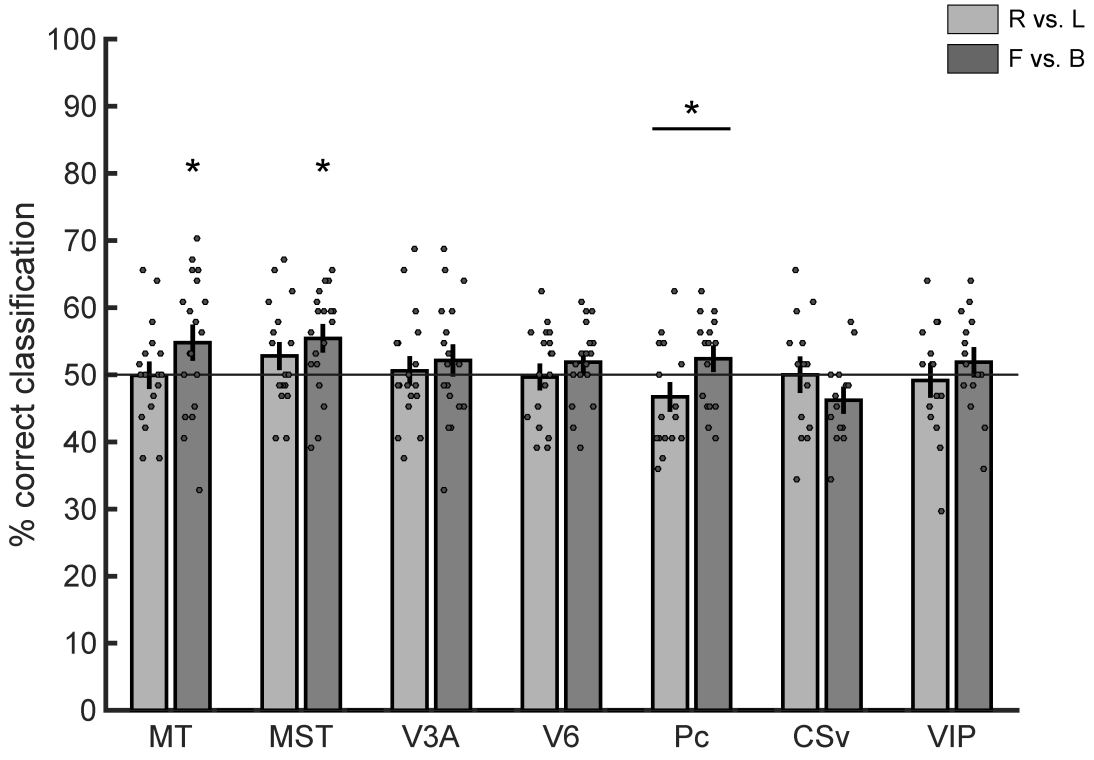

Figure 25: Decoding performance for directional implied motion in the visual motion areas MT, MST, V3A, V6, Pc, CSv and VIP. Error bars show the group average (n = 19 for the first 4 of them, n =14 for CSv, n = 17 for Pc and n = 15 for VIP) with the SEM and the scattered dots over each bar show the individual results. The horizontal line highlights the chance level (50%) of decoding. Asterisks are presented over the ROIs that have significant corrected p values. Asterisk over the line corresponds to the significant difference between the conditions for the relevant ROI.

In the parietal cortex ROIs group, the decoding of R vs. L implied motion directions was possible only in intraparietal sulcus area IPS0 (accuracy = 55%, p = 0.023, corrected) significantly better than chance (Figure 26). Decoding of F vs. B implied motion directions, however, was only possible in SPL1 (accuracy = 55%, p = 0.031, corrected) and to some degree in IPS0 (accuracy = 55%, uncorrected p = 0.017, corrected p = 0.059). Moreover, there was a significant difference in the decoding performances between the R vs. L and F vs. B implied motion conditions in SPL1 (t (18) = -2.98, p = 0.079, two-sided t-test) (Figure 26). Nevertheless, the decoding performances for both the R vs. L and the F vs. B implied motion conditions in IPS1, IPS2, IPS3, IPS4 and IPS5 were at the chance level (see Table 3 for the values).

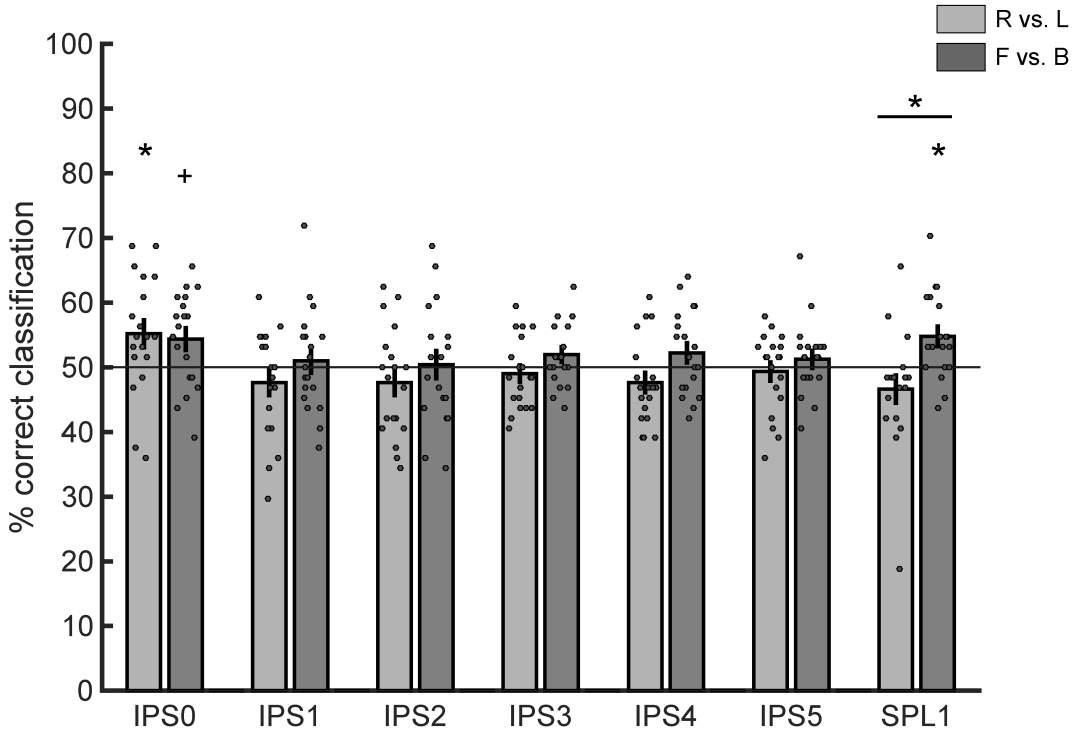

Figure 26: Decoding performance for directional implied motion in the posterior parietal cortex (IPS0 – IPS5, SPL1). Error bars show the group average (n = 19) with the SEM and the scattered dots over each bar show the individual results. The horizontal line highlights the chance level (50%) of decoding. Asterisks are presented over the ROIs that have significant corrected p values. Plus sign (+) is presented over the ROI that has significant uncorrected p value.

Implied motion decoding results						
ROI	Right vs. Left			Forward vs. Backward		
	accuracy	uncor. p	cor. p	accuracy	uncor. p	cor. p
Foveal	58.63	0.001	0.001	53.7	0.017	0.036
Peripheral	56.08	0.001	0.001	56.66	0.002	0.002
V1	61.18	0.001	0.001	54.93	0.002	0.012
V2	60.85	0.001	0.001	57.64	0.001	0.001
V3	61.51	0.001	0.001	56.41	0.001	0.001
V4	62.5	0.001	0.001	54.02	0.016	0.056
VO1	52.63	0.077	0.252	54.85	0.006	0.015
VO2	51.48	0.215	0.555	52.63	0.082	0.259
PHC1	50.9	0.314	0.711	52.63	0.081	0.259
PHC2	50.08	0.475	0.885	51.72	0.196	0.486
V3B	57.23	0.001	0.007	54.27	0.008	0.034
LO1	55.01	0.001	0.001	52.05	0.157	0.329
LO2	55.34	0.004	0.012	54.85	0.01	0.019
MT	49.91	0.542	0.976	54.76	0.004	0.047
MST	52.79	0.071	0.375	55.42	0.002	0.018
V3A	50.57	0.369	0.909	52.13	0.132	0.568
V6	49.67	0.59	0.982	51.89	0.144	0.64
Pc	46.69	0.96	1	52.38	0.113	0.479
CSv	50	0.539	0.971	46.2	0.982	1
VIP	49.16	0.664	0.995	51.87	0.208	0.64
IPS0	55.18	0.007	0.023	54.35	0.017	0.058
IPS1	47.61	0.916	1	50.98	0.305	0.79
IPS2	47.61	0.908	1	50.41	0.433	0.887
IPS3	49.01	0.727	0.99	51.97	0.152	0.515
IPS4	47.61	0.918	1	52.22	0.123	0.46
IPS5	49.34	0.646	0.99	51.23	0.26	0.724
SPL1	46.62	0.976	1	54.76	0.006	0.031

Table 3: The results of the decoding implied motion directions. Accuracy values correspond to percentages. Uncor p stands for uncorrected p values and cor. p stands for family-wise error corrected p values.

5.2.1 Eye – Tracking Results

The analysis of the eye-tracking data showed a high fixation accuracy across all tested subjects (n = 9) in all conditions (mean deviation in implied motion runs over all subjects: 0.7923 ± 0.3645). Between the experimental conditions there were no differences in fixation position (one-way ANOVA with four factors [experimental conditions]: $F_{3,24} = 0.53$, $p = 0.67$). Mauchly's test indicated that the assumption of sphericity had been violated ($X^2(5) = 15.32$, $p = 0.009$). Therefore, degrees of freedom were corrected using Greenhouse-Geisser estimates of sphericity ($\varepsilon = 0.53$, corrected $F_{1.58,\ 12.64} = 0.53$, $p = 0.56$). Moreover, the post-doc paired t-tests comparing distances to fixation for different conditions produced non-significant results. Below there are two figures showing one subjects (Figure 27) and all recorded subjects (Figure 28) fixation during all different experimental conditions.

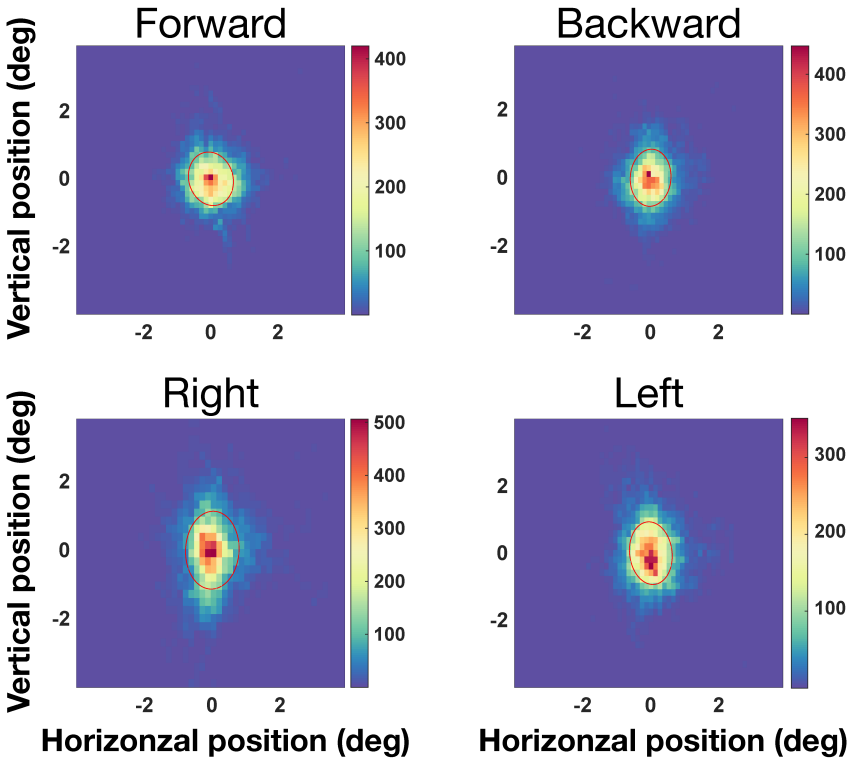

Figure 27: Histograms of the eye position (in visual degrees) of a subject for each implied motion condition is shown to visualize fixation accuracy. The red lines depict the 50% confidence ellipse.

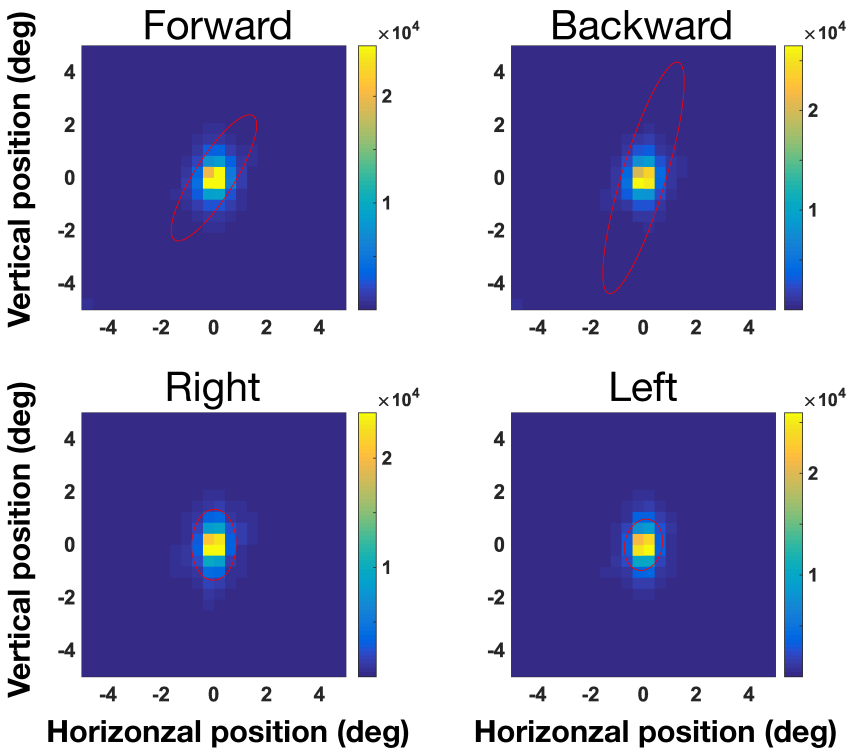

Figure 28: Histograms of the eye positions (in visual degrees) of all measured subjects (n = 9) for each implied motion condition is shown to visualize fixation accuracy. The red lines depict the 50% confidence ellipse.

5.3 Discussion

The current experiment aimed to investigate the neural mechanisms involved in implied motion processing. More specifically, I looked at the early visual cortex areas (V1-V3), higher visual areas (V3B, V4, LO1, LO2, VO1, VO2, PHC1, PHC2), motion responsive areas and parietal cortex areas (IPS0-IPS5, SPL1) to examine whether these regions contain reliable direction-selective information of implied motion stimuli. Since it has been proposed that V5/MT+ is involved in processing implied motion I looked at this area with its subunits (i.e. MST and V5/MT) and other visual motion responsive areas (V3A, V6, Pc, CSv, VIP) as well.

5.3.1 Right - Left decoding

Our results have shown that the BOLD activity patterns in all of the early visual areas (V1, V2, V3), ventral visual area V4, object-processing areas V3B, LO1, LO2, and parietal cortex area IPS0 in response to the R vs. L implied motion stimuli carry directional information that can be detected with linear machine-learning classifiers and correctly labelled according to their implied motion direction. The direction information was conveyed by the heading direction of the foreground objects. For R vs. L condition the stimuli were prepared in a way that the background motion would correspond to the opposite direction compare to the foreground object. As the participants were instructed to fixate at the fixation cross that was at the centre of the stimuli, where the foreground objects were present, our assumption was that the decodable motion direction would correspond to the implied motion direction of the objects in motion, rather than the background motion. Interestingly, the classification of the implied motion directions was also possible in the peripheral representation of the EVC (Peripheral EVC) which was not stimulated by the foreground objects. The results suggest that higher-level cognitive processes that detect implied motion direction based on context and object configuration feed back their predictions beyond the retinal representation of the given object to cover the entire context-providing visual space in early visual cortex. As presented here, the reliable decoding of implied motion direction information from the Peripheral EVC is in line with the predictive coding theory, and exemplifies how top-down information is integrated with the bottom-up processing in the early visual cortex similarly as demonstrated before for colours of objects (Bannert and Bartels, 2013).

5.3.2 Forward - Backward decoding

The decoding results of the Forward versus Backward implied motion directions were similar to that of the Right-Left condition, except for foveal EVC, V1, V4, LO1 and Pc that had preference for decoding either of the conditions better than the other. Activity patterns in all of the early visual areas (V1-V3) allowed significantly above chance classification of Forward versus Backward implied motion directions. For this condition, however, foveal and peripheral EVC distinction is not valid as it is for the Right versus Left condition. This is because the foreground objects used in this condition were not completely fitting into the central visual area that corresponds to the checkerboard stimulus used to simulate and define foveal EVC (see Figure 29 for clarification). Therefore, we are cautious about interpreting the results for this condition, especially in early visual areas.

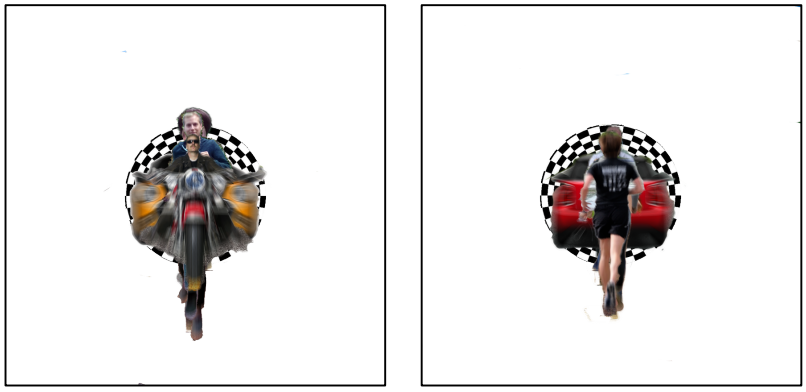

Figure 29: Foreground objects used in Forward (left) and Backward (right) implied motion stimuli overlapped on the checkerboard that was used for foveal early visual cortex localizer.

5.3.3 Comparing the decoding performance of the two direction pairs

Lateral visual area LO2 was the only ROI that showed very similar result for both conditions while the decoding accuracies were significantly over chance level. The decoding results from early visual areas were overall higher for the R vs. L implied motion condition and the performance differences between the conditions were significant for Foveal EVC, V1, V4, LO1, Pc and SPL1. Is it possible that the difference between foreground objects in the F vs. B condition were reflected in the activity patterns of these areas and these differences made it easier for the classifier to distinguish the activity patters belonged to these implied motion directions? The decoding accuracies obtained for the R vs. L condition were significantly higher in Foveal EVC and V1 compare to the F vs. B condition, which contradicts this idea. Might it be

possible that these differences actually made it more difficult for the classifier to learn the direction related information? According to the results obtained from the early visual areas, this could be the case. Nevertheless, motion areas V5/MT and MST allowed decoding of implied motion directions only for forward-backward axis.

5.3.4 Encoding of implied motion directions in the primary visual cortex

Our results showed that the activity patterns in the primary visual cortex (V1) allow decoding of both right-left and forward-backward implied motion directions significantly better than chance. Previous studies showed that the activity patterns in V1 allow decoding the orientation of a uniform visual grating (Kamitani and Tong, 2005) even the stimuli were rendered to be invisible (Haynes and Rees, 2005). Besides orientation decoding, activity patterns in V1 also allow decoding of motion directions of random dots and plaid patterns (Kamitani and Tong, 2006; Seymour et al., 2009; Hong et al., 2012; van Kemenade et al., 2014). The stimuli we used in our experiment were more naturalistic, high-level and the directional motion information were conveyed by the orientation of foreground objects and motion blur. To our knowledge, there is no evidence for V1 to encode high-level object orientation or implied motion directions. Both types of information (i.e. object-orientation and implied motion direction) are complex and relevant to higher visual areas, given that V1 processes rather low-level visual features. The information about implied motion directions is most likely fed back to V1 from higher visual areas. Hence, our results showing significantly above chance decoding in V1 is a novel finding and it is consistent with the previous study that showed presence of contextual feedback to this area (Muckli et al., 2015).

5.3.5 Are direction-selective neurons responsible for decoding direction?

Decoding the direction information of the retinal motion that results from objects moving in space is one of the fundamental tasks of the visual system. Yet, the neural mechanisms underlying the perception of motion direction are still unknown. It is generally assumed that the brain constructs its percept of the direction of motion from the selective responses of direction-selective neurons (Newsome and Pare, 1988; Salzman et al., 1990; Blanke et al., 2002). Some of the brain areas we investigated were previously reported to show direction-selective responses, for instance, the early visual areas (Orban et al., 1986; Nishida et al., 2003), visual area V4 (Tolias et al., 2005), V5/MT (Dubner and Zeki, 1971; Zeki, 1974). Moreover, a psychophysics study reported that adaptation to implied motion results in transfer of motion direction aftereffect to real motion (Winawer et al., 2008). The transfer of adaptation from implied motion to real motion suggests that implied motion processing recruits direction selective

neurons. Our results showing significant decoding of implied motion directions from early visual areas (V1-V3), higher visual area V4, and motion areas V5/MT and MST is consistent with this view. Thus, direction-selective neurons are likely to account for the decoding of motion directions. Nevertheless, an alternative explanation is discussed in the General Discussion & Conclusion section.

5.3.6 Involvement of object-processing areas LO1 and LO2

The two subunits of the human LOC are LO1 and LO2, and they are located between dorsal V3 and V5/MT+ (Larsson and Heeger, 2006). It was shown that LOC has selectivity for real motion patterns and global patterns of implied motion when tested with Glass patterns, suggesting an overlap between the neural populations responding to both types of motion (Krekelberg et al., 2005). Previous fMRI study has shown that LO is sensitive to mirror-reversed images of objects and treats mirror-reversed images of objects and scenes as different images (Dilks et al., 2011). The authors of the study did not distinguish between LO1 and LO2, and presented the images of objects without a contextual background. Might it be the case that mirror-reserved sensitivity of these areas allowed successful classification of right-left implied motion directions? The stimuli we used for rightward implied motion were mirror-reversed versions of the ones that we used for leftward implied motion. However, the stimuli set for both right and left implied motion conditions contained normal and mirror-reversed versions of the background images irrespective of the foreground images. Therefore, there is not a straightforward answer to this question, although it might be possible, it is not very probable. According to our results we think that there may be difference in sensitivity between LO1 and LO2 for encoding of implied motion directions. The activity patterns in LO2 allowed above chance decoding of both right-left and forward-backward implied motion directions, whereas decoding in LO1 was significantly above chance only for right-left implied motion directions and the difference between R vs. L and F vs. B implied motion conditions was significant. Previously it was suggested that LOC contains “car-selective” neurons (Grill-Spector et al., 1999). Given that our stimuli contained cars as foreground objects one may argue that the results are driven by these neurons. However, the same cars that were used in right implied motion block were also used in left implied motion block, and the same was true for forward and backward implied motion blocks. Moreover, cars were one of the various objects that we used in our block-design experiment, therefore it is very unlikely that the decoding results are driven by car-selective neurons, unless these neurons also show selectivity to other objects (e.g. birds) and at the same time show high sensitivity to object orientation. Although, those cases would be against the proposition of neurons being specifically selective for cars.

6 CHAPTER III: Testing for generalization of motion directions

6.1 Summary

Does the human brain generalize motion directions regardless of the motion type? In the previous chapters I showed that I was able to decode both real and implied motion directions from BOLD activity responses from various visual areas. In this chapter I wanted to answer our main experimental question: does the brain generalize real and implied motion directions? This would mean that the directions I used in my stimuli would elicit specific activity patterns about direction content that could be learnt by the linear classifier I have been using. For this, I used all the data that I collected in the following way: the real motion data as training set and the implied motion data as the test set. The training set was used for classifier to learn about directional patterns in BOLD responses to real motion directions, the testing set was used to assess the performance of the classifier for accurately labelling each tested sample according to the direction of motion it implied. Our results showed that for the Right versus Left motion directions the activity patterns in lateral occipital area LO2, and for the Forward versus Backward motion directions the activity patterns in ventral occipital area VO1 contained information about the direction content that generalizes from real to implied motion. These findings suggest that similar neural patterns were evoked in these regions for a given real motion direction, as well as for the same direction of implied motion. Given that both regions where the generalized codes were found are located in the ventral stream and involved in processing of objects, our results suggest a strong interaction between dorsal and ventral pathways for processing motion direction, and a crucial role of the ventral stream in the perception of motion.

6.2 Results

In order to test for the generalization of motion direction information in our ROIs, I ran a cross-classification analysis. A linear classifier was trained on directional real motion data and the directional implied motion data was used as a test-set. As it can be seen from the figures below, for many of the ROIs the decoding performance was at around the chance level. Nevertheless, for statistical inference I performed permuting direction labels for each axis 1000 times for each ROI and then applied FWE correction for multiple comparisons (described with more details in the Methods section). The results showed that for each direction axis there was one object-processing brain area that contained generalized information about motion directions (i.e. from real motion to implied motion).

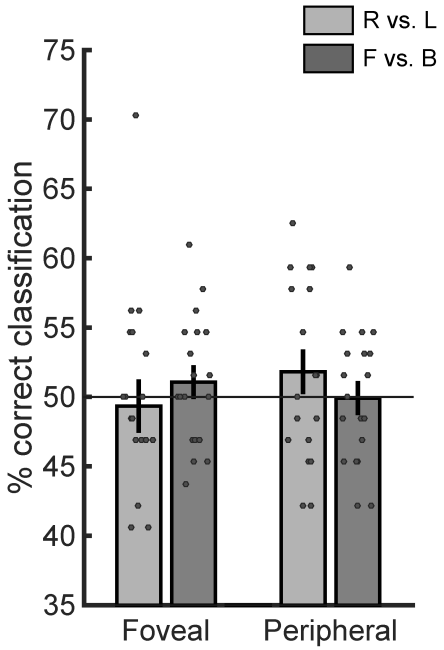

Figure 30: Cross-classification results for the Foveal and the Peripheral representations of the early visual cortex. Error bars show the group average (n = 19) with the SEM and the scattered dots over each bar show the individual results. The horizontal line highlights the chance level (50%) of decoding.

The cross-classification analysis of R vs. L motion directions revealed that the activity patterns in lateral occipital area LO2 (accuracy = 53%, p = 0.042, corrected) allows the classifier to predict the direction information of the seen implied motion after being trained on real motion data (Figure 34). Although the mean accuracy values were close to the chance level, the decoding performances of these directions in V3 (accuracy = 53 %, uncorrected p = 0.023, corrected p = 0.066) and V3B (accuracy = 53 %, uncorrected p = 0.027, corrected p = 0.074) reached statistical significance before applying FWE-wise multiple correction (Figure 32 & Figure 34). Decoding of these directions across the datasets was at the chance level for the rest of the ROIs.

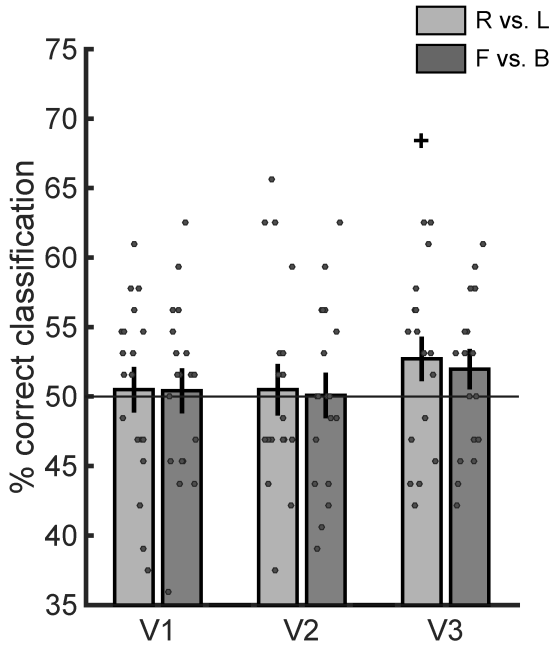

Figure 32: Cross-classification results in the early visual cortex (V1-V3). Error bars show the group average (n = 19) with the SEM and the scattered dots over each bar show the individual results. The horizontal line highlights the chance level (50%) of decoding. Plus sign (+) is presented over the ROI that has significant uncorrected p value.

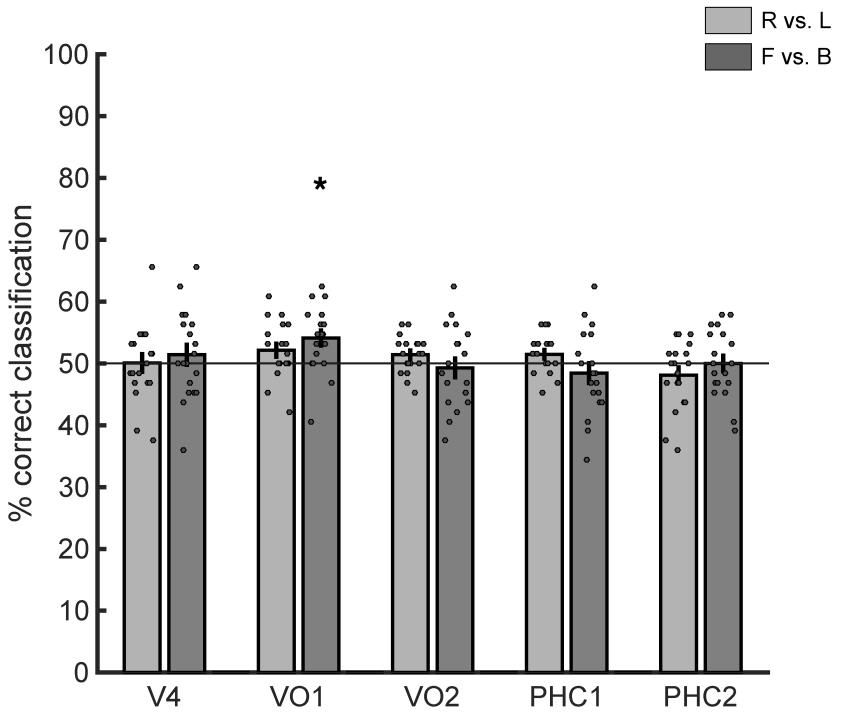

Figure 32: Cross-classification results in the ventral – temporal cortex (V4, VO1, VO2, PHC1, PHC2). Error bars show the group average (n = 19) with the SEM and the scattered dots over each bar show the individual results. The horizontal line highlights the chance level (50%) of decoding. Asterisks are presented over the ROIs that have significant corrected p values.

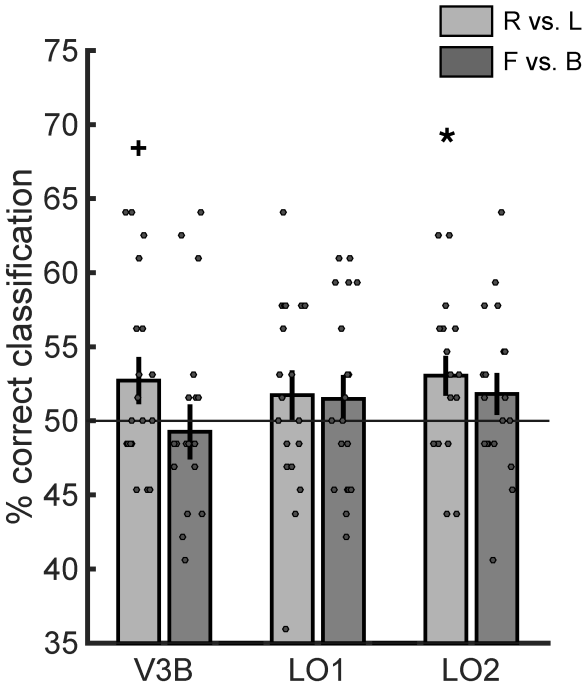

Figure 34: Cross-classification results in the dorso-lateral areas (V3B, LO1, LO2). Error bars show the group average (n = 19) with the SEM and the scattered dots over each bar show the individual results. The horizontal line highlights the chance level (50%) of decoding. Asterisks are presented over the ROIs that have significant corrected p values. Plus sign (+) is presented over the ROI that has significant uncorrected p value.

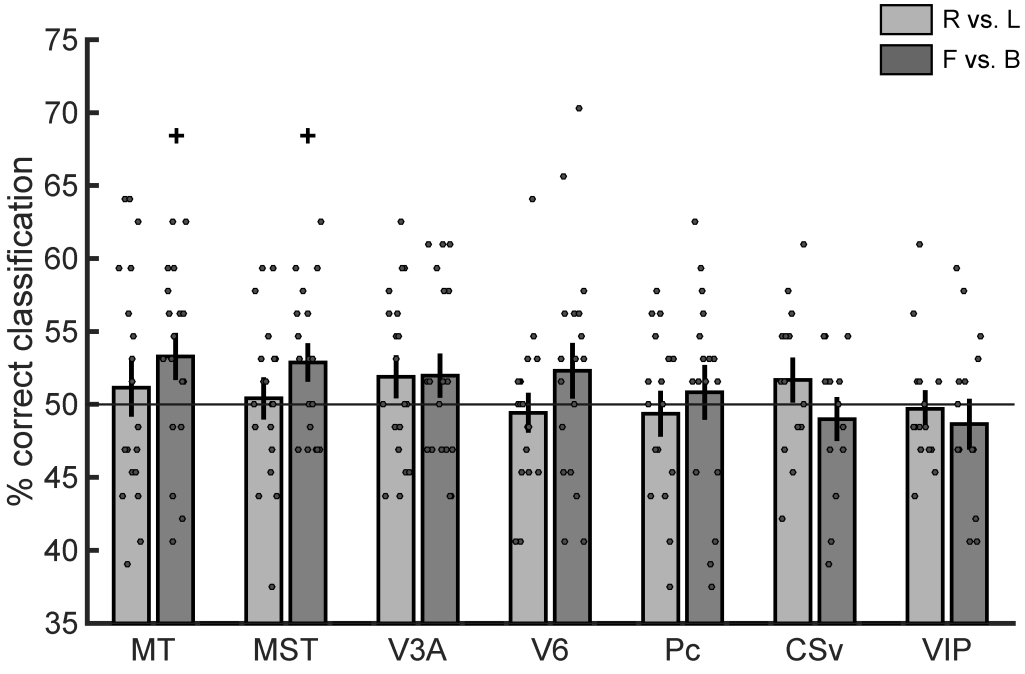

Figure 34: Cross-classification results in the visual motion areas MT, MST, V3A, V6, Pc, CSv and VIP. Error bars show the group average (n = 19 for the first 4 of them, n =14 for CSv, n = 17 for Pc and n = 15 for VIP) with the SEM and the scattered dots over each bar show the individual results. The horizontal line highlights the chance level (50%) of decoding. Plus signs (+) are presented over the ROIs that have significant uncorrected p value.

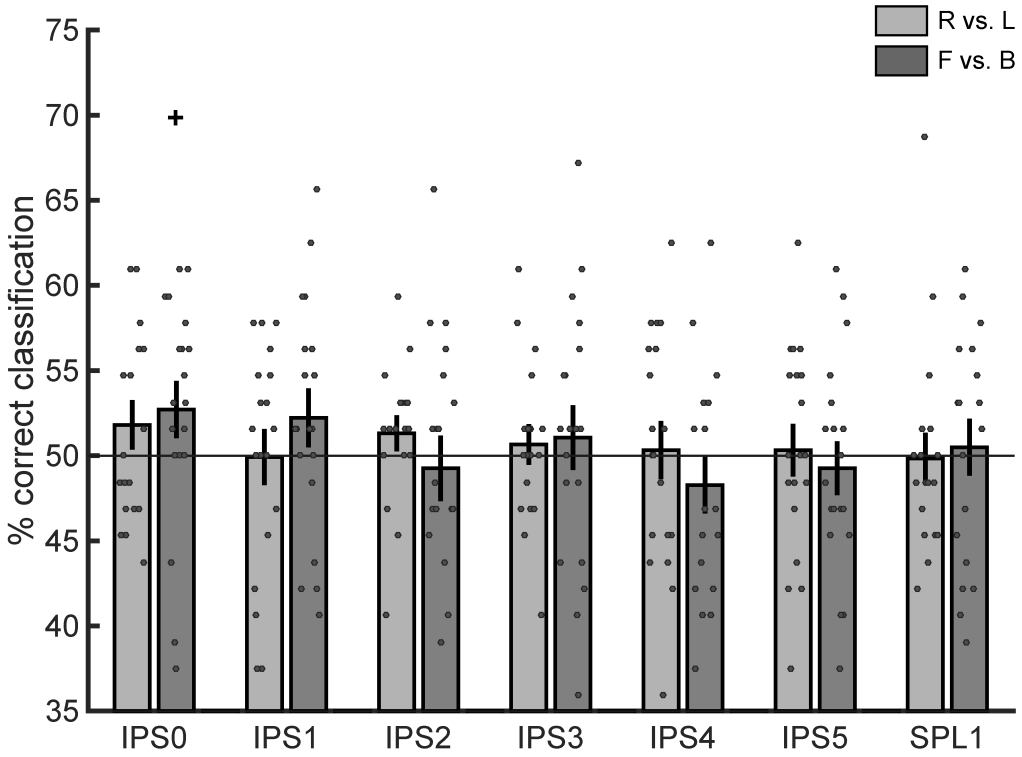

Figure 35: Cross-classification results in in the parietal cortex (IPS0 – IPS5, SPL1). Error bars show the group average (n = 19) with the SEM and the scattered dots over each bar show the individual results. The horizontal line highlights the chance level (50%) of decoding. Plus sign (+) is presented over the ROI that has significant uncorrected p value.

For decoding of F vs. B motion directions the ventral occipital area VO1 (accuracy = 54%, p = 0.009, corrected) allowed significantly above chance decoding of implied motion directions although the linear classifier was only trained on real motion data (Figure 32). Moreover, in V5/MT (accuracy = 53 %, uncorrected p = 0.004, corrected p = 0.107), MST (accuracy = 53 %, uncorrected p = 0.014, corrected p = 0.168) and IPS0 (accuracy = 53 %, uncorrected p = 0.026, corrected p = 0.167) the decoding performances reached significance before applying FWE-wise multiple correction (Figure 34 & Figure 35). Decoding of these directions across the datasets were at the chance level for the rest of the ROIs.

6.3 Discussion

It has been proposed that common mechanisms maybe involved in real and implied motion processing in the human brain (Kourtzi and Kanwisher, 2000; Senior et al., 2000; Krekelberg et al., 2005). Directionality is one of the features of both types of motion. We thought that if common mechanisms are involved in processing of both motion types, then motion directions may have similar representations in the brain. Moreover, object processing areas may contain directional information of the both motion types. In order to test this, I examined 27 brain regions, such as early visual, ventral, lateral and parietal, object processing and motion processing areas to check whether response activity patterns for the same directions are similar. To do this, I used a linear classifier and trained it on directional real motion data and then used directional implied motion data to test its performance. The results showed that for the Right versus Left motion directions the activity patterns in lateral occipital area LO2 and for the Forward versus Backward motion directions the activity patterns in ventral occipital area VO1 contained information about the direction content that generalizes from real to implied motion. Both of these findings are very interesting since these high level visual areas are involved in object processing.

The lateral occipital complex is a large area that contains at least two visual field maps, one of being the lateral occipital LO2, and in the human brain it is located between dorsal V3 and V5/MT+ and it is selectively responsive to objects (Malach et al., 1995; Larsson and Heeger, 2006). In comparison to its neighbour area LO1, LO2 was shown to be significantly more responsive to objects compare to scrambled versions of the objects and faces (Larsson and Heeger, 2006) and was reported to be causally involved in processing of object shape (Silson et al., 2013). In our previous experiments (see Chapter I & II) we found that LO2 allows decoding of both real and implied motion directions for both in Right versus Left and Forward versus Backward conditions. Moreover, according to the results of our current experiment, the information about right and left motion directions appears to generalize across real and implied motion in LO2. A previous fMRI study found that LO is sensitive to sense information of scenes and objects and treats mirror-reversed images of objects as two different images (Dilks et al., 2011), without distinguishing between LO1 and LO2. A double dissociation between LO1 and LO2 were demonstrated in a TMS study, showing that disruption to LO1 (but not LO2) significantly perturbs orientation discrimination, while disruption to LO2 (but not LO1) significantly disturbs shape discrimination (Silson et al., 2013). Considering these findings and our results for these areas, the shapes of the foreground objects might be more relevant information for implied motion direction encoding than their orientations.

VO1 was shown to respond preferentially to objects compared to faces and shows colour selectivity (Brewer et al., 2005). Moreover, it was shown that stimulus colour can accurately be decoded from VO1 (Brouwer and Heeger, 2009; Seymour et al., 2009; Bannert and Bartels, 2018). The results of our previous experiments (see Chapter I & II) showed that decoding of both R vs. L and F vs. B real motion directions and F vs. B implied motion directions is possible from this area. In this experiment, we showed that the activity patterns in VO1 contains information about forward and backward direction content that is shared between real and implied motion.

Initially we thought that motion areas and/or early visual areas could be potential candidates for decoding the generalized motion information. However, none of these areas allowed significantly correct predictions of seen implied motion directions when the directions were learnt from the response patters to the real motion stimuli. Perhaps future studies can reveal whether the uncorrected significant decoding performances from V3 and V3B for right-left directions, and from V5/MT, MST and IPS0 for forward-backward directions reflect the presence of generalized direction information in these areas on different dataset.

Overall, our results suggest that there is a generalized information about motion direction in the higher visual areas. For right-left axis the direction representations are encoded in LO2, for forward-backward motion axis they are encoded in VO1 (Figure 36). These novel findings to our knowledge have not been reported before and are important to take into account when investigating motion processing in the human brain. Although we are not the first ones, we raise the question about the validity of motion and object processing pathways in the human brain. Given that our findings suggest strong interaction between these pathways for processing motion direction, dorsal and ventral pathways should not be thought to work independently for motion and object processing respectively.

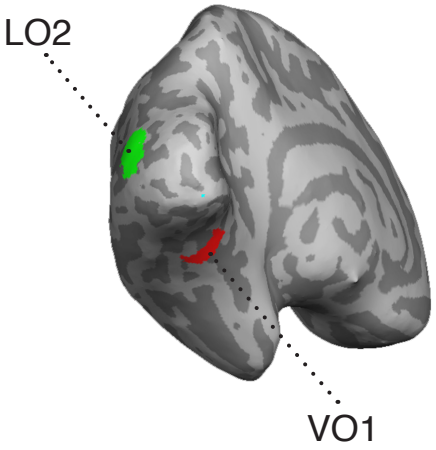

Figure 36: Locations of the higher visual areas lateral occipital LO2 and ventral occipital VO1 are shown on the left hemisphere of a single subject. These are the brain areas that encode generalized information of the observed real and implied motion directions.

7 Chapter IV: Univariate analyses of BOLD responses to real motion directions

7.1 Summary

The aim of the current chapter was threefold. Firstly, we wanted to examine whether forward real motion differentially modulates BOLD responses in comparison to backward real motion. Several studies have reported evidence for what is called “looming” bias. That is, because of its ecological saliency, the expanding sensory signals are processed differently than contracting signals. Several auditory and multisensory studies confirmed the existence of such bias across different datasets, however in our knowledge there has not been an fMRI study directly investigating the bias throughout regions of the visual cortex and posterior parietal cortex. We wanted to check whether there was a sign of such asymmetry in our dataset. Secondly, we wanted to check for mean BOLD signal differences to Right and Left real motion stimuli. Although we expected to observe no such difference, eliminating the existence of such possibility would be an extra level of control that MVPA results cannot be explained by difference in BOLD amplitudes for the Right versus Left real motion condition. Thirdly, given that our previous analyses found differences in multivariate encoding between Right versus Left and Forward versus Backward real motion processing in some of the ROIs, we wanted to check whether motion on right-left axis corresponded to higher mean BOLD signal, or vice versa. Our results showed that a multitude of visual high-level regions had a considerably stronger BOLD response to backward compared to forward motion, especially in the areas V6, IPS0 and IPS1. This is surprising, as previous behavioural results provide evidence mostly for higher saliency of forward motion across sensory modalities. I discuss these findings in context of predictive coding, and neural efficiency, in that both of these concepts would predict our results. As expected, we did not find right-left preferences. With regard to preferences for motion axes, the vast majority of ROIs showed higher BOLD responses for motion along the forward-backward compared to the right-left axis. As stimuli for both axes were not directly comparable, this finding is primarily relevant for the interpretation of the multivariate results presented in Chapter I.

7.2 Results

In order to test whether forward or backward real motion stimuli corresponds to higher BOLD signal in any of the ROIs I contrasted the mean beta values in response to forward and backward conditions. The results are shown in the Figure 37 for each ROI. Group averaged mean beta values of difference between two conditions were significant (t-test against zero) for nine out of twenty-seven areas according to the two-tailed t-tests, after applying multiple comparisons correction (i.e. Bonferroni-Holm correction for 27 ROIs) this number dropped to three. These areas were IPS1 ($t(13) = -5.22$; $p = 0.004$, corrected), V6 ($t(13) = -4.15$; $p = 0.028$, corrected) and IPS0 ($t(13) = -3.95$; $p = 0.001$, corrected). The areas that had significant uncorrected p values were V5/MT ($t(13) = -2.26$; $p = 0.041$, uncorrected), V3A ($t(13) = -2.19$; $p = 0.046$, uncorrected), IPS2 ($t(13) = -3.69$; $p = 0.002$, uncorrected), IPS3 ($t(13) = -3.35$; $p = 0.005$, uncorrected), Pc ($t(11) = -2.75$; $p = 0.018$, uncorrected) and CSv ($t(9) = -2.92$; $p = 0.016$, uncorrected).

The results of the same analysis applied for right and left real motion directions are shown in Figure 38. The two-tailed t-tests revealed that the difference of BOLD responses in none of the ROIs were statistically significant.

The Figure 39 shows the results of the univariate analysis of BOLD responses to real motion in depth (i.e. forward + backward) in contrast to translational motion (i.e. right + left) across the ROIs. Group averaged mean beta values of difference between two motion axes were significant (t-test against zero) for twenty-four out of twenty-seven areas according to the two-tailed t-tests, after applying multiple comparisons correction (i.e. Bonferroni-Holm correction for 27 ROIs) this number dropped to ten. The areas that had significant corrected p values were Peripheral EVC ($t(16) = 4.47$; $p = 0.008$, corrected), V3 ($t(16) = 3.76$; $p = 0.032$, corrected), V4 ($t(16) = 6.66$; $p = 0.0001$, corrected), VO1 ($t(16) = 6.11$; $p = 0.0003$, corrected), VO2 ($t(16) = 7.32$; $p = 0.00004$, corrected), LO1 ($t(16) = 4.48$; $p = 0.008$, corrected), MST ($t(16) = 4.20$; $p = 0.013$, corrected), V5/MT ($t(16) = 3.71$; $p = 0.034$, corrected), PHC1 ($t(16) = 7.18$; $p = 0.00005$, corrected), PHC2 ($t(16) = 7.67$; $p = 0.00002$, corrected). The areas that had significant uncorrected p values were V1 ($t(16) = 3.33$; $p = 0.0042$, uncorrected), V2 ($t(16) = 3.19$; $p = 0.0056$, uncorrected), LO2 ($t(16) = 2.80$; $p = 0.0128$, uncorrected), V3A ($t(16) = 2.69$; $p = 0.0161$, uncorrected), V3B ($t(16) = 3.49$; $p = 0.003$, uncorrected), V6 ($t(16) = 2.73$; $p = 0.0146$, uncorrected), IPS1 ($t(16) = 2.72$; $p = 0.015$, uncorrected), IPS2 ($t(16) = 2.84$; $p = 0.0117$, uncorrected), IPS3 ($t(16) = 2.46$; $p = 0.0254$, uncorrected), IPS5 ($t(16) = 2.38$; $p = 0.0297$, uncorrected), SPL1 ($t(16) = 3.32$; $p = 0.0043$, uncorrected), Pc ($t(14) = 3.02$; $p = 0.009$, uncorrected), CSv ($t(12) = 2.24$; $p = 0.0442$, uncorrected).

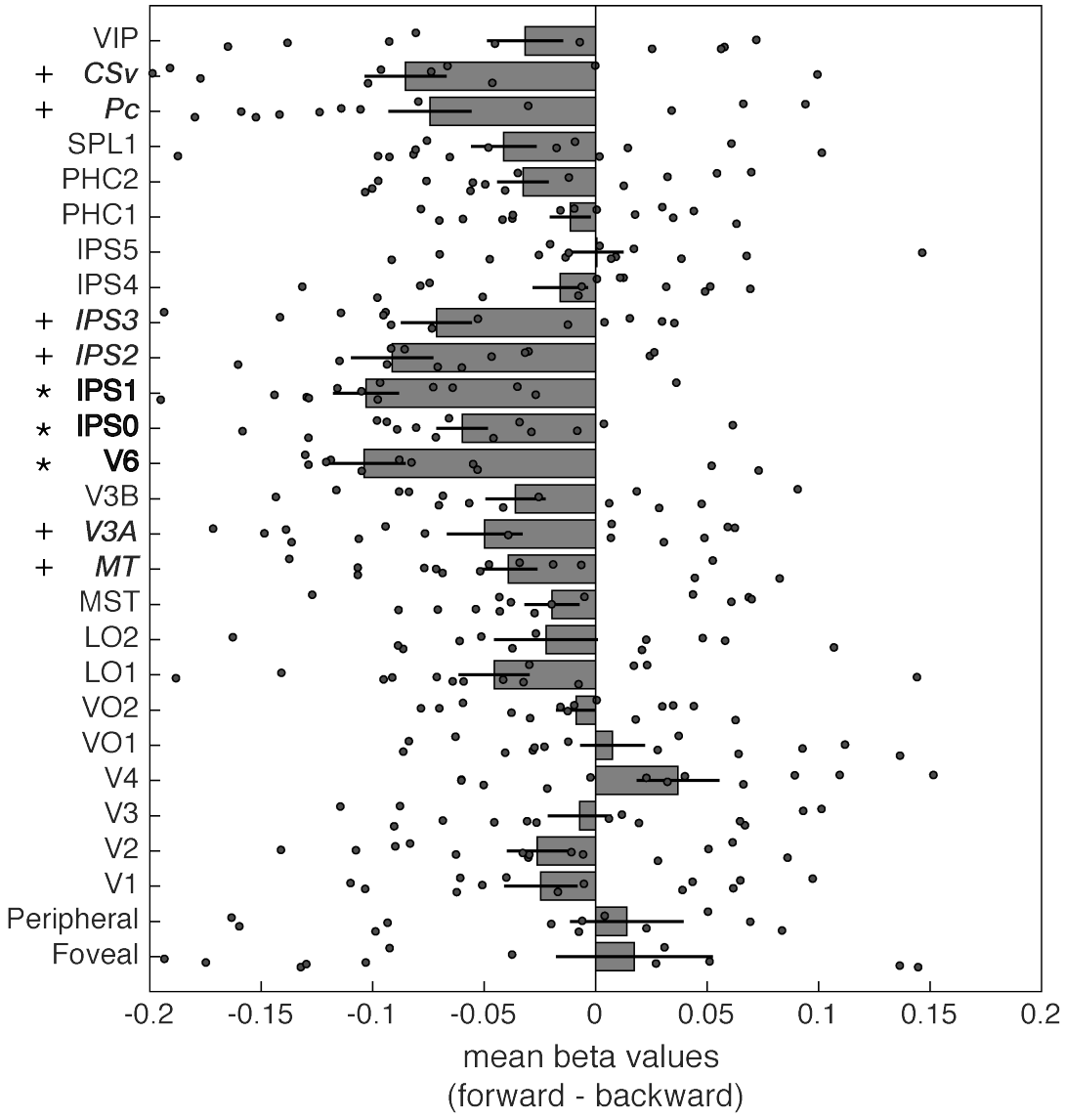

Figure 37: Difference of mean beta values between real forward and backward motion conditions for each ROI. Error bars show the group average (n = 14 for all except for Pc (n = 12), CSv (n = 10) and VIP (n = 10)) with the SEM and the scattered dots over each bar show the individual results. The ROIs that had significant corrected p values ($p < 0.05$) are marked with bold font and asterisks and the ones with significant uncorrected p values ($p < 0.05$) are marked with italic font and plus signs. on the y-axis

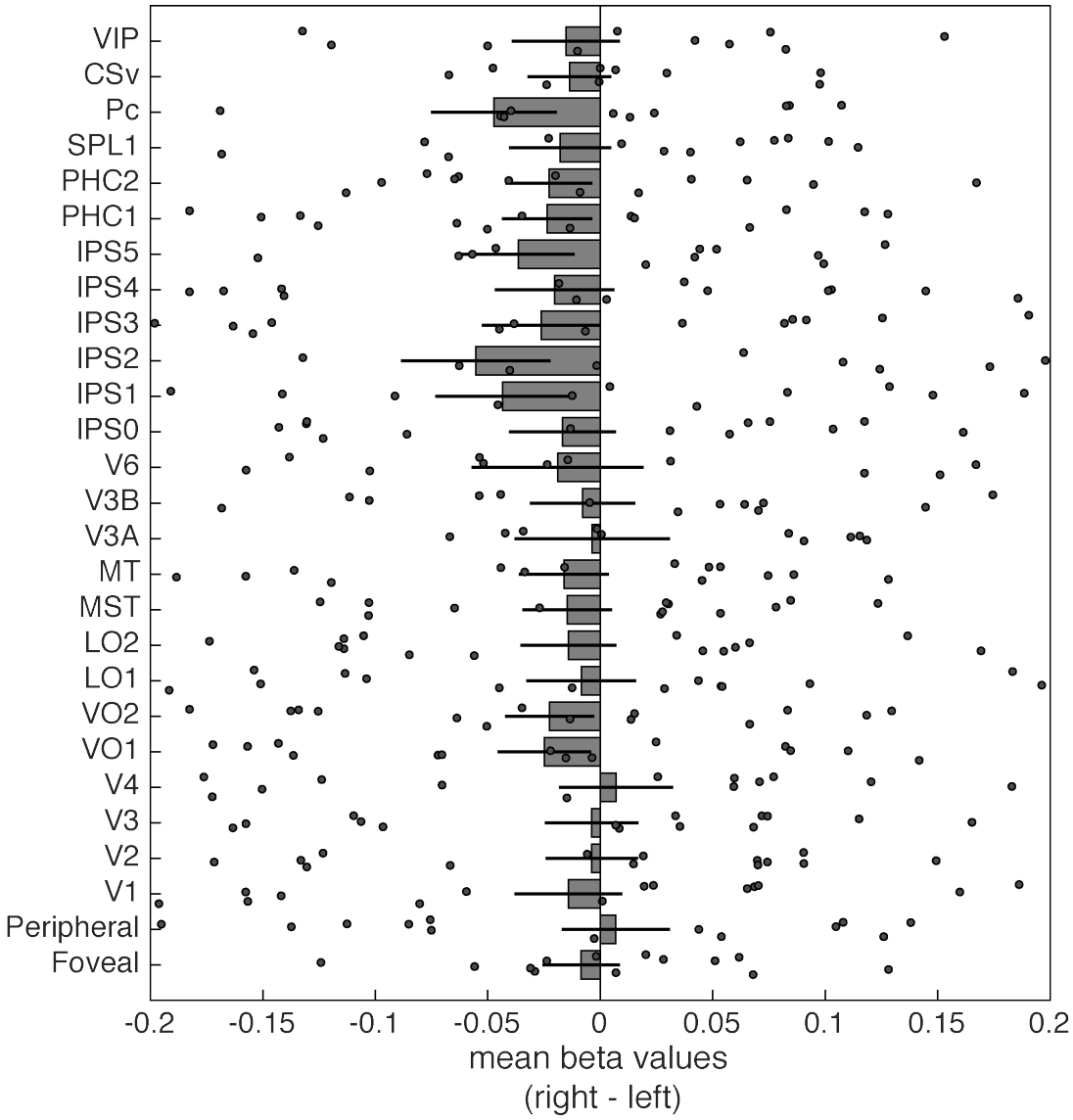

Figure 38: Difference of mean beta values between real right and left motion conditions for each ROI. Error bars show the group average (n = 14 for all except for Pc (n = 12), CSv (n = 10) and VIP (n = 11)) with the SEM and the scattered dots over each bar show the individual results. For none of the ROIs the difference in mean BOLD signal was significant.

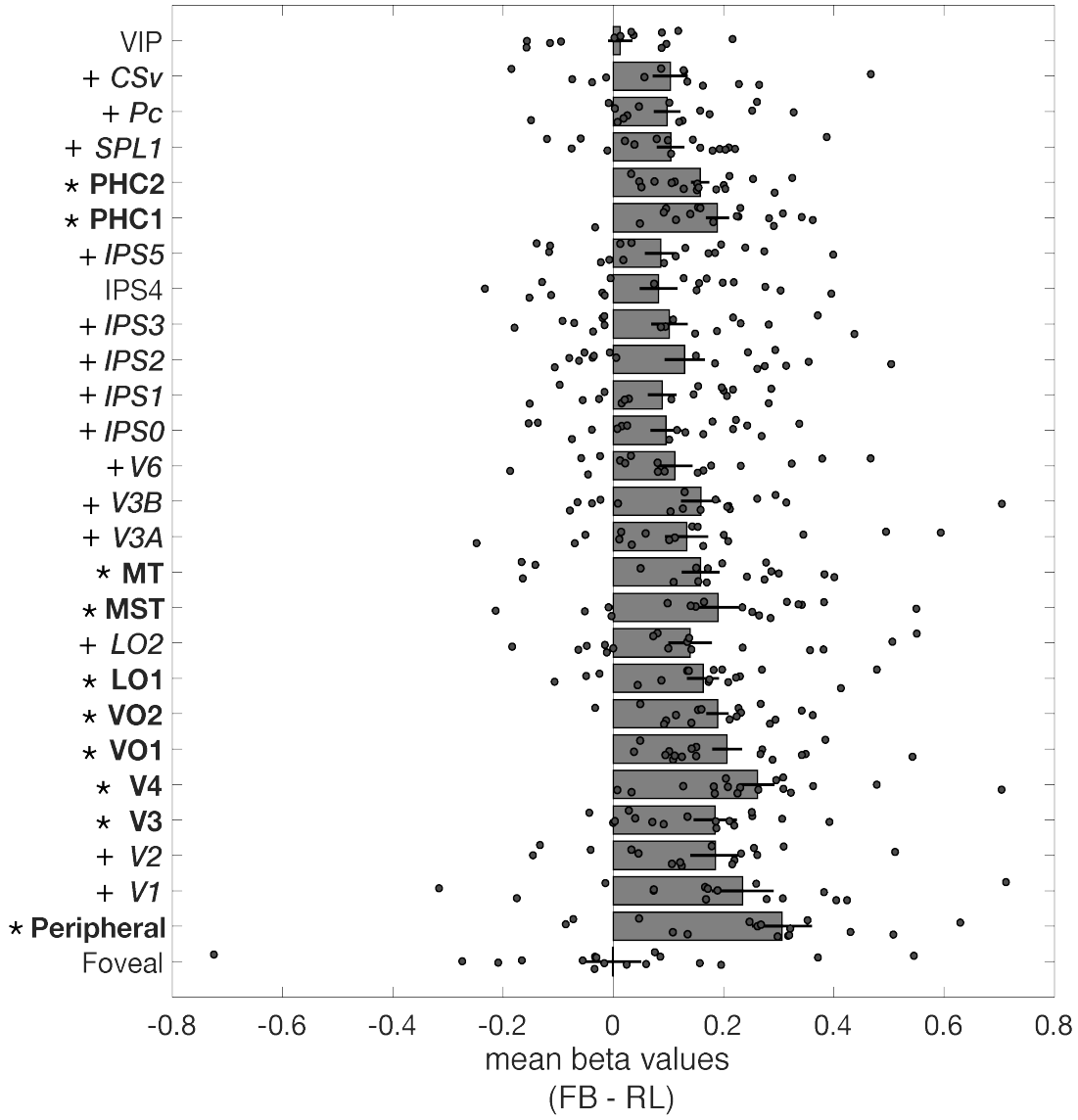

Figure 39: Difference of mean beta values between real motion in depth (forward + backward) and translational (right + left) motion for each ROI. Error bars show the group average (n = 17 for all except for Pc (n = 15), CSv (n = 13) and VIP (n = 13)) with the SEM and the scattered dots over each bar show the individual results. The ROIs that had significant corrected p values ($p < 0.05$) are marked with bold font and asterisks and the ones with significant uncorrected p values ($p < 0.05$) are marked with italic font and plus signs. on the y-axis

7.3 Discussion

Our results showed that there was a significant difference in mean BOLD responses in motion area V6 and in intraparietal sulcus areas IPS0 and IPS1 in response to Forward and Backward real motion stimuli. Some of the other motion areas (V5/MT, V3A, Pc, CSv) and intraparietal sulcus areas (IPS2, IPS3) also showed tendency (i.e. significant uncorrected p values) to have difference in mean BOLD responses. However, these results do not mean that we found an evidence in our dataset for the previously reported 'looming' bias as we tested for the difference in both directions (i.e. two-tailed t-test). The difference between conditions was calculated by subtracting the values for Backward condition from Forward condition. Therefore, negative values correspond to higher beta values for the Backward condition. When tested whether the difference in any of the ROIs was in favour of the looming bias (i.e. one-tailed t-test) the statistics were in favour of the null hypothesis. In the following subchapters I will discuss the possible reasons for our unexpected finding and how it relates to the previous studies.

Furthermore, in response to Right and Left real motion stimuli there were no significant differences between mean BOLD signals across the ROIs. This null finding matches our expectation. The stimulus was matched completely between Right and Left conditions except for the motion direction and we did not have any reason to expect difference in processing these motion signals. Furthermore, this null finding is meaningful as it confirms that the results of our first experiment (see Chapter I) cannot be explained by the mean BOLD signal differences to either right or left real motion directions.

At last, we showed that the mean BOLD signal is stronger in response to motion in depth in comparison to motion on lateral axis (or translational motion). In our study, as the participants were instructed in both conditions to maintain attention, and perform a uniform task across all conditions. Attention is hence unlikely to account for the effects observed here.

7.3.1 Efficiency account for lower BOLD signal

In response to backward moving stimuli the averaged mean BOLD responses were greater than they were to forward moving stimuli. The difference was significant in motion area V6 and intraparietal sulcus areas IPS0 and IPS1, but not in early visual areas. This finding contradicts with the previous researches indicating looming bias resulting in stronger cortical BOLD activation compared to the receding motion (Seifritz et al., 2002; Wittmann et al., 2010; Tyll et al., 2013). In our study we did not look beyond the visual and parietal areas, however we could not detect any positive correlation between BOLD signal strength and looming motion

across 27 ROIs. According to the “neural efficiency” hypothesis cortical neural activity is reduced in experts compare to non-experts (Neubauer and Fink, 2009) and glucose metabolic rate changes in brain areas that are associated with learning some tasks (Haier et al., 1992). Previous fMRI study which compared brain activations between athletes and non-athletes found that athletes had lower cortical activation in task-sensitive brain areas during the processing of sports related and sport unrelated visuo-spatial task than non-athletes (Guo et al., 2017). Indeed, the areas we found significant difference in BOLD responses are sensitive to visual motion. For example, the visual area V6 is a high-level motion responsive area that was shown to have a strong preference for coherent motion and optic flow (Pitzalis et al., 2006; Pitzalis et al., 2010) and gives strong differential response to egomotion-compatible optic flow in comparison to egomotion-incompatible flow (Cardin and Smith, 2010). Similarly, IPS0 and IPS1 were shown to have differential activations for coherent and incoherent motion (Helfrich et al., 2013). If we consider neural efficiency in a broader term (rather than only explaining between subject effects) in respect to learning by experience, then it would be less surprising to have found lower BOLD response to forward motion compare to backward motion, in cortical areas that show differential responses to different motion types. Therefore, the observed BOLD signal differences in the brain areas that are involved in motion possibly reflects that these areas are more efficient in processing forward motion in comparison to backward motion.

7.3.2 Predictive coding of forward motion

Alternative explanation for weaker BOLD signal in response to forward moving stimuli compare to backward moving stimuli would be that humans have higher expectation for forward motion because of the real world statistics of encountering similar motion types in comparison to backward motion. Expectations are prior information driven brain states that predict the probable upcoming sensory information and are employed to reduce computational burden in visual perception (Summerfield and Egner, 2009). During a lifetime an individual encounters forward motion signals more frequently and thus processes those more often than backward motion signals. For instance, optic flow signals during locomotion share similar characteristics with our forward motion stimuli. As it was mentioned in the Predictive coding in vision chapter, the predictable stimuli result in weaker or lower BOLD signal compare to unpredictable stimuli (Alink et al., 2010). Such findings were consistently replicated by several studies for processes in early visual cortex and beyond (Meyer and Olson, 2011; Todorovic et al., 2011; Kok et al., 2012). It is therefore possible that visual motion and IPS areas are more efficient in predicting and therefore processing forward moving textures than backward moving textures and this is reflected in reduced BOLD signal.

7.3.3 Eye – movements

The optokinetic system minimizes retinal image motion by acting as a simple negative feedback system. Optokinetic nystagmus (OKN) is a class of small eye movements that are elicited by global visual motion and acts as a visual gaze stabilization system (reflex) (Ilg, 1997). In humans OKN asymmetries with respect to the direction of motion was reported in vertical axis. Such that gain (i.e. eye movement accuracy) for upward pattern motion is shown to be higher than downward pattern motion (van den Berg and Collewijn, 1988). In our forward motion stimuli, the lower hemi-field was dominated with downward motion, whereas in the backward stimuli the same hemi-field was dominated with upward motion. Given that posterior part of IPS is involved in control of eye-movements, it is not unlikely that differential activity strength in the areas covering this region corresponds to gain related mechanisms. Moreover, it was shown that eye-movements also activate V5/MT, Pc (precuneus) and potentially V6 (Konen et al., 2004). Therefore, we consider the stronger BOLD signal for backward motion in IPS and motion area V6 to reflect the lower gain for downward pattern motion.

8 GENERAL DISCUSSION & CONCLUSION

This thesis aimed to answer the core question whether the actual information content about directionality of motion is encoded the same way when humans view physical motion compared to when implied motion is perceived. It is a complex question and that only modern multivariate pattern analysis (MVPA) techniques allow to answer. Also, it required collecting a multitude of fMRI datasets that allowed to ask several additional questions related to neural encoding of real and implied motion in the human brain.

First, I examined multivariate encoding of direction information evoked by our real motion stimuli that contained two pairs of opposing directions (i.e. right, left, forward, backward). I found that directional information is encoded within numerous visual areas, from early visual to higher parietal and ventral areas, and that directions can be predicted with linear machine learning classifiers from BOLD activity responses. The areas that encode motion direction information are not limited to motion responsive areas, and include even some of the object responsive areas, posterior parietal areas as well as anterior ventral regions.

Second, I examined multivariate encoding of implied motion directions evoked by viewing static images containing objects in context. I found that directional information in implied motion stimuli can be decoded from all early visual areas and some higher visual areas. A key finding is that the peripheral part of the early visual cortex encoded all implied motion directions. Importantly, this part of cortex was not stimulated by the foreground object and hence did not receive bottom-up information about directionality. This result can only be accounted for by considering that feedback information from higher-level regions informs the peripheral early visual cortex representations about foveally presented implied motion information.

Third, I examined whether directional motion information is encoded by similar patterns for both, real and implied motion. I found that in select cortical regions, the neural codes for motion directions are shared between real and implied motion. For right and left directions the shared information is encoded in the lateral occipital area LO2, for forward and backward directions it is encoded in the ventral occipital area VO1. The summary of the decoding results from the investigated brain areas are shown in Table 4.

Finally, I examined net-BOLD signal amplitudes across distinct motion direction and motion axes. I found that motion region V6 and some regions in the posterior parietal cortex show a bias for processing backward real motion in contrast to forward real motion.

The findings of each experiment were presented in detail within separate chapters and they were also discussed within their own chapter. In this section I will emphasize some of the points that I already discussed and will provide additional insights while considering all the results I presented in this thesis.

ROI	Real Motion		Implied Motion		Generalization	
	R vs. L	*F vs. B*	*R vs. L*	*F vs. B*	*R vs. L*	*F vs. B*
Foveal	Y	Y	Y	Y	N	N
Peripheral	Y	Y	Y	Y	N	N
V1	Y	Y	Y	Y	N	N
V2	Y	Y	Y	Y	N	N
V3	Y	Y	Y	Y	U	N
V4	Y	Y	Y	U	N	N
VO1	Y	Y	N	Y	N	**Y**
VO2	N	Y	N	N	N	N
PHC1	N	Y	N	N	N	N
PHC2	N	N	N	N	N	N
V3B	Y	Y	Y	Y	U	N
LO1	Y	Y	Y	N	N	N
LO2	Y	Y	Y	Y	**Y**	N
V5/MT	Y	Y	N	Y	N	U
MST	U	Y	N	Y	N	U
V3A	Y	Y	N	N	N	N
V6	Y	Y	N	N	N	N
Pc	N	Y	N	N	N	N
CSv	U	N	N	N	N	N
VIP	N	Y	N	N	N	N
IPS0	Y	Y	Y	U	N	U
IPS1	Y	Y	N	N	N	N
IPS2	Y	Y	N	N	N	N
IPS3	Y	Y	N	N	N	N
IPS4	Y	Y	N	N	N	N
IPS5	U	N	N	N	N	N
SPL1	Y	Y	N	Y	N	N

Table 4: The summary of the decoding results of all three experiments for each ROI. This table answers the following question for a given ROI; “Does this area (first column) allow decoding of (for example) R vs. L real motion directions?”. If the activity patterns within a given ROI allowed significantly better than chance classification of the direction pairs the relevant cells contain Y for Yes (corrected for multiple comparisons across all ROIs), N for No (corrected), and U for Yes (uncorrected).

8.1 Directional information encoding in early visual areas

Previous studies (Kamitani and Tong, 2006; Seymour et al., 2009; Beckett et al., 2012; Wang et al., 2014) reported significant above chance decoding of real motion directions in V1,V2 and V3. However, these studies only used random dots as stimuli which is highly reductionist and artificial, and they had smaller number of subjects and did not have comparable condition to the F vs. B condition. Moreover, to my knowledge, no prior studies investigated these areas for their multivariate encoding of implied motion directions. Our results showed that BOLD response patterns in early visual areas V1, V2 and V3 contain directional information that allowed the linear machine classifier to learn and to predict both real and implied right-left and forward-backward motion directions of the viewed stimuli. However, our results suggest that the patters of the directional information are not common for real and implied motion, thus we could not find any evidence for generalization in these areas.

For my first experiment I created directional real motion stimuli for right, left, forward and backward directions. The aim was to engage a maximal number of directionally selective units, in order to maximize the overlap to the subset of units potentially involved in coding implied motion. Hence, real motion stimuli were created such that the static component frames had natural image statistics (known to activate neurons more effectively) by using Fourier-scrambled natural images, and motion was presented at a wide range of motion velocities. Moving textures are categorically different than moving dot displays and the former are ecologically more relevant to the visual system. Until now it was not known if the previous findings of decoding motion direction of random dot kinetograms are comparable to natural motion direction stimulation. For real motion, the decoding performance in V1 was significantly different between the R vs. L and F vs. B conditions, and was better for the R vs. L directions. Such preference for a motion axis was not present in V2 or V3; these areas had very similar results for both R vs. L and F vs. B conditions. Among early visual areas the decoding performance was lowest in V1 and highest in V3 for both conditions.

Overall, while our results confirm that decoding motion directions from early visual areas is possible, they also further show that the decoding does not depend on using moving dots as stimuli or within a certain speed range. Furthermore, decoding motion directions across two different motion axes allowed us to show that Peripheral EVC and V1 have a preference for encoding R vs. L motion directions compare to F vs. B motion directions, which was not shown before.

In my second experiment, I used the directional implied motion stimuli that I carefully created for this experiment. The direction information was conveyed by the heading direction of the foreground objects. For the R vs. L condition the stimuli were prepared in a way that the background motion would correspond to the opposite direction compare to the foreground object. As the participants were instructed to fixate at the fixation cross that was at the centre of the stimuli, where the foreground objects were present, our assumption was that the decodable motion direction would correspond to the implied motion direction of the objects in motion, rather than the background motion. Interestingly, the classification of the implied motion directions was also possible in the peripheral representation of the EVC (Peripheral EVC) which was not stimulated by the foreground objects. The results suggest that higher-level cognitive processes that detect implied motion direction based on context and object configuration feed back their predictions beyond the retinal representation of the given object to cover the entire context-providing visual space in early visual cortex. As presented here, the reliable decoding of implied motion direction information from the Peripheral EVC is in line with the predictive coding theory, and exemplifies how top-down information is integrated with the bottom-up processing in the early visual cortex similarly as demonstrated before for colours of objects (Bannert and Bartels, 2013).

8.2 A closer look to the responses of V5/MT, MST, LO1 and LO2

The core question that this thesis investigated was whether the human brain generalizes the direction information of real and implied motion in specific brain areas. If it does so, then the areas that encode motion-invariant direction information should be integrating motion and object responses to represent the direction of both real and implied motion stimuli. The human LOC is the most specialized area for object processing (Malach et al., 1995; Grill-Spector et al., 2000; Kourtzi and Kanwisher, 2001; Self and Zeki, 2005), and for motion processing in the human brain the area V5/MT+ is highly crucial (Zeki, 1991; Zeki et al., 1993; Moutoussis and Zeki, 2006, 2008; Zeki, 2015). Although human V5/MT is known as a motion area, a previous fMRI study reported object-selective responses (higher responses for intact than for scrambled images of objects) in V5/MT+ (Kourtzi et al., 2002). More specifically, the object-selective responses that they observed in V5/MT+ were for moving objects and for static objects defined by depth cues, but not for static 2D objects. Moreover, they showed that human V5/MT+ has even higher object-selectivity responses than the LOC. The shape responses in V5/MT+ was also reported in another study, which also found the responses to be significantly stronger to motion-defined shapes than to colour-defined shapes (Self and Zeki, 2005). The shape responses of the LOC, however, were shown to be equal to both colour- and motion-defined shapes, and the responses were higher when the shapes were defined by more than one cue, such as both colour and

motion (Self and Zeki, 2005). Moreover, V5/MT+ activation was also observed in response to dynamically changing illumination of coloured Mondrians (Bartels and Zeki, 2000) and was found to be correlated with subjective experience of colour during free viewing of a movie (Bartels and Zeki, 2004). Furthermore, LOC activity was reported in response to coherent motion of random-dots (Murray et al., 2003) and it was shown to strongly correlate with the reported motion percept (Moutoussis et al., 2005). Overall, previous research on human V5/MT+ and LOC suggest that these neighbouring areas are involved in more processes than what they are specialized for, and the results of my experiments provide multivariate evidence for this to be really the case. In my first experiment I found that the LOC areas, LO1 and LO2, encode direction information of real motion stimuli for both right-left and forward-backward axes. These results contradict with the previous findings suggesting LO1 and LO2 are not motion selective (Larsson and Heeger, 2006). The same was true for V5/MT. However, MST showed a preference for encoding of forward-backward directions.

In my second experiment I found that LO1 and LO2 encode implied right-left motion directions, and LO2 also encode implied forward-backward directions. In contrast, V5/MT and MST encode only forward-backward implied motion directions. It might be that encoding of real motion directions are done by different neuronal populations than of implied motion directions. However, the results of my third experiment showed that the right-left motion directions of both real and implied motion are encoded in similar patterns in LO2, and the forward-backward directions of both motion types are encoded in somewhat similar patterns in V5/MT and MST. These results suggest that there is a common code for motion directions for right-left in LO2 and for forward-backward (arguably) in V5/MT and MST. Is it possible that LO2 contain direction-selective neurons as well? Unfortunately, my research can raise this question but cannot provide an answer to it. Nevertheless, the fact that the better decoding performances were obtained in LO2 in comparison to ones of V5/MT (and MST) is highly interesting, and overlaps with our hypothesis that object processing areas should be involved in processing of implied motion directions, especially if there is a generalization of this information.

8.3 Contributions of ventral areas in motion processing

The human ventral occipital cortex contains several retinotopically organized areas, such as V4, VO1, VO2, PHC1 and PHC2. The visual area V4 was first identified in rhesus monkeys (Zeki, 1971) and was shown to contain neurons that are selective to wavelength (Zeki, 1973), and later it was also identified in humans as an area specialized for processing of colour (Lueck et al., 1989; McKeefry and Zeki, 1997; Zeki and Bartels, 1999; Gallant et al., 2000). VO areas, located anterior to V4, were reported to have similar response profiles (Arcaro et al., 2009) and

were shown to respond preferentially to objects compared to faces and to show colour selectivity (Wade et al., 2002; Brewer et al., 2005). Moreover, it was shown that stimulus colour can accurately be decoded from V4 and VO1 (Brouwer and Heeger, 2009; Seymour et al., 2009; Bannert and Bartels, 2018). Much later, two visual field maps anterior to the human visual area V4 were identified as VO1 and VO2 and proposed to be part of a VO cluster (Brewer et al., 2005). More recently two other visual field maps anterior to VO2 were identified as PHC1 and PHC2 (Arcaro et al., 2009). An fMRI study which looked at all of these ventral areas (V4, VO1, VO2, PHC1, PHC2) showed that these areas respond significantly stronger to scene stimuli than to face stimuli, although V4 and VO1 do not discriminate between scene, object or scrambled stimuli, scene stimuli exhibit significantly stronger response than objects and scrambled stimuli in VO2, PHC1 and PHC2 (Arcaro et al., 2009). Among these areas only V4 was shown to contain direction-selective neurons (Tolias et al., 2005) and to encode motion directions of random dots (Kamitani and Tong, 2006; Seymour et al., 2009). Moreover, V4 was shown to be selective for the global structure of Glass patterns implying motion, although this selectivity was reported to be carried by a different subpopulation of neurons than for those selective for real motion (Krekelberg et al., 2005). However, no other study examined V4 for its involvement in implied motion processing. None of the other ventral areas were reported to be involved in motion processing. Thus, the responses of the other ventral areas to both real and implied motion was unknown until now. I found that decoding of the real motion directions was also possible from the activity patterns in VO1, VO2 and PHC1. For VO2 and PHC1 only the decoding of F vs. B real motion directions worked, while for V4 and VO1 decoding of both R vs. L and F vs. B real motion directions was possible. These results strongly suggest that motion directions are encoded in these ventral areas. Moreover, the response patterns in V4 and VO1 also allowed decoding of implied motion directions significantly above chance. Most interestingly, I found that the activity patterns in VO1 contains information about forward and backward direction content that is shared between real and implied motion. These novel findings highlight the importance of ventral occipital areas for processing both real and implied motion. Furthermore, amplify the knowledge of functions of relatively new visual areas VO1, VO2, PHC1 and PHC2.

8.4 “Motion direction decoding” versus “object orientation decoding”

The results of our first experiment clearly demonstrated that the decoding of real motion directions of viewed stimuli is possible from fMRI BOLD responses and not limited to areas that were previously reported. The results of our second experiment, however, are ambiguous regarding the content of decoded information. Could it be that what we decoded from responses to implied motion stimuli was object orientation information, rather than motion direction information? I think this question may have different answers for different areas. The

generalization results suggest that we can rule out the possibility of object orientation decoding in VO1, LO2, V5/MT, MST, V3, V3B and IPS0. Also, the early visual areas are unlikely to encode object orientation since it is a rather high level process. The stimuli we used in our implied motion experiment were naturalistic, high-level and the directional motion information were conveyed by the orientation of foreground objects and motion blur. Considering the receptive field properties and previous reports on stimuli selectivity responses, the results of V4, VO2 and LO1 might be reflecting object orientation encoding of these areas. Especially for LO1 this alternative interpretation of the second experiments' results would be probable, given that this area was reported to show robust orientation selective adaptation (Larsson and Heeger, 2006)

8.5 Directional information in the implied motion stimuli

The direction information of the implied motion stimuli was conveyed by the heading direction of the foreground objects. For the R vs. L conditions the stimuli were prepared in a way that the background motion would correspond to the opposite direction compared to the foreground object. For the F vs. B conditions the backgrounds were blur-free and the implied motion of the foreground objects were relative to the stable scenery. Hence there was no motion implied in the background. As the participants were instructed to fixate at the fixation cross that was at the centre of the stimuli where the foreground objects were present, our assumption was that the decodable motion direction would correspond to the implied motion direction of the objects in motion, rather than the relative motion of background scenes. However, in theory, some of the areas could be coding for the motion direction of the background, rather than the unified implied motion perception induced by the heading direction of the foreground object. For instance, the peripheral representation of the early visual cortex (Peripheral EVC) received only bottom-up information corresponding to the background of the stimuli, especially for the R vs. L conditions. The background itself did not contain directional information, however as I previously discussed, the feedback this area received would have provided the contextual information of the foreground objects, and therefore this area might have encoded the relative direction of the background, rather than that of the foreground object. That would mean that the information this area encodes in response to rightward implied motion would be 'left', and vice versa. Therefore, one should not think that above chance decoding of implied motion directions from an area necessarily corresponds to perceived implied motion direction. However, above chance decoding of implied motion directions means that these brain areas encode the differential information that is present in the stimuli, which is in our case motion directions. What I explained so far applies exclusively for the results of my second experiment that were obtained with cross-validation analysis and do not apply to the results of my third experiment. The cross-classification analysis of the motion directions potentially allows to detect if an area was

consistently encoding the background motion directions. In that case, that area would have significant below-chance decoding, as the classifier was trained on the real motion data. However, when I tested the areas that show below-chance decoding I found that none of them was significantly different than the chance level of decoding. Hence, I conclude that none of the brain areas investigated encodes the directionality implied by the background scenes and the results of the implied motion decoding corresponds to the perceived implied motion directions.

9 STATEMENT OF CONTRIBUTIONS

This doctoral thesis contains unpublished findings that are presented in four separate chapters. Each of the chapters can potentially be submitted to scientific journals for publication. As the author of this thesis I created, programmed, prepared the experimental stimuli and the experimental design, collected and analysed the data, created the figures and wrote the thesis. The main research questions were introduced to me by my supervisor Andreas Bartels, who advised me during the planning and designing of the experiments and the data analyses. He also reviewed and provided feedback for the drafts of this thesis.

10 REFERENCES

Albright TD (1984) Direction and orientation selectivity of neurons in visual area MT of the macaque. J Neurophysiol 52:1106-1130.

Albright TD, Desimone R, Gross CG (1984) Columnar organization of directionally selective cells in visual area MT of the macaque. J Neurophysiol 51:16-31.

Alink A, Schwiedrzik CM, Kohler A, Singer W, Muckli L (2010) Stimulus predictability reduces responses in primary visual cortex. J Neurosci 30:2960-2966.

Alink A, Euler F, Kriegeskorte N, Singer W, Kohler A (2012) Auditory motion direction encoding in auditory cortex and high-level visual cortex. Hum Brain Mapp 33:969-978.

Andersen RA (1989) Visual and eye movement functions of the posterior parietal cortex. Annu Rev Neurosci 12:377-403.

Arcaro MJ, McMains SA, Singer BD, Kastner S (2009) Retinotopic organization of human ventral visual cortex. J Neurosci 29:10638-10652.

Ball W, Tronick E (1971) Infant responses to impending collision: optical and real. Science 171:818-820.

Bannert MM, Bartels A (2013) Decoding the yellow of a gray banana. Curr Biol 23:2268-2272.

Bannert MM, Bartels A (2017) Invariance of surface color representations across illuminant changes in the human cortex. Neuroimage 158:356-370.

Bannert MM, Bartels A (2018) Human V4 Activity Patterns Predict Behavioral Performance in Imagery of Object Color. J Neurosci 38:3657-3668.

Bartels A, Zeki S (2000) The architecture of the colour centre in the human visual brain: new results and a review. Eur J Neurosci 12:172-193.

Bartels A, Zeki S (2004) Functional brain mapping during free viewing of natural scenes. Human Brain Mapping 21:75-85.

Bartels A, Logothetis NK, Moutoussis K (2008) fMRI and its interpretations: an illustration on directional selectivity in area V5/MT. Trends Neurosci 31:444-453.

Beckett A, Peirce JW, Sanchez-Panchuelo RM, Francis S, Schluppeck D (2012) Contribution of large scale biases in decoding of direction-of-motion from high-resolution fMRI data in human early visual cortex. Neuroimage 63:1623-1632.

Benson NC, Butt OH, Datta R, Radoeva PD, Brainard DH, Aguirre GK (2012) The Retinotopic Organization of Striate Cortex Is Well Predicted by Surface Topology (vol 22, pg 2081, 2012). Current Biology 22:2284-2284.

Berger DR (2003) Spectral Texturing for Real-Time Applications. ACM SIGGRAPH 2003 Sketches & Applications

Bisley JW, Zaksas D, Droll JA, Pasternak T (2004) Activity of neurons in cortical area MT during a memory for motion task. J Neurophysiol 91:286-300.

Blake R, Shiffrar M (2007) Perception of human motion. Annu Rev Psychol 58:47-73.

Blanke O, Landis T, Safran AB, Seeck M (2002) Direction-specific motion blindness induced by focal stimulation of human extrastriate cortex. European Journal of Neuroscience 15:2043-2048.

Brewer AA, Liu J, Wade AR, Wandell BA (2005) Visual field maps and stimulus selectivity in human ventral occipital cortex. Nat Neurosci 8:1102-1109.

Brouwer GJ, van Ee R (2007) Visual cortex allows prediction of perceptual states during ambiguous structure-from-motion. J Neurosci 27:1015-1023.

Brouwer GJ, Heeger DJ (2009) Decoding and Reconstructing Color from Responses in Human Visual Cortex. Journal of Neuroscience 29:13992-14003.

Burr D (1980) Motion smear. Nature 284:164-165.

Burr D (2000) Motion vision: Are 'speed lines' used in human visual motion? Current Biology 10:R440-R443.

Cardin V, Smith AT (2010) Sensitivity of human visual and vestibular cortical regions to egomotion-compatible visual stimulation. Cereb Cortex 20:1964-1973.

Chen J, Sperandio I, Henry MJ, Goodale MA (2019) Changing the Real Viewing Distance Reveals the Temporal Evolution of Size Constancy in Visual Cortex. Curr Biol 29:2237-2243 e2234.

Colby CL, Duhamel JR, Goldberg ME (1993) Ventral intraparietal area of the macaque: anatomic location and visual response properties. J Neurophysiol 69:902-914.

Cutting JE (2002) Representing motion in a static image: constraints and parallels in art, science, and popular culture. Perception 31:1165-1193.

Dilks DD, Julian JB, Kubilius J, Spelke ES, Kanwisher N (2011) Mirror-Image Sensitivity and Invariance in Object and Scene Processing Pathways. Journal of Neuroscience 31:11305-11312.

Dubner R, Zeki SM (1971) Response properties and receptive fields of cells in an anatomically defined region of the superior temporal sulcus in the monkey. Brain Res 35:528-532.

Dupont P, De Bruyn B, Vandenberghe R, Rosier AM, Michiels J, Marchal G, Mortelmans L, Orban GA (1997) The kinetic occipital region in human visual cortex. Cereb Cortex 7:283-292.

Erlikhman G, Gurariy G, Mruczek REB, Caplovitz GP (2016) The neural representation of objects formed through the spatiotemporal integration of visual transients. Neuroimage 142:67-78.

Fan RE, Chang KW, Hsieh CJ, Wang XR, Lin CJ (2008) LIBLINEAR: A Library for Large Linear Classification. J Mach Learn Res 9:1871-1874.

Fischer E, Bulthoff HH, Logothetis NK, Bartels A (2012) Human areas V3A and V6 compensate for self-induced planar visual motion. Neuron 73:1228-1240.

Franconeri SL, Simons DJ (2003) Moving and looming stimuli capture attention. Percept Psychophys 65:999-1010.

Freyd JJ (1983) The mental representation of movement when static stimuli are viewed. Percept Psychophys 33:575-581.

Freyd JJ (1987) Dynamic mental representations. Psychol Rev 94:427-438.

Freyd JJ, Finke RA (1984) Representational momentum. Journal of Experimental Psychology: Learning, Memory, and Cognition 10:126-132.

Gallant JL, Shoup RE, Mazer JA (2000) A human extrastriate area functionally homologous to macaque V4. Neuron 27:227-235.

Geisler WS (1999) Motion streaks provide a spatial code for motion direction. Nature 400:65-69.

Ghazanfar AA, Neuhoff JG, Logothetis NK (2002) Auditory looming perception in rhesus monkeys. Proc Natl Acad Sci U S A 99:15755-15757.

Gibson JJ (1966) The problem of temporal order in stimulation and perception. J Psychol 62:141-149.

Goebel R, Khorram-Sefat D, Muckli L, Hacker H, Singer W (1998) The constructive nature of vision: direct evidence from functional magnetic resonance imaging studies of apparent motion and motion imagery. Eur J Neurosci 10:1563-1573.

Goodale MA, Milner AD (1992) Separate visual pathways for perception and action. Trends Neurosci 15:20-25.

Greenlee MW (2000) Human cortical areas underlying the perception of optic flow: brain imaging studies. Int Rev Neurobiol 44:269-292.

Grill-Spector K, Kushnir T, Hendler T, Malach R (2000) The dynamics of object-selective activation correlate with recognition performance in humans. Nat Neurosci 3:837-843.

Grill-Spector K, Kushnir T, Edelman S, Avidan G, Itzchak Y, Malach R (1999) Differential processing of objects under various viewing conditions in the human lateral occipital complex. Neuron 24:187-203.

Guo ZP, Li AM, Yu L (2017) "Neural Efficiency" of Athletes' Brain during Visuo-Spatial Task: An fMRI Study on Table Tennis Players. Frontiers in Behavioral Neuroscience 11.

Hagen MC, Franzen O, McGlone F, Essick G, Dancer C, Pardo JV (2002) Tactile motion activates the human middle temporal/V5 (MT/V5) complex. Eur J Neurosci 16:957-964.

Haier RJ, Siegel B, Tang C, Abel L, Buchsbaum MS (1992) Intelligence and Changes in Regional Cerebral Glucose Metabolic-Rate Following Learning. Intelligence 16:415-426.

Hansen T, Olkkonen M, Walter S, Gegenfurtner KR (2006) Memory modulates color appearance. Nat Neurosci 9:1367-1368.

Haxby JV, Grady CL, Horwitz B, Ungerleider LG, Mishkin M, Carson RE, Herscovitch P, Schapiro MB, Rapoport SI (1991) Dissociation of Object and Spatial Visual Processing Pathways in Human Extrastriate Cortex. P Natl Acad Sci USA 88:1621-1625.

Haynes JD, Rees G (2005) Predicting the orientation of invisible stimuli from activity in human primary visual cortex. Nature Neuroscience 8:686-691.

Hebart MN, Gorgen K, Haynes JD (2014) The Decoding Toolbox (TDT): a versatile software package for multivariate analyses of functional imaging data. Front Neuroinform 8:88.

Hedges JH, Gartshteyn Y, Kohn A, Rust NC, Shadlen MN, Newsome WT, Movshon JA (2011) Dissociation of neuronal and psychophysical responses to local and global motion. Curr Biol 21:2023-2028.

Helfrich RF, Becker HG, Haarmeier T (2013) Processing of coherent visual motion in topographically organized visual areas in human cerebral cortex. Brain Topogr 26:247-263.

Holm S (1979) A Simple Sequentially Rejective Multiple Test Procedure. Scand J Stat 6:65-70.

Hong SW, Tong F, Seiffert AE (2012) Direction-selective patterns of activity in human visual cortex suggest common neural substrates for different types of motion. Neuropsychologia 50:514-521.

Ilg UJ (1997) Slow eye movements. Prog Neurobiol 53:293-329.

Ilg UJ (2008) The role of areas MT and MST in coding of visual motion underlying the execution of smooth pursuit. Vision Research 48:2062-2069.

Johansson G (1973) Visual-Perception of Biological Motion and a Model for Its Analysis. Perception & Psychophysics 14:201-211.

Kamitani Y, Tong F (2005) Decoding the visual and subjective contents of the human brain. Nature Neuroscience 8:679-685.

Kamitani Y, Tong F (2006) Decoding seen and attended motion directions from activity in the human visual cortex. Current Biology 16:1096-1102.

Kim CY, Blake R (2007) Brain activity accompanying perception of implied motion in abstract paintings. Spat Vis 20:545-560.

Kok P, Jehee JFM, de Lange FP (2012) Less Is More: Expectation Sharpens Representations in the Primary Visual Cortex. Neuron 75:265-270.

Konen CS, Kastner S (2008) Representation of eye movements and stimulus motion in topographically organized areas of human posterior parietal cortex. J Neurosci 28:8361-8375.

Konen CS, Kleiser R, Wittsack HJ, Bremmer F, Seitz RJ (2004) The encoding of saccadic eye movements within human posterior parietal cortex. Neuroimage 22:304-314.

Kourtzi Z, Kanwisher N (2000) Activation in human MT/MST by static images with implied motion. J Cogn Neurosci 12:48-55.

Kourtzi Z, Kanwisher N (2001) Representation of perceived object shape by the human lateral occipital complex. Science 293:1506-1509.

Kourtzi Z, Bulthoff HH, Erb M, Grodd W (2002) Object-selective responses in the human motion area MT/MST. Nat Neurosci 5:17-18.

Krekelberg B, Vatakis A, Kourtzi Z (2005) Implied motion from form in the human visual cortex. J Neurophysiol 94:4373-4386.

Krekelberg B, Dannenberg S, Hoffmann KP, Bremmer F, Ross J (2003) Neural correlates of implied motion. Nature 424:674-677.

Larsson J, Heeger DJ (2006) Two retinotopic visual areas in human lateral occipital cortex. J Neurosci 26:13128-13142.

Livingstone M, Hubel D (1988) Segregation of form, color, movement, and depth: anatomy, physiology, and perception. Science 240:740-749.

Logothetis NK, Schall JD (1989) Neuronal correlates of subjective visual perception. Science 245:761-763.

Lorteije JA, Kenemans JL, Jellema T, van der Lubbe RH, de Heer F, van Wezel RJ (2006) Delayed response to animate implied motion in human motion processing areas. J Cogn Neurosci 18:158-168.

Lorteije JAM, Kenemans JL, Jellema T, van der Lubbe RHJ, Lommers MW, van Wezel RJA (2007) Adaptation to real motion reveals direction-selective interactions between real and implied motion processing. J Cognitive Neurosci 19:1231-1240.

Lueck CJ, Zeki S, Friston KJ, Deiber MP, Cope P, Cunningham VJ, Lammertsma AA, Kennard C, Frackowiak RS (1989) The colour centre in the cerebral cortex of man. Nature 340:386-389.

Maier JX, Ghazanfar AA (2007) Looming biases in monkey auditory cortex. J Neurosci 27:4093-4100.

Malach R, Reppas JB, Benson RR, Kwong KK, Jiang H, Kennedy WA, Ledden PJ, Brady TJ, Rosen BR, Tootell RB (1995) Object-related activity revealed by functional magnetic resonance imaging in human occipital cortex. Proc Natl Acad Sci U S A 92:8135-8139.

Masse NY, Hodnefield JM, Freedman DJ (2017) Mnemonic Encoding and Cortical Organization in Parietal and Prefrontal Cortices. J Neurosci 37:6098-6112.

Maunsell JH, Newsome WT (1987) Visual processing in monkey extrastriate cortex. Annu Rev Neurosci 10:363-401.

McKeefry DJ, Zeki S (1997) The position and topography of the human colour centre as revealed by functional magnetic resonance imaging. Brain 120:2229-2242.

McKeefry DJ, Burton MP, Vakrou C, Barrett BT, Morland AB (2008) Induced deficits in speed perception by transcranial magnetic stimulation of human cortical areas V5/MT+ and V3A. J Neurosci 28:6848-6857.

Meyer T, Olson CR (2011) Statistical learning of visual transitions in monkey inferotemporal cortex. Proc Natl Acad Sci U S A 108:19401-19406.

Mikami A, Newsome WT, Wurtz RH (1986) Motion selectivity in macaque visual cortex. II. Spatiotemporal range of directional interactions in MT and V1. J Neurophysiol 55:1328-1339.

Mishkin M, Ungerleider LG, Macko KA (1983) Object Vision and Spatial Vision - 2 Cortical Pathways. Trends in Neurosciences 6:414-417.

Moutoussis K, Zeki S (2006) Seeing invisible motion: a human FMRI study. Curr Biol 16:574-579.

Moutoussis K, Zeki S (2008) Motion processing, directional selectivity, and conscious visual perception in the human brain. Proc Natl Acad Sci U S A 105:16362-16367.

Moutoussis K, Keliris G, Kourtzi Z, Logothetis N (2005) A binocular rivalry study of motion perception in the human brain. Vision Res 45:2231-2243.

Movshon JA, Newsome WT (1996) Visual response properties of striate cortical neurons projecting to area MT in macaque monkeys. J Neurosci 16:7733-7741.

Muckli L, Kohler A, Kriegeskorte N, Singer W (2005) Primary visual cortex activity along the apparent-motion trace reflects illusory perception. PLoS Biol 3:e265.

Muckli L, Kriegeskorte N, Lanfermann H, Zanella FE, Singer W, Goebel R (2002) Apparent motion: event-related functional magnetic resonance imaging of perceptual switches and States. J Neurosci 22:RC219.

Muckli L, De Martino F, Vizioli L, Petro LS, Smith FW, Ugurbil K, Goebel R, Yacoub E (2015) Contextual Feedback to Superficial Layers of V1. Curr Biol 25:2690-2695.

Murray SO, Olshausen BA, Woods DL (2003) Processing shape, motion and three-dimensional shape-from-motion in the human cortex. Cereb Cortex 13:508-516.

Murray SO, Boyaci H, Kersten D (2006) The representation of perceived angular size in human primary visual cortex. Nat Neurosci 9:429-434.

Nanez JE (1988) Perception of Impending Collision in 3-Week-Old to 6-Week-Old Human Infants. Infant Behav Dev 11:447-463.

Nau M, Schindler A, Bartels A (2018) Real-motion signals in human early visual cortex. Neuroimage 175:379-387.

Nawrot M, Blake R (1991) The Interplay between Stereopsis and Structure from Motion. Perception & Psychophysics 49:230-244.

Neubauer AC, Fink A (2009) Intelligence and neural efficiency. Neurosci Biobehav Rev 33:1004-1023.

Neuhoff JG (1998) Perceptual bias for rising tones. Nature 395:123-124.

Newsome WT, Pare EB (1988) A Selective Impairment of Motion Perception Following Lesions of the Middle Temporal Visual Area (Mt). Journal of Neuroscience 8:2201-2211.

Nichols TE, Holmes AP (2002) Nonparametric permutation tests for functional neuroimaging: A primer with examples. Human Brain Mapping 15:1-25.

Nishida S, Sasaki Y, Murakami I, Watanabe T, Tootell RB (2003) Neuroimaging of direction-selective mechanisms for second-order motion. J Neurophysiol 90:3242-3254.

Oosterhof NN, Wiestler T, Downing PE, Diedrichsen J (2011) A comparison of volume-based and surface-based multi-voxel pattern analysis. Neuroimage 56:593-600.

Orban GA, Kennedy H, Bullier J (1986) Velocity sensitivity and direction selectivity of neurons in areas V1 and V2 of the monkey: influence of eccentricity. J Neurophysiol 56:462-480.

Orban GA, Van Essen D, Vanduffel W (2004) Comparative mapping of higher visual areas in monkeys and humans. Trends in Cognitive Sciences 8:315-324.

Orban GA, Dupont P, De Bruyn B, Vogels R, Vandenberghe R, Mortelmans L (1995) A motion area in human visual cortex. Proc Natl Acad Sci U S A 92:993-997.

Parker A, Alais D (2007) A bias for looming stimuli to predominate in binocular rivalry. Vision Res 47:2661-2674.

Pereira F, Mitchell T, Botvinick M (2009) Machine learning classifiers and fMRI: a tutorial overview. Neuroimage 45:S199-209.

Pitzalis S, Fattori P, Galletti C (2012) The functional role of the medial motion area V6. Front Behav Neurosci 6:91.

Pitzalis S, Sereno MI, Committeri G, Fattori P, Galati G, Patria F, Galletti C (2010) Human v6: the medial motion area. Cereb Cortex 20:411-424.

Pitzalis S, Galletti C, Huang RS, Patria F, Committeri G, Galati G, Fattori P, Sereno MI (2006) Wide-field retinotopy defines human cortical visual area v6. J Neurosci 26:7962-7973.

Rao RPN, Ballard DH (1999) Predictive coding in the visual cortex: a functional interpretation of some extra-classical receptive-field effects. Nature Neuroscience 2:79-87.

Ross J, Badcock DR, Hayes A (2000) Coherent global motion in the absence of coherent velocity signals. Curr Biol 10:679-682.

Salzman CD, Britten KH, Newsome WT (1990) Cortical microstimulation influences perceptual judgements of motion direction. Nature 346:174-177.

Sarma A, Masse NY, Wang XJ, Freedman DJ (2016) Task-specific versus generalized mnemonic representations in parietal and prefrontal cortices. Nat Neurosci 19:143-149.

Schellekens W, van Wezel RJ, Petridou N, Ramsey NF, Raemaekers M (2016) Predictive coding for motion stimuli in human early visual cortex. Brain Struct Funct 221:879-890.

Schiff W, Oldak R (1990) Accuracy of judging time to arrival: effects of modality, trajectory, and gender. J Exp Psychol Hum Percept Perform 16:303-316.

Schiff W, Caviness JA, Gibson JJ (1962) Persistent fear responses in rhesus monkeys to the optical stimulus of "looming". Science 136:982-983.

Schlack A, Albright TD (2007) Remembering visual motion: Neural correlates of associative plasticity and motion recall in cortical area MT. Neuron 53:881-890.

Seifritz E, Neuhoff JG, Bilecen D, Scheffler K, Mustovic H, Schachinger H, Elefante R, Di Salle F (2002) Neural processing of auditory looming in the human brain. Curr Biol 12:2147-2151.

Self MW, Zeki S (2005) The integration of colour and motion by the human visual brain. Cereb Cortex 15:1270-1279.

Senior C, Ward J, David AS (2002) Representational momentum and the brain: An investigation into the functional necessity of V5/MT. Vis Cogn 9:81-92.

Senior C, Barnes J, Giampietro V, Simmons A, Bullmore ET, Brammer M, David AS (2000) The functional neuroanatomy of implicit-motion perception or representational momentum. Curr Biol 10:16-22.

Serences JT, Boynton GM (2007) The representation of behavioral choice for motion in human visual cortex. Journal of Neuroscience 27:12893-12899.

Sereno MI, Huang RS (2006) A human parietal face area contains aligned head-centered visual and tactile maps. Nature Neuroscience 9:1337-1343.

Seymour K, Clifford CWG, Logothetis NK, Bartels A (2009) The Coding of Color, Motion, and Their Conjunction in the Human Visual Cortex. Current Biology 19:177-183.

Silson EH, McKeefry DJ, Rodgers J, Gouws AD, Hymers M, Morland AB (2013) Specialized and independent processing of orientation and shape in visual field maps LO1 and LO2. Nat Neurosci 16:267-269.

Silver MA, Ress D, Heeger DJ (2005) Topographic maps of visual spatial attention in human parietal cortex. J Neurophysiol 94:1358-1371.

Simoncelli EP, Olshausen BA (2001) Natural image statistics and neural representation. Annu Rev Neurosci 24:1193-1216.

Smith AT, Greenlee MW, Singh KD, Kraemer FM, Hennig J (1998) The processing of first- and second-order motion in human visual cortex assessed by functional magnetic resonance imaging (fMRI). J Neurosci 18:3816-3830.

Sperandio I, Chouinard PA, Goodale MA (2012) Retinotopic activity in V1 reflects the perceived and not the retinal size of an afterimage. Nature Neuroscience 15:540-542.

Summerfield C, Egner T (2009) Expectation (and attention) in visual cognition. Trends Cogn Sci 13:403-409.

Todorovic A, van Ede F, Maris E, de Lange FP (2011) Prior expectation mediates neural adaptation to repeated sounds in the auditory cortex: an MEG study. J Neurosci 31:9118-9123.

Tolias AS, Keliris GA, Smirnakis SM, Logothetis NK (2005) Neurons in macaque area V4 acquire directional tuning after adaptation to motion stimuli. Nat Neurosci 8:591-593.

Tootell RB, Reppas JB, Dale AM, Look RB, Sereno MI, Malach R, Brady TJ, Rosen BR (1995) Visual motion aftereffect in human cortical area MT revealed by functional magnetic resonance imaging. Nature 375:139-141.

Tootell RB, Mendola JD, Hadjikhani NK, Ledden PJ, Liu AK, Reppas JB, Sereno MI, Dale AM (1997) Functional analysis of V3A and related areas in human visual cortex. J Neurosci 17:7060-7078.

Treue S, Husain M, Andersen RA (1991) Human perception of structure from motion. Vision Res 31:59-75.

Tyll S, Bonath B, Schoenfeld MA, Heinze HJ, Ohl FW, Noesselt T (2013) Neural basis of multisensory looming signals. Neuroimage 65:13-22.

Ungerleider LG, Haxby JV (1994) 'What' and 'where' in the human brain. Curr Opin Neurobiol 4:157-165.

van den Berg AV, Collewijn H (1988) Directional asymmetries of human optokinetic nystagmus. Exp Brain Res 70:597-604.

van Kemenade BM, Seymour K, Christophel TB, Rothkirch M, Sterzer P (2014) Decoding pattern motion information in V1. Cortex 57:177-187.

Van Oostende S, Sunaert S, Van Hecke P, Marchal G, Orban GA (1997) The kinetic occipital (KO) region in man: an fMRI study. Cereb Cortex 7:690-701.

Vetter P, Grosbras MH, Muckli L (2015) TMS over V5 disrupts motion prediction. Cereb Cortex 25:1052-1059.

Wade AR, Brewer AA, Rieger JW, Wandell BA (2002) Functional measurements of human ventral occipital cortex: retinotopy and colour. Philos Trans R Soc Lond B Biol Sci 357:963-973.

Wallach H, O'Connell DN (1953) The kinetic depth effect. J Exp Psychol 45:205-217.

Wandell BA, Dumoulin SO, Brewer AA (2007) Visual field maps in human cortex. Neuron 56:366-383.

Wang HX, Merriam EP, Freeman J, Heeger DJ (2014) Motion Direction Biases and Decoding in Human Visual Cortex. Journal of Neuroscience 34:12601-12615.

Wang L, Mruczek REB, Arcaro MJ, Kastner S (2015) Probabilistic Maps of Visual Topography in Human Cortex. Cerebral Cortex 25:3911-3931.

Wibral M, Bledowski C, Kohler A, Singer W, Muckli L (2009) The timing of feedback to early visual cortex in the perception of long-range apparent motion. Cereb Cortex 19:1567-1582.

Winawer J, Huk AC, Boroditsky L (2008) A motion aftereffect from still photographs depicting motion. Psychol Sci 19:276-283.

Wittmann M, van Wassenhove V, Craig AD, Paulus MP (2010) The neural substrates of subjective time dilation. Front Hum Neurosci 4:2.

Zeki S (1991) Cerebral akinetopsia (visual motion blindness). A review. Brain 114 (Pt 2):811-824.

Zeki S (2015) Area V5-a microcosm of the visual brain. Front Integr Neurosci 9:21.

Zeki S, Bartels A (1999) The clinical and functional measurement of cortical (in)activity in the visual brain, with special reference to the two subdivisions (V4 and V4 alpha) of the human colour centre. Philos Trans R Soc Lond B Biol Sci 354:1371-1382.

Zeki S, Watson JD, Frackowiak RS (1993) Going beyond the information given: the relation of illusory visual motion to brain activity. Proc Biol Sci 252:215-222.

Zeki SM (1971) Cortical projections from two prestriate areas in the monkey. Brain Res 34:19-35.

Zeki SM (1973) Colour coding in rhesus monkey prestriate cortex. Brain Res 53:422-427.

Zeki SM (1974) Functional organization of a visual area in the posterior bank of the superior temporal sulcus of the rhesus monkey. J Physiol 236:549-573.